THE UTILITY OF L-TYROSINE BASED POLYCARBONATE COPOLYMERS CONTAINING POLY(ETHYLENE GLYCOL) AS A DEGRADABLE CARRIER FOR THE RELEASE OF A HYDROPHOBIC PEPTIDE MOLECULE

by

ISAAC JOHN KHAN

A dissertation submitted to the

Graduate School-New Brunswick

Rutgers, the State University of New Jersey

and

The Graduate School of Biomedical Sciences

University of Medicine and Dentistry of New Jersey

In partial fulfillment of the requirements

For the degree of

Doctor of Philosophy

Graduate Program in Biomedical Engineering

Written under the direction of

Joachim Kohn, Ph.D.

And approved by

_____

_____

_____

_____

New Brunswick, New Jersey

October, 2009

ABSTRACT OF THE DISSERTATION

THE UTILITY OF L-TYROSINE BASED POLYCARBONATE COPOLYMERS CONTAINING POLY(ETHYLENE GLYCOL) AS A DEGRADABLE CARRIER FOR THE RELEASE OF A HYDROPHOBIC PEPTIDE MOLECULE

By ISAAC JOHN KHAN

Dissertation Director:

Joachim Kohn, Ph.D.

The utility of biodegradable polymers as localized drug delivery carriers is an ongoing area of research where investigators attempt to deliver a wide range of hydrophobic small molecules and peptides. The long-term (≥ 1 year), controllable and sustained release of such molecules from these solid carriers has not been demonstrated due to the complexity of the reaction-diffusion mechanisms that occur in these hydrated polymers. The goal of the present research was to characterize the release of the hydrophobic peptide voclosporin from a class of biodegradable amorphous polymers based on desaminotyrosyl-tyrosine alkyl ester (DTR) and desaminotyrosyl-tyrosine ester, (DT), and the monomer polyethylene glycol (PEG). Four areas of study were presented: (i) the modulation of drug release and polymer erosion as a function of poly(DTR-co-y % DT-co-z % PEG_{1K} carbonate) homo-, co- and terpolymer compositions, (ii) the changes in polymer morphology and a proposed theory to account for drug retention exhibited by

these polymers after prolonged hydration, (iii) the instability of voclosporin in the presence of the terpolymer carriers and the need for formulations containing antioxidants and (iv) the demonstration of selected PEG-containing polycarbonate formulations as a drug delivery vehicle for potential ophthalmic applications. The polycarbonate terpolymers were shown to undergo hydration-induced microphase separation, where the mobility of the PEG_{1K} length in the composition enabled this behavior. The limited access of water to regions containing only PEG was believed to cause both drug retention and a slowdown in polymer erosion in these matrices. Drug-polymer interaction between DTE-co-DT segments of the polymer and voclosporin was also suspected to play a role in drug retention. *In vivo in vitro* correlation (IVIVC) values of 3 to 4 obtained from rabbit implantation studies implied that both drug release and polymer resorption would be enhanced if these carriers were placed within the human body. Select tyrosine-based polycarbonate terpolymer matrices were well tolerated in the sensitive regions of the rabbit's eye. An outcome of this research is the development of a polymer platform that can serve as an implantable medical device matrix to deliver drugs to patients for the treatment of chronic diseases and disorders of the eye.

Acknowledgements

I thank the following individuals for their assistance during my graduate studies. First, I would like to thank my mother, Ursula Khan, and father, Z. Lionel Khan (now deceased) and my sisters (especially Bernine Khan, Ph.D.) and brother, and friends (especially Elina Tzatzalos), for their continued emotional support during these past four years. I thank my advisor, Prof. Joachim Kohn, Ph.D., for his guidance and the opportunities he created for me to perform this work. I thank my committee members, Prof. Troy Shinbrot, Ph.D., Prof. David Shreiber, Ph.D., and Poonam Velagaleti, Ph.D. I acknowledge the invaluable assistance of Prof. Sanjeeva Murthy, Ph.D. (expertise in polymer physics), Carmine Iovine (project-related activities & expertise in polymers), Poonam Velagaleti, Ph.D. (project-related activities & expertise in pharmaceutical analytical methods), Prof. Steven Buyske, Ph.D. (expertise in statistics), and Prof. Das Bolikal, Ph.D. (polymer chemistry). In addition, I thank Matthew Laughland and Lulu Wang for their technical assistance on polymer synthesis and performance testing; Mehdi Ashraf-Khorassani, Ph.D., for his analytical services at Virginia Tech; Lux Biosciences Inc. for their financial support and project related activities; Brian Gilger, DVM, and the staff at NCSU Veterinary School for the animal work; Aurora Costache, Ph.D., for optimization of polymer-drug interaction using MOE; Tom Emge, Ph.D. (Rutgers X-ray Laboratory); William Heller, Ph.D., beamline scientist at ORNL; Steven Weigand, Ph.D., beamline scientist at APS; Bill Schneider and Eric Paduch at the Rutgers Physics Machine Shop; the office staff and professors at BME and NJCBM; and all Kohn group members (past and present).

Dedication

To my late father, Z. Lionel Khan

…generous in spirit, generous in resources, and generous in love

October 3, 1929 – February 6, 2008

Table of Contents

List of Tables

List of Figures

List of Abbreviations

Greek letters

β_i^*, β_{ij}^*, β_{ijk}^*	coefficients for polynomial terms (response surface analysis)
δ_{ij}	coefficient for polynomial term (response surface analysis)
λ	wavelength
η	predicted response
η_p	persistence factor
σ	distribution of interdomain spacing
θ	angle

Roman letters

A	$\exp[-q^2\sigma^2/2]$
ACN	acetonitrile
ANOVA	analysis of variance
API	active pharmaceutical ingredient
APS	Advanced Photon Source
AUC	area under curve
BHA	butylated hydroxyl anisole, or 2,5-di-tert-butyl-4-hydroxyanisole
BHT	butylated hydroxyl toluene, or 2,6-di-tert-butyl-4-methylphenol
C_{drug}	concentration of free drug (units: mass/volume)
Cs	drug solubility
CsA	cyclosporine A

$C_{polymer}$	polymer concentration in composite matrix (gram polymer/device volume)
CDS	central diffuse scattering
d	interdomain spacing (units: length)
D	drug diffusion coefficient (units: surface area/time)
DCM	dichloromethane, or methylene chloride
DMF	dimethyl formamide
DSC	differential scanning calorimetry
DT	deaminotyrosyl tyrosine ester carbonate
DTE	desaminotyrosyl tyrosine ethyl ester
DTM	desaminotyrosyl tyrosine methyl ester
DTR	desaminotyrosyl tyrosine alkyl ester
DT*t*Bu	tertiary-butyl desaminotyrosyl-tyrosine ester
ELSD	evaporative light scattering detector
f	function
FWHM	full width at half maximum
GLP	good laboratory practice
GPC	gel permeation chromatography
h	constant
HCl	hydrochloric acid
HFIR	high flux isotope reactor
HPLC	high performance liquid chromatography
HSD	honestly significant difference
I	intensity

I_0	intensity at q = 0 (ZP model)
I_{CDS}	intensity of central diffuse scattering at q = 0
IPA	isopropyl alcohol
IVIVC	*in vitro in vivo* correlation
k_1	early-stage drug diffusion rate coefficient
k_2	late-stage drug diffusion rate coefficient
k_{dis}	drug dissolution rate coefficient
k_S	coefficient of proportionality
KDR	kinetic drug release
LOD	limit of detection
logP	partition coefficient (water/octanol)
LOQ	limit of quantification
LSD	least significant difference
M_n	number average molecular weight
M_p	peak molecular weight
M_t	fractional drug release at time t
M_w	weight average molecular weight
MeOH	methanol
MW	molecular weight
n	sample size
N/A	not available
NaOH	sodium hydroxide
NMR	nuclear magnetic resonance

NZW	New Zealand White
NJCBM	New Jersey Center for Biomaterials
ORNL	Oak Ridge National Laboratory
p	probability
P(q)	elastic scattering function
PBS	phosphate buffered saline
PD	polydispersity (M_w/M_n)
PEG	polyethylene glycol
PEG_{1K}	polyethylene glycol, molecular weight 1,000 Da
PGA	poly(glycolic acid)
PLGA	poly(lactic acid-co-glycolic acid)
PLA	poly(lactic acid)
PLLA	poly(L-lactic acid)
POE	poly(ortho ester)
PVA	poly(vinyl alcohol)
q	scattering vector
q_{max}	value of q at maximum intensity
r	Pearson correlation coefficient
R	radius of phase separated domains
R_g	radius of gyration
S	drug mass bound per mass of polymer matrix (gram drug/gram polymer)
S(q)	structure factor
SANS	small angle neutron scattering

SAXS	small angle x-ray scattering
S.D.	standard deviation
SEM	scanning electron microscopy
t	time
T_g	glass transition temperature (units: °C)
T_m	melting point (units: °C)
T_p	processing temperature (units: °C)
TEM	transmission electron microscopy
TGA	thermogravimetric analysis
TFA	trifluoroacetic acid
TPGS	tocopheryl polyethylene glycol 1000 succinate
wt	weight
UV	ultraviolet
Vit C	Vitamin C, or L-ascorbic acid
Vit E	Vitamin E, or (±)-α-tocopherol
vol	volume
WAXS	wide angle x-ray scattering
x	spatial distance
x_i, x_j, x_k,	compositional mixture components
ZP	Zernike-Prins

Units

Å	angstroms
µl	microliters
µm	micrometers
kGy	kilogray (1 kGy = 0.1 Mrad)
M	Molar
MHz	megahertz
mg	milligrams
ml	milliliters
N	Normality

1 Introduction and background

1.1 Introduction

The goal of this work is to develop a customizable polymeric bioerodible carrier for the delivery of the hydrophobic peptide voclosporin from a library of L-tyrosine based polycarbonate polymers invented in the Kohn laboratory. This research will lay the groundwork for the development of a long-term implantable controlled drug delivery device suitable for ophthalmic applications. Voclosporin is a cyclic 11-amino acid peptide molecule which is a derivative of the immunosuppressant cyclosporine A, and is currently in clinical trials as a next-generation treatment for inflammatory diseases such uveitis, dry eye syndrome and blepharitis (1). Voclosporin, like its parent compound cyclosporine A, suppresses lymphocyte proliferation and T-cell activation by forming an active drug-cyclophilin complex that inhibits the enzyme calcineurin[1], but is 3-4 times more potent (2). This cyclic peptide molecule does not possess any significant three-dimensional conformational structure; there is only a short segment of beta sheet held in a rigid configuration by four intramolecular hydrogen bonds (3, 4). A majority of the amino acids that make up the peptide are either non-natural or are N-methylated, leaving only the N-H on amino acids 5, 2, 7 and 8 available to hydrogen bond with the C=O on amino acids 2, 5, 11 and 6, respectively. Overall, the molecule is extremely hydrophobic

[1] Calcineurin plays a vital role in T-cell development for host immunity.

and therefore sparingly soluble in aqueous media, but readily soluble in many organic solvents. The chemical structure of voclosporin is shown in Figure 1.1.

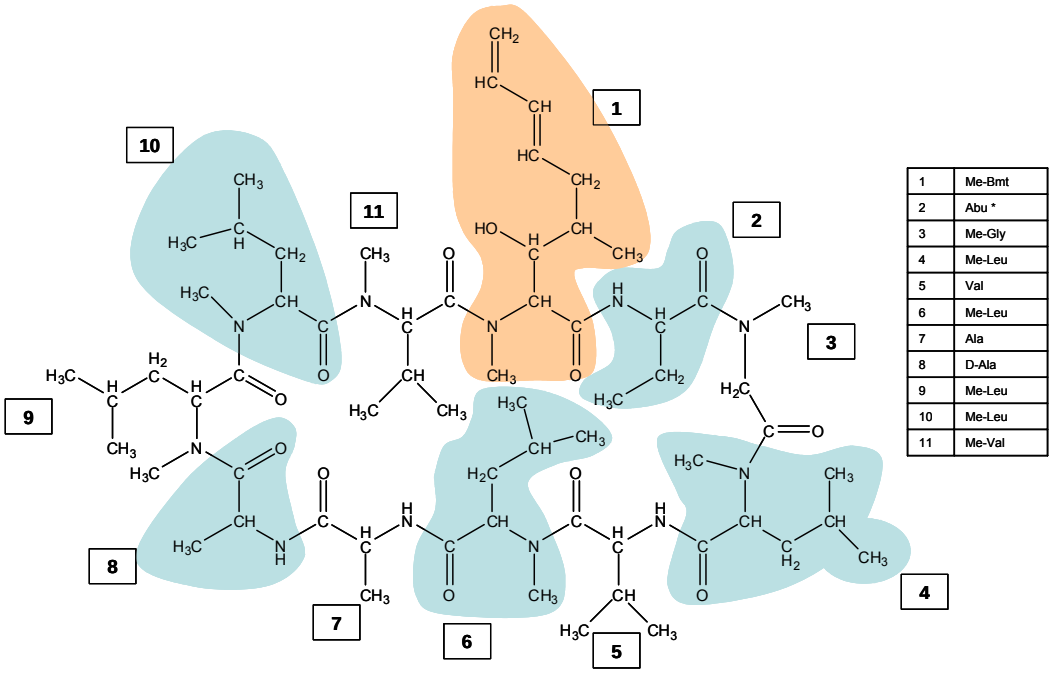

Figure 1.1. Chemical composition of voclosporin. Me-Bmt = (4R)-4-[(E)-2-butenyl]-4,N-dimethyl-L-threonine; Abu = α-aminobutyric acid.

The library of L-tyrosine based polymers used in this research consists of homo-, co- and terpolymers of poly(desaminotyrosyl-tyrosine alkyl ester carbonate), abbreviated as DTR, polymerized with polyethylene glycol (PEG) and/or desaminotyrosyl-tyrosine ester carbonate (DT). In this work, the alkyl groups R = M (methyl) and R = E (ethyl) are investigated. The main advantages of studying this family of bioresorbable polymers for ophthalmic applications is the ability to fine tune its chemical and physical properties to match the desired requirements of a suitable matrix for controlled drug delivery, and to use a material that generates biocompatible byproducts from polymer degradation that is

tolerable to the sensitive regions of the eye. The chemical structure of this class of polymers is shown in Figure 1.2.

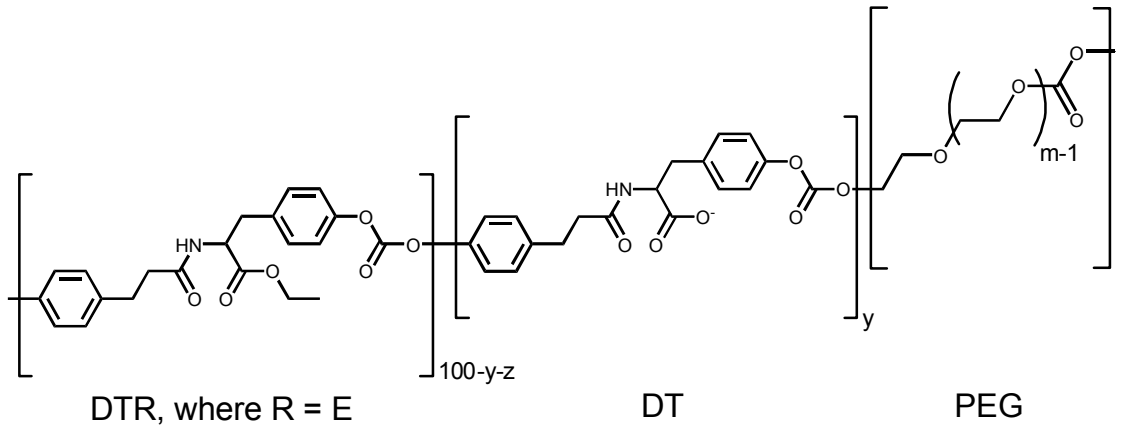

Figure 1.2. Chemical composition of poly(DTR-co-y% DT-co-z% PEG_{1K} carbonate), where 'R' = ethyl (E) as shown. DT segment has no 'R' pendant group, instead, it contains a carboxyl functional group (shown in figure in the ionized form COO^-). The polymer composition is a random distribution of the three monomers DTR, DT and PEG_{1K}.

The sustained local administration of therapeutic levels of the peptide voclosporin for the treatment of ocular diseases and disorders, while the matrix undergoes controlled bioresorption for a predetermined period, is a challenging task. In an attempt to achieve this goal, the following work was performed: (a) homo-, co- and terpolymers from the library of L-tyrosine polycarbonates were utilized as carriers for the drug voclosporin to understand how *in vitro* drug release and *in vitro* polymer erosion can be modulated as a function of the hydrated matrix composition, (b) the hydrated structure of homo-, co- and terpolymers of L-tyrosine polycarbonates was probed using neutron and x-ray scattering techniques to examine the changes in the interchain distance of polymer chains and the hydration-induced phase separation of PEG domains in order to understand how these

features affect drug release, (c) the effect of thermal and radiation exposure on the drug stability in the presence of PEG-containing polycarbonate terpolymers during device fabrication was investigated; the use of antioxidants were required to protect the drug during these operations, and (d) drug release and polymer erosion from sterile PEG-containing polycarbonate terpolymers were evaluated *in vivo* to determine the extent to which these polymeric systems behaved differently relative to *in vitro* conditions. The information contained within this body of work may provide a basic understanding of the utility of L-tyrosine based polycarbonates as a delivery platform for a range of other hydrophobic (or hydrophilic) peptides and small molecules for use in a wide range of tissue regeneration and drug delivery applications.

1.2 Clinical need

The treatment of ophthalmic inflammatory diseases and disorders is an active area of research. These disease states affect tens of millions of people worldwide. Within the United States, 3.2 million people are affected by dry-eye syndrome alone, and the number of these cases increases to approximately 30 million worldwide (5). Topical administration of drug-containing solutions, emulsions, gels and/or viscous ointments is generally the preferred method of treatment for front-of-the-eye diseases due to the ease of application (6, 7). However, the major disadvantage of topical administration is that drug cannot effectively penetrate the corneal layer, and the irrigation system of the eye rapidly washes out the drug. In order to improve drug bioavailability several ophthalmic delivery methods are available, such as iontophoresis (8), periocular injections (9) and the placement of drug-coated metallic devices into the conjunctival region of the eye (10).

Other less intrusive and less cumbersome approaches to localized ophthalmic drug delivery favors the use of implantable bioerodible polymeric carriers.

These carriers can be fabricated into many forms, such as films, rods, nano/microparticles and *in situ* forming gels. The implantation of these drug-loaded bioerodible matrices into the sublayer of the conjunctival region of the eye has several advantages (11, 12): (i) improved bioavailability of the drug, (ii) less systemic side effect of the drug due to localized dosing, (iii) controllable, sustained and accurate dosing of the patient, (iv) improvement in drug shelf life without the use of preservatives, (v) better patient compliance and (vi) solubilization and metabolism of the polymer byproducts that eliminate the need for surgical removal of the matrix after the drug is exhausted. Disadvantages include (i) the potential for "drug dumping" as matrix fragments, (ii) foreign-body sensation due to the presence of the implant (the eye is very sensitive) and (iii) the difficulty of removing an eroding implant in patients having an allergic reaction to the drug.

Given the fact that there is no commercially available biodegradable product for the long-term treatment of chronic inflammatory or infectious diseases of the eye, the current research will provide a viable solution to a problem that is long overdue.

1.3 Drug release from bioerodible polymers for ophthalmic applications

There are several examples of bioerodible polymeric matrices having potential use in ocular drug delivery, ranging from the commonly used biomaterials poly(L-lactic acid), PLLA, and poly(lactic acid-co-glycolic acid), PLGA (13), to more customized and novel materials. Albertsson, et al., incorporated the beta-blocker timolol maleate used to treat glaucoma in fast degrading poly(adipic anhydride) microspheres (14). These drug-

loaded particles, when incorporated into the *in situ* gelling polysaccharide Gelrite®, were designed to increase the precorneal residence time of a topical administration by several hours. Di Colo, et al., used physical blends of poly(ethylene oxide) with poly(methyacrylic acid-co-methyl methacrylate)-sodium to form mucoadhesive gels containing the antibiotic ofloxacin for treating ocular bacterial infections (15). The placement of this gel into the conjunctival space of the eye demonstrated drug release via an erosion-controlled behavior of the polymer carrier. Heller and coworkers designed poly(ortho esters) compositions to modulate the release of the antiproliferative agent 5-fluorouracil to prevent blockage of a trabeculectomy in glaucoma filtering surgery (16, 17). The potential route of administration for this carrier is via injection. Hamalainen, et al., used poly(vinyl methyl ether-maleic anhydride) to study the release of a variety of drug molecules, including a model peptide [D-Ala2]-leucine enkephalinamide, to demonstrate the feasibility of using a synthetic polymer to release proteins to the eye (18).

The examples above demonstrate a relatively short-term control of drug release. Additionally, it is important to realize that each drug had a unique association with its surrounding polymeric matrix, and it may not be possible to make a generalized statement regarding the drug release profile and other performance characteristics of the system.

1.4 Release of cyclosporine A from polymers

Cyclosporine A (CsA) and voclosporin are identical in chemical structure with the exception that voclosporin has a conjugated double bond within the first amino acid (refer to Figure 1.1). It is therefore reasonable to expect that most of the physiochemical

properties of both drugs would be similar. There is substantial literature on the controlled release of cyclosporine A from polymers, mainly PLLA and PLGA microparticles (19-22). Of particular note is the work of Gref, et al. (19), using microspheres composed of PLLA-PEG copolymers. In this study, the *in vitro* hydrolysis of the PLLA-PEG ester bond caused a 10 % loss of PEG from the matrix during the course of six weeks, resulting in an augmentation in CsA release. Other examples of cyclosporine in polymeric carriers include the fabrication of drug loaded microspheres from the biodegradable polymer polycaprolactone (23), the structurally-related family of novel degradable copolymers poly(terepthalate-co-phosphate) that modulated erosion and provided near zero order drug release for several weeks (24) and an episcleral drug-loaded implant composed of the non-degradable polymer silicone utilized by Lee, et al. (25), to rapidly deliver therapeutic dosage of the drug to the entire cornea at sufficient levels that could prevent allograft rejection after corneal surgery.

1.5 Benefits and limitations of tyrosine-based polycarbonate polymers

Several excellent reviews of synthetic and natural biodegradable polymeric biomaterials are given by Nair and Laurencin (26), Merkli, et al. (27), Coulembier, et al. (28), Okada (29), and Ray and Bousmina (30). These articles represent an extensive selection of matrix candidates having wide-ranging chemistry. The choice of a suitable polymer candidate was left to the experience of the researcher and the design requirements of the product of interest. In this work we investigate the family of tyrosine-based polycarbonates for use as a suitable ocular drug matrix material, specifically, the homo-, co- and terpolymers of poly(DTR-co-y%DT-co-z% PEG_{nK} carbonate) of which similar libraries of these biodegradable polymers have been studied

within the Kohn laboratory for the past fifteen years (31-35). These polymers contain three hydrolytically labile bonds: the carbonate bonds in the backbone of the chain, the ester bonds connecting pendant groups and the amide bonds in the backbone that can be cleaved *in vivo* by enzymes (32).

Some of the key benefits and limitations of this class of biodegradable tyrosine-based polycarbonate polymers are briefly described. Their advantages are (i) the breakdown products are naturally occurring substances that are non-toxic and easily metabolized in the human body, (ii) there is controlled degradation that occurs via hydrolysis of the ester or carbonate bonds (32, 33), (iii) the amide bond in the backbone is relatively stable towards enzymatic degradation for polymers exhibiting low water content (36), (iv) the acidity of the byproducts of degradation is not significant[2] when compared to the amounts observed in the widely used biodegradable polymers of PLLA, PLGA and their copolymers (37), and (v) the library of polymers presents a wide selection from which to choose a desired physical property, such as a low glass transition temperature (T_g) for thermal processing or a material having an amorphous/liquid crystalline-like behavior. The disadvantages of these polymers include (i) the bulk eroding nature can cause fragmentation of a degrading implant and (ii) the rate of mass loss may be low due to the limited aqueous solubility of the degraded byproducts.

Modifications of the chemical, physical and/or biological effect of the tyrosine-based polycarbonates can be performed in several ways. The incorporation of PEG into the main backbone chain of the polycarbonates was shown to decrease the hydrophobic nature of the polymer, to lower its glass transition temperature, to make the polymer more

---

[2] The work of Schachter (37) demonstrates less acidity from degradation byproducts of tyrosine-based polyarylates compared to PLGA.

flexible and to alter the adhesion of proteins and biological cells onto its surface (34, 38-41). The incorporation of carboxyl functionality at the pendant group site (obtained from polymer synthesis with monomers containing COOH groups; referred to as DT-containing monomer) decreased the hydrophobicity of the polymer and endowed the polymer with the potential for dissolution in an aqueous medium (32, 42). With these modifications, varying amounts of DT and/or PEG can add a dimension of tunability to the structure-property relationship for this class of polymers.

1.6 Mechanisms affecting drug release from polymer carriers

Understanding the interplay between the mechanisms of polymer erosion, polymer swelling and de-swelling, polymer-drug interaction, drug dissolution control and pure drug diffusion is a formidable task. These processes are important to consider when describing the release of the hydrophobic drug from the L-tyrosine based polycarbonate terpolymers. A comprehensive listing of potential factors influencing drug release from biodegradable polymers, as well as empirical and computational modeling of erodible systems, is given by Siepmann, et al., (43).

The erosion of degradable polymers is initiated by water uptake followed by chemical degradation of the polymer chains (typically by hydrolysis) leading to chain fragmentation, solubilization of oligomeric/monomeric byproducts and the mass transport of these species out of the matrix (44). Polymer erosion can have additional complexity, such as the lowering of the local pH that accelerate chemical degradation as observed with PLGA microspheres (45) or by the *in situ* changing composition of the polymer matrix as shown in this work.

Another key factor influencing polymer erosion is its hydrophobic/hydrophilic nature and the corresponding three-dimensional polymer chain structure. An example of the importance of polymer structure is given by Breitenbach, et al., (46). In this study the authors examined the erosion of microspheres composed of the hydrophilic poly(vinyl alcohol) backbone grafted with hydrophobic poly(lactic-co-glycolic acid), PVA-g-PLGA. They found that the PVA-g-PLGA matrix containing high molecular weight (MW) PLGA chains initially displayed negligible mass loss characterized by a lag phase that preceded a sigmoidal decay in polymer mass loss. This initial lag phase in erosion was absent in PVA-g-PLGA containing low MW PLGA due to the solubility of the short chain PLGA byproducts. Nuclear magnetic resonance (NMR) analysis of the polymer degradation byproducts indicated a selective chain scission site for high MW PVA-g-PLGA on the backbone of the PVA at the PLGA graft site, whereas for low MW PVA-g-PLGA chain scission was predominantly at the pendant PLGA. These findings demonstrated the importance of water accessibility within a three-dimensional polymer structure for the occurrence of hydrolysis.

Wan, et al., (47) studied the biphasic protein release from a set of poly(ortho ester)-polyethylene glycol-poly(ortho ester) (POE-PEG-POE) triblock polymers. This article presented two findings that are similar to the current work of voclosporin release from the polycarbonate terpolymers. These similarities include (i) a rapid loss in MW for these polymers within two weeks followed by a slow rate of MW degradation and (ii) an initial burst followed by a lag phase for drug release. The authors also speculated that selective PEG loss from the polymer matrix might have occurred.

Finally, a brief overview on the role of polymer-drug interaction is given. The association of proteins with polymers in solution (48-50) or the adsorption of proteins onto polymer surfaces may be explained by their electrostatic interactions, hydrogen bonding capability, hydrophobic interactions, hydration forces and/or van der Waals forces (51-53). Additional factors to consider include physical properties such as the polymer molecular weight and protein conformation, as well as environmental conditions such as pH, temperature and salt concentration (54, 55). With so many parameters it is difficult to predict how a peptide or protein molecule will be released from a polymeric carrier. Further complexity arises from the effects of processing conditions for device fabrication.

1.7 Modeling drug diffusion from degradable polymers

Several treatises for the mathematical modeling of diffusion, swelling and erosion controlled systems for drug delivery using biodegradable polymers exist in the literature [Arifin (56); Fan & Singh (57); Kanjickal (58)] and will not be repeated in this document. However, some useful approaches to modeling these degradable systems as it pertains to drug delivery are worth mentioning.

Batycky, et al., (59) provided an erosion model for drug-loaded PLGA microspheres where the main feature of the model was the formation and expansion of a porous network. An observed lag phase for drug release was described by drug entrapment within the polymer before the development of the matrix porosity. Drug release was modeled using desorption kinetics from an evolving polymer structure comprised of micro-, meso- and macropores. Lemaire, et al., (60) used a simplified modeling approach to porous network development (based on the work of Batycky) to

simulate the effects of diffusion and erosion on drug release kinetics. Recently, Kang, et al. (61), provided scanning electron microscopy (SEM) images as evidence of the dynamic nature of the porous structure in PLGA where they demonstrated the opening and closing of these pores.

Several researchers model the effect of erosion on drug release by using a diffusivity coefficient that is time-dependent. For example, Faisant, et al., (45) augmented pure diffusion with a term that accounted for the MW of the degrading polymer:

Eq. 1.1: $$D(MW) = D_0 + \frac{h}{MW(t)}$$

where D_0 is the pure diffusivity coefficient, 'h' is a constant, and MW(t) is the decreasing molecular weight that follows first order kinetics. Faisant, et al., (62) also used Monte Carlo simulations to estimate the matrix porosity and drug diffusivity in a degrading polymer.

He, et al., (63) used a model that accounted for a triphasic drug release profile, namely, an initial burst phase followed by an intermediate zero-order release phase, then a final second burst phase that was attributed to rapid polymer erosion. The model described the initial phase release by using an analytical solution to Fick's second law with the diffusion coefficient augmented by the rate of polymer chain scission. The near zero-order drug release was modeled as pure diffusion where D_o described the diffusivity in a non-degrading non-eroding polymer. The final burst was modeled using a mathematical description of fractional drug release (M_t) of the form,

Eq. 1.2:
$$M_t = \frac{\exp[f(t)]}{1+\exp[f(t)]}$$

that expressed the effect of polymer erosion. M_t increases exponentially when f(t) was small, and M_t approaches the asymptotic value of 1 when f(t) was large (or at infinity). The values for f(t) were always positive, i.e., f(t) > 0. The model gave an excellent fit of the experimental data for several bioerodible formulations such as the oligomers of D,L-lactic acid, poly(D,L-lactic acid) and poly(D,L-lactide-co-ε-caprolactone), but was not helpful in understanding the underlying mechanism for polymer erosion and drug release.

The mass balance equation for drug release from a matrix system as given by Grassi & Grassi (64) accounted for one-dimensional diffusion in a thin film, swelling of the polymer matrix due to water uptake and dissolution of a hydrophobic drug:

Eq. 1.3:
$$\frac{\partial C_{drug}}{\partial t} = \frac{\partial}{\partial x}\left(D\frac{\partial C_{drug}}{\partial x} - \frac{DC_{drug}}{\rho}\frac{\partial \rho}{\partial x}\right) + k_{dis}\left(C_s - C_{drug}\right)$$

Singh, et al. (65), described a model system that addressed both one-dimensional diffusion and net desorption of the drug that follow Langmuir equilibrium kinetics. The use of Langmuir kinetics required that irreversible adsorption of drug did not occur.

Eq. 1.4:
$$\frac{\partial C_{drug}}{\partial t} = D\frac{\partial^2 C_{drug}}{\partial x^2} - C_{polymer}\frac{\partial S}{\partial t}$$

Craig (66) reviewed work in the literature on erosion-controlled versus drug-controlled dissolution systems for solid dispersions of hydrophobic drugs within water-

soluble matrices. These systems may provide some assistance in modeling the controlled dissolution of voclosporin from the hydrophobic polycarbonate terpolymers. Other excellent reviews are given by Miller-Chou, et al. (67) on polymer dissolution models, by Costa, et al. (68) on the empirical modeling of drug release from polymers, and by Narasimhan (69) on mathematical models for drug release from dissolving polymeric systems. Treatises on modeling drug dissolution-limited systems can be found by Ayres & Lindstrom (70), Lindstrom & Ayes (71), Chandrasekaran, et al. (72), and Fan & Singh (57).

1.8 Scattering techniques to study of polymeric structure and chain mobility

Small angle neutron scattering (SANS) is a useful tool for measuring structural information on the order of 10 to 1,000 Å in polymers using deuterated water or by deuteration of the polymer as a contrast medium (73-75). An excellent generalized overview of the technique of SANS is given by Wignall, et. al. (76). Similarly, small angle x-ray scattering (SAXS) is useful tool for measuring structural information on the same length scale as SANS, except that water or radiolabeling is not used as a contrast medium. Instead, the contrast comes from the difference in electron density of the atoms making up the polymer structure, and this difference can be probed for the presence of microphase separated domains. Wide angle x-ray scattering (WAXS) can be used to measure the intrachain distances of polymers on the order of 10 Å, and is generally performed in conjunction with SAXS. These scattering techniques are complementary to each other, but are by no means the only available methods available. Transmission electron microscopy (TEM), solid state NMR, polarization microscopy and staining techniques are a few examples of other complementary techniques. An excellent

introductory treatment of the theory and applications of neutron and x-ray scattering in polymers is available in a textbook written by Roe (77). Key information from this book is repeated below in this manuscript to aid the reader in understanding the neutron and x-ray data presented in Chapter 4.

The signal detected by neutron and x-ray scattering is the intensity I(q), defined as

Eq. 1.5: $$I(q) \equiv \frac{d\Sigma}{d\Omega} = \frac{\text{scattered photon flux through a solid angle in a given direction}}{\text{incident photon flux}}$$

where $d\Sigma/d\Omega$ is the differential scattering cross section. The measured intensity I(q) is proportional to the summation of the electron density of atoms in the polymer chain for x-ray scattering, or is proportional to the amount of deuterated water detected in the sample for neutron scattering. The scattering vector, q, is the resultant vector of the incident and scattering vectors that is related to the structural features of interest in the polymer. The signals located at q are manifestations of an interference pattern, where q is dependant on the incident wavelength, λ, and the scattering angle 2θ by the relationship:

Eq. 1.6: $$q = \frac{4\pi \sin\theta}{\lambda}$$

It is customary to use q instead of 2θ since data collected as I(q) versus q can be compared across different equipment setups. Two critical requirements for these techniques are that (i) the scattering must be elastic (i.e., no energy transfer must occur between the incident photon and the electron or atom nuclei) so that the wavelength will

remain constant and (ii) the scattering must be coherent (i.e., no phase change in the traveling wave) so that interference can occur.

Examples of the use of SAXS/WAXS for detection of structural changes within a hydrated solid biodegradable polymer are given by King, et al., (78), with poly(glycolic acid) (PGA), by Noorsal, et al. (79), with poly(glycolide-co-trimethylene carbonate), and by Shekunov, et al. (80), with PEG hydrogels crosslinked with a urethane bond.

1.9 Organization of thesis

In this chapter an overview of the field of degradable polymers and drug delivery challenges was presented with many citations from the literature for a more in-depth treatment of the subject. A cursory introduction to the field of scattering techniques was also given. Within the remaining body of the thesis, data is presented from studies using the library of tyrosine-based polycarbonate polymers containing DT and/or PEG_{1K} that explored their utility as a suitable platform for the delivery of the hydrophobic peptide molecule voclosporin with a potential application for localized therapy for front-of-the-eye inflammatory diseases. Chapter 2 describes the materials and experimental methods used throughout the work. Chapter 3 presents the *in vitro* performance of selected polycarbonates in terms of their drug release and polymer erosion behavior and compares some of these characteristics to the well established family of biodegradable biomaterials, poly(lactic-co-glycolic acid). The morphology of the hydrated polycarbonates is addressed in Chapter 4 with a focus on examining the structural changes that occur within PEG-containing co- and polycarbonate terpolymers, and a proposed explanation is given for why drug release was difficult from these carriers after extended periods of hydration. Chapter 5 addresses the effect of the PEG-containing polycarbonates on the stability of

the drug during thermal and radiation exposure. This information becomes important in Chapter 6 for animal studies where data is presented on the *in vivo in vitro* correlation for drug release. The thesis ends in Chapter 7 with a discussion of the future potential of this work.

2 Materials and methods

This chapter describes the details of the materials and methods used throughout this work. The synthesis procedure of the tyrosine-based polycarbonates is given for reference only. Basic polymer characterization test methods using proton nuclear magnetic resonance spectroscopy (^{1}H-NMR) for chemical structure confirmation, gel permeation chromatography (GPC) for polymer molecular weight determination, thermogravimetic analysis for polymer decomposition temperature determination, and differential scanning calorimetry for polymer glass transition temperature (T_g) determination were performed for all polycarbonates. Procedural methods for evaluating the stability of the drug voclosporin after thermal and radiation exposure in the presence of these polymers are given. The use of antioxidants was required to protect the drug, and these methods are also outlined. Test article fabrication, *in vitro* performance test methods for polymer degradation, polymer mass loss and kinetic drug release (KDR) from polymers, as well as experimental mixture design methods are given. The resulting data obtained from these performance testing demonstrate the utility of these degradable polycarbonates to function as a drug delivery vehicle. Methods of examining the hydrated structure of these polymers using the scattering techniques of SANS, SAXS and WAXS provide a means to correlate the drug release behavior to the dynamics of the polymer structure. Lastly, methods for evaluating the *in vivo* performance of these polymers in a rabbit model are described.

2.1 Materials

2.1.1 Active pharmaceutical ingredient (API)

Voclosporin (Isotechnika Inc., Edmonton Alberta, Canada) lot numbers 1505673 / batch 11, 1505674 / batch 13, 187852 / batch 21, 187854 / batch 22 and 187855 / batch 23 were used for all studies. The API was stored in amber vials or other suitable light sensitive containers either at room temperature or in the refrigerators at -4 °C.

2.1.2 Reagents and chemicals

The monomers desaminotyrosyl tyrosine ethyl ester (DTE), desaminotyrosyl tyrosine methyl ester (DTM) and *tertiary*-butyl desaminotyrosyl-tyrosine ester (DT*t*Bu) were made by synthetic chemists at the New Jersey Center for Biomaterials (NJCBM) at Rutgers University using the procedure outlined by Hooper, et al. (36).

The following commercially available chemicals were purchased and used as received. Trifluoroacetic acid, 99 % (TFA), cat.# 139720025 from Acros Organics Inc., subsidiary of Thermo Fisher Scientific Inc., Morris Plains, NJ. N,N-dimethylformamide (DMF), cat.# DX1726 from EMD Chemicals Inc., Darmstadt, Germany. Bis(trichloromethyl) carbonate (triphosgene), cat.# 15217; and polyethylene glycol 1,000 (PEG_{1K}), cat.# 81190 from Fluka Chemie GmbH, Buchs, Switzerland. Acetonitrile, HPLC-grade (ACN), cat.# 34851; deuterium oxide, 99 %, cat.# 151882; Dulbecco's phosphate buffered saline (PBS), pH 7.4, cat.# D8537; phosphate buffered saline, pH 7.4, powdered form, cat.# P-3813; d^6-methyl sulfoxide (d^6-DMSO), cat.# 02621HE; water, HPLC-grade, cat.# 270733; and water with 0.1 % TFA , cat.# 576905 from Sigma-Aldrich Chemicals Inc. (St. Louis, MO). Sodium hydroxide (NaOH), 0.5N solution, cat.#

S-360 from Spectrum Chemicals Inc. (Gardena, CA). Dichloromethane (DCM), cat.# D143; hydrochloric acid (HCl), 12.1N, cat.# A144c; methanol (MeOH), HPLC-grade, cat.# A542; pyridine, ACS-grade, cat.# P368; and 2-propanol (IPA), cat.# A416 from Thermo Fisher Scientific Inc., Waltham, MA.

2.1.3 Polystyrene standards

The following polystyrene standards were used for calibration of the GPC system: polystyrene, Mp 523,000 (cat.# 2013-9001); polystyrene, Mp 204,500 (cat.# 2013-7001); polystyrene, Mp 96,000 (cat.# 2013-5001); polystyrene, Mp 30,230 (cat.# 2013-2001); and polystyrene, Mp 7,200 (cat.# 2012-8001) from Polymer Laboratories Inc., a subsidiary of Varian Inc. (Palo Alto, CA).

2.1.4 Tyrosine-based polycarbonates

All tyrosine-based polycarbonates were made by synthetic chemists at the NJCBM at Rutgers University via a condensation reaction using the procedure of Pesnell (81) with minor modifications. DCM was added to a reaction flask containing the varying amounts of the monomers desaminotyrosyl tyrosine alkyl ester (either DTE or DTM), DT*t*Bu and PEG_{1K} that depended on the desired final composition. Pyridine, a nucleophilic base, was added to the mixture to (i) promote the *in-situ* formation of phosgene from triphosgene and (ii) to neutralize hydrochloric acid formed during the reaction. The reaction mixture was stirred at room temperature during which time a solution of triphosgene in DCM was added dropwise over a period of 80 minutes. The mixture was stirred for an additional 30 minutes after complete addition of the triphosgene. TFA was added in volume equal to half of the reaction mixture for

deprotection of polymers containing DT*t*Bu, and the mixture was stirred for an additional 18 hours. The reaction was quenched with 0.2 M HCl and the polymer was washed three times with 0.2 M HCl. The resulting polymer was grounded in a 50/50 (vol./vol.) mixture of chilled IPA/deionized water, recovered by filtration and dried in a vacuum oven at 40°C. The polymers were further purified by preparing a 15% solution (wt./vol.) of polymer in DCM and precipitating the solution with a 50/50 (vol./vol.) mixture of IPA/MeOH. The purification step was repeated three times. The final purified solution was filtered using a 1μm glass fiber membrane filter (Acrodisc® 37 mm, cat.# 4524T, Pall Lifesciences Inc., Ann Arbor, MI), cast as a thin film into a Teflon® dish under a laminar flow hood, and left to dry under nitrogen gas for at least 48 hours at room temperature.

A shorthand notation for these polymers, Ryyzz(1K), will be used to designate polymer compositions, where the two digits 'yy' refer to the mole percent of DT and the two digits 'zz' refer to the mole percent of PEG_{1K}. The remaining composition is the mole percent of DTR, where R is either E (for ethyl) or M (for methyl). For polymer compositions with a notation such as E0304.5(1K), the decimal point indicates a fraction. For example, this polymer composition is described as having 3 % DT and 4.5 % PEG_{1K}, with the remaining composition being 92.5 % DTE.

2.1.5 Poly(DL-lactic acid-co-glycolic acid), PLGA

PLGA 50:50, molecular weight 40,000-75,000 (cat.# P2191), PLGA 75:25, molecular weight 66,000-107,000 (cat.# P1941) and PLGA 85:15 (cat.# 430471) were purchased from Sigma-Aldrich Chemicals Inc. (St. Louis, MO) and were used as received.

2.1.6 Antioxidants

The following antioxidants given in Table 2-1 were purchased from a commercial vendor and were used as received.

Table 2-1. List of commercially available antioxidants.

Chemical	Vendor	Catalog Number	Lot Number
2,6-di-*tert*-butyl-4-methylphenol (butylated hydroxyl toluene, BHT)	Sigma-Aldrich Chemical Inc.	B1378	058K0134
2,5-di-*tert*-butyl-4-hydroxyanisole (butylated hydroxyl anisole, BHA)	Sigma-Aldrich Chemical Inc.	44,732-3	S33693-098
(±)-α-tocopherol (Vitamin E)	Sigma-Aldrich Chemical Inc.	258024	038K3743
L-ascorbic acid (Vitamin C)	Sigma-Aldrich Chemical Inc.	255564	08627TH
Tocopheryl polyethylene glycol 1000 succinate (TPGS)	N/A	N/A	N/A

2.2 Experimental methods

2.2.1 Polymer chemical structure

The chemical structure of the polymer was determined by ^{1}H-NMR. A sample of approximately 20 mg was dissolved in 0.75 ml d^{6}-DSMO and analyzed on a Varian VNMRS 500 MHz machine (Varian Inc., Palo Alto, CA).

2.2.2 Polymer molecular weight

The molecular weight of the polymer was measured using a GPC system consisting of a Waters 717 Plus Autosampler, Waters 2414 Refractive Index Detector,

Waters 515 HPLC Pump, serial PLgel columns (5 μm beads; 10^4 Å and 10^2 Å pores size; 30 cm long; Polymer Laboratories Inc., subsidiary of Varian Inc., Palo Alto, CA), PLgel 5 μm guard column and Empower® 2 Software (Waters Inc., Milford, MA). The columns were operated at room temperature with DMF containing 0.1% TFA as the mobile phase at a flow rate of 0.8 ml/min. A sample of approximately 20 mg was dissolved in 1 ml DMF containing 0.1 % TFA and filtered with a 0.45 μm Teflon® filter (13mm diameter, cat.# 6766-1304, Whatman Inc., Florham Park, NJ). The TFA was added to neutralize any basic impurities in the DMF that would enhance polymer degradation. The injection volume was 20 μl and run time for the analysis was 25 minutes. Molecular weights were determined relative to polystyrene standards. The sample size (n) for each formulation was $n \geq 2$.

2.2.3 Polymer residual solvent and decomposition temperature

The total polymer residual solvent content and polymer decomposition temperature were measured using a Thermogravimetric Analyzer (TGA) Model TGA/SDTA851e with STARe software version 19.10 (Mettler-Toledo Inc., Columbus, OH) or similar equipment. A sample of approximately 10 mg was heated from 25 to 400 °C at a rate of 10 °C per minute.

2.2.4 Glass transition temperature of polymer

The glass transition temperature (T_g) of the polymer was measured using a Differential Scanning Calorimeter (DSC) Model DSC 823e (Mettler-Toledo Inc., Columbus, OH) or similar equipment. A sample of approximately 5 to 15 mg was heated from -50 to 200 °C at a rate of 10 °C per minute, and then kept at 200 °C for 5 minutes to

erase the thermal history of the polymer (first heat cycle). The sample was cooled and then heated again from -50 °C to 200 °C at a rate of 10 °C per minute (second heat cycle).

2.2.5 Heat stability of voclosporin in polymer

The thermal stability of voclosporin in the presence of the following seven polymers was investigated: M1218(1K), M1420(1K), M1224(1K), E1218(1K), E1420(1K), E1224(1K) and 1:1 blend of E1224(1K)+PLGA 50:50. Test samples were prepared by dissolving 8.5 parts of polymer to 1.5 parts of voclosporin (by weight) in DCM, then casting into a Teflon® dish as a thin film. The drug loaded films were left to dry under nitrogen gas in a laminar flow hood at room temperature for a minimum of 48 hours.

Test samples (approximately 10 mg) were accurately weighed before heat treatment and placed separately into 8 ml amber glass vials. The vials were then immersed into a hot oil bath that was maintained at the desired temperature. All drug-loaded samples were heat treated in triplicate at 60 °C, 100 °C and 130 °C for times of 30 minutes and 180 minutes. Control samples were comprised of (1) polymers with no API that were used to determine if there were any interference peaks during thermal decomposition, (2) API only that was used to measure the effect of thermal exposure on drug in the absence of polymer and (3) non heat-treated samples that were kept at room temperature.

Test solutions were prepared for high performance liquid chromatography (HPLC) analysis by dissolving each sample in 1 ml of DCM for a minimum of 1 hour, followed by the addition of 6.5 ml of MeOH. An aliquot of 200 µl of the solution was

diluted in 1800 µl of ACN:water (50:50, by vol.) and was tested using the HPLC method given in Section 2.2.12.

2.2.6 Heat stability of voclosporin in polymer with antioxidants

The thermal stability of voclosporin in M1224(1K) in the presence of the following five antioxidants was investigated: BHT, BHA, Vitamin E, Vitamin C and TPGS. Sample preparation and analysis was the same as Section 2.2.5 with the following exceptions: (1) antioxidant levels of 0.1 % and 1 % per weight of polymer was added to the formulation prior to solvent casting, (2) Vitamin C is water soluble and was therefore dissolved in 1:1 water:MeOH (vol./vol.) prior to addition to the drug-polymer mixture, (3) a heat treatment schedule of 100 °C for 60 and 180 minutes was used and (4) the linear gradient for mobile phases A and B for HPLC was changed to account for each antioxidant (refer to Table 2-2).

2.2.7 Gamma radiation stability of voclosporin in polymer

Test samples were prepared as given in Section 2.2.18. Packaging and sterilization was performed as given in Section 2.2.20. These samples were from the same sterilization lot as the rabbit subcutaneous study. Control samples were comprised of (1) API only that was used to measure the effect of radiation exposure on drug in the absence of polymer and (2) non-sterile samples that were kept at room temperature.

Test solutions were prepared for HPLC analysis by dissolving each sample in 1 ml of DCM for a minimum of 1 hour, followed by an addition of 6.5 ml of MeOH. An aliquot of 200 µl of the solution was diluted in 1800 µl of ACN:HPLC-grade water (50:50, by vol.) and was tested using the HPLC method given in Section 2.2.12.

Table 2-2. HPLC linear gradient method for detection of antioxidants used in polycarbonates.

Antioxidant	HPLC linear gradient method
BHT	0 min: 50 % A and 50 % B; 3 min: 35 % A and 65 % B; 4 min: 35 % A and 65 % B; 6 min: 30 % A and 70 % B; 6.5 min: 0 % A and 100 % B; 12 min: 0 % A and 100 % B; 13 min: 50 % A and 50 % B.
BHA	0 min: 40 % A and 60 % B; 0.5 min: 40 % A and 60 % B; 5 min: 25 % A and 75 % B; 6 min: 0 % A and 100 % B; 11 min: 0 % A and 100 % B; 12 min: 40 % A and 60 % B.
Vitamin E	0 min: 30 % A and 70 % B; 7.5 min: 25 % A and 75 % B; 8 min: 0 % A and 100 % B; 11 min: 0 % A and 100 % B; 12 min: 30 % A and 70 %B.
Vitamin C	0 min: 65 % A and 35 % B; 2 min: 65 % A and 35 % B; 2.5 min: 30 % A and 70 % B; 7 min: 30 % A and 70 % B; 7.5 min: 0 % A and 100 % B; 13 min: 0 % A and 100 % B; 65 min: 35 % A and 50 % B.
TPGS	0 min: 30 % A and 70 % B; 3 min: 30 % A and 70 % B; 4 min: 15 % A and 85 % B; 9 min: 15 % A and 85 % B; 10 min: 30 % A and 70 % B.

2.2.8 Gamma radiation stability of voclosporin in polymer with antioxidants

The gamma radiation stability of voclosporin in M1224(1K) in the presence of the following five antioxidants was investigated: BHT, BHA, Vitamin E, Vitamin C and TPGS. Test samples were prepared by dissolving 8.5 parts of polymer to 1.5 parts of voclosporin (by weight) in DCM. Antioxidant levels of 0.1 % and 1 % per weight of polymer were added to the formulation prior to solvent casting. Since Vitamin C is water soluble, it required a slight modification in preparation by first dissolving in 1:1 water:MeOH (vol./vol.) prior to addition to the drug-polymer mixture. All formulations were cast into a Teflon® dish as a thin film. The drug loaded films were left to dry under nitrogen gas in a laminar flow hood at room temperature for a minimum of 48 hours.

Samples were individually packaged in ziplock bags and sent to Sterigenics Inc. (Charlotte, NC) for gamma sterilization. A sterilization dose of 22 kGy ± 10 % was determined by Sterigenics Inc. from bioburden (aerobes and fungi) testing of the devices. Minimum and maximum gamma radiation doses were recorded at 21.1 and 23.4 kGy, respectively. Non-sterile samples were packaged in ziplock bags and kept at room temperature in the laboratory.

Test solutions were prepared for HPLC analysis by dissolving each sample in 1 ml of DCM for a minimum of 1 hour, followed by an addition of 6.5 ml of MeOH. An aliquot of 200 µl of the solution was diluted in 1800 µl of ACN:water (50:50, by vol.) and was tested using the HPLC method given in Section 2.2.12 with the exception of the linear gradient for mobile phases. The linear gradient for mobile phases A and B for HPLC analysis of each antioxidant is given in Table 2-2.

2.2.9 Compression molding of polymer

For drug loaded samples, a mixture of 'a' parts of polymer to 'b' parts of voclosporin (by weight) was dissolved in DCM to make a 5 to 20 % (wt./vol.) solution. For placebo samples, the polymer was dissolved in DCM to make a 5 to 20 % (wt./vol.) solution. The solution was cast into a Teflon® dish as a thin film and left to evaporate under nitrogen gas in a laminar flow hood at room temperature for a minimum of 48 hours. The dried drug-loaded film was placed between stainless steel plates lined with Reynolds® parchment paper (Alcoa Consumer Products Inc., Richmond, VA) and spaced apart by custom stainless steel shims 'c' mm thick. The plates were placed between the platens of a Carver Press (model 4122, Carver Inc., Wabash, IN) that was heated to a processing temperature, T_p. The sequential steps of the compression molding process

were: (1) heat soaked at T_p with no pressure for 2 minutes, (2) slow ramp up of the pressure from 0 to 15,000 lbs over 1.5 minutes, (3) constant pressure at 15,000 lbs for 0.5 minutes and (4) slow decrease of the pressure from 15,000 lbs to zero over 1 minute. All steps were performed at constant temperature T_p.

2.2.10 Fabrication of test samples for *in vitro* performance testing

Compression molded films (placebo and API) were prepared according to Section 2.2.9 with the parameters 'a' = 7 parts, 'b' = 3 parts, 'c' = 0.18 mm and a processing temperature, T_p, as given in Table 2-3, unless stated otherwise. Test articles were made by punching 6 mm disks from the compression molded film. The thickness and weight of each sample were recorded.

Table 2-3. Process parameters for compression molding polymer film with and without API.

Polymer composition	Process temperature, T_p (°C)	Polymer composition	Process temperature, T_p (°C)
E0000(1K)	130	poly(DT carbonate)	130
E1200(1K)	130	poly(PEG_{1K} carbonate)	60
E0018(1K)	60	M1218(1K)	70
E1218(1K)	60-70	M1420(1K)	70
E0400(1K)	130	M1224(1K)	80
E0800(1K)	130	E1818(1K)	70
E0006(1K)	100	E2418(1K)	70
E0012(1K)	85	E4018(1K)	70
E1206(1K)	100	E6018(1K)	70
E1212(1K)	85	E1420(1K)	70
E0418(1K)	60	E1224(1K)	70
E0818(1K)	60	E1230(1K)	60
E0304.5(1K)	100	PLGA 50:50	90
E0904.5(1K)	100	PLGA 75:25	90
E0313.5(1K)	70	PLGA 85:15	90
E0913.5(1K)	70		
E0609(1K)	85		

2.2.11 *In vitro* polymer degradation

Each polymer sample with or without API was cut from compression molded film (refer to Section 2.2.9 for thermal processing method). Each sample of approximately 20 to 40 mg was immersed in 20 ml PBS at pH 7.4 and 37 °C. The PBS solution was changed weekly. At various time points, duplicate samples were removed from the PBS and blotted dry, then stored frozen at -20 °C. The samples were analyzed for molecular weight using the GPC method outlined in Section 2.2.2.

2.2.12 *In vitro* kinetic drug release (KDR) testing

Each drug-loaded disk contained within a Teflon® mesh basket was inserted into a 40 ml amber vial with PBS at pH 7.4 and incubated in a shaking water bath (model SW22, Julabo Inc., Vista, CA) at 37 °C. The volume of PBS was adjusted and recorded throughout the study to ensure that sink conditions were maintained. At various time intervals each mesh basket containing the sample was lifted from its vial and blown with nitrogen gas to remove solution droplets from the basket back into the vial. The basket was then rinsed with tap distilled water, blotted dry, transferred into fresh pre-warmed PBS in a clean vial and placed back into the shaking water bath at 37 °C. An equal volume of ACN was added to the remaining drug elutant solution to dissolve any drug from the walls of the glass vial prior to analysis.

The sample mixture was analyzed on an HPLC system consisting of a Waters Separations Alliance 2695 Module, Waters 2487 Dual λ Absorbance Ultraviolet (UV) Detector and Empower Pro® Software (Waters Inc., Milford, MA). The column was a Perkin-Elmer Pecosphere C18 (33x4.6mm; 3μm particle size; cat.# 0258-1064, Waltham,

MA). The mobile phase A was water with 0.1 % TFA and mobile phase B was ACN with 0.1 % TFA. The column was operated at 60 ± 1 °C at a flow rate of 0.8 ml/min using a linear gradient of A and B (0 min: 30 % A and 70 % B; 7.5 min: 25 % A and 75 % B). The sample injection volume was 100 µl and the drug was detected at 210 nm. External drug standards of 1, 10 and 50 µg/ml of ACN:PBS (50:50, by vol.) and a blank (ACN:PBS, 50:50, by vol.) were run along with the unknown test sample concentrations. The limit of quantification (LOQ) and limit of detection (LOD) for the determination of voclosporin quantity using HPLC were measured at 25 ng/ml and 6.3 ng/ml, respectively. The sample size (n) for each drug-loaded polymer formulation was n = 3.

2.2.13 *In vitro* polymer erosion testing

The drug-loaded sample contained within a Teflon® mesh basket was inserted into a 40 ml amber vial with 5 ml PBS at pH 7.4 and placed into an incubator oven (cat.# 31746, Precision Scientific Inc., Chicago, IL) at 37 °C. At various time intervals each mesh basket containing the sample was lifted from its vial and blown with nitrogen gas to remove solution droplets from the basket back into the vial. The basket was then rinsed with tap distilled water, blotted dry, transferred into fresh pre-warmed PBS in a clean vial and placed back into the incubator at 37 °C.

The test sample mixture was prepared by adding 150 µl of 0.1 N sodium hydroxide solution to the elutant solution and incubated for 4 hours at room temperature, followed by the addition of 384 µl of 0.5N hydrochloric acid and incubation for 30 minutes at room temperature. The mixture was frozen, then lyophilized in a Labconco FreeZone 2.5 lyophilizer (Labconco Inc., Kansas City, MO) operating at -45 ± 5 °C and <

0.1 millibar. The lyophilized powder was reconstituted in 1 ml of a solvent mixture containing ACN: water:MeOH (25:50:25, by vol.), then filtered using a 0.45 μm Teflon® filter. The base treatment converted all solubilized oligomers into desaminotyrosyl tyrosine ester (DT) monomer and PEG_{1K} monomer, and the acid treatment was used to neutralize the base. The destruction of voclosporin using this method was not important.

The test sample mixture was analyzed on an HPLC system consisting of a Waters Separations Alliance 2695 Module, Waters 2487 Dual λ Absorbance Ultraviolet (UV) Detector, Sedex Evaporative Light Scattering Detector, ELSD, Model 75 (Sedere Inc, Cedex, France) and Empower Pro® Software (Waters Inc., Milford, MA). The column was a Perkin-Elmer Pecosphere C18 (33x4.6mm; 3μm particle size). The mobile phase A was water with 0.1 % TFA and mobile phase B was ACN with 0.1 % TFA. The column was operated at 25 ± 1 °C at a flow rate of 0.8 ml/min using a linear gradient of A and B (0 min: 95 % A and 5 % B; 15 min: 60 % A and 40 % B; 16 min: 50 % A and 50 % B; 17 min: 5 % A and 95 % B; 20 min: 5 % A and 95 % B; 21 min: 95 % A and 5 % B). The sample injection volume was 60 μl. The DT monomer was detected at 220 nm with the UV Detector and the PEG_{1K} was detected with the ELSD. The ELSD was set at a temperature of 40 °C, pressure of 3.3 bar and a gain of 9. External DT monomer standards of 12.5, 125 and 200 μg/ml in ACN:water:MeOH (25:50:25, by vol.), external PEG_{1K} standards of 50, 125, 250, 450 and 625 μg/ml in ACN:water:MeOH (25:50:25, by vol.) and a blank (ACN:water:MeOH, 25:50:25, by vol.) were run along with the unknown test sample concentrations. The sample size (n) for each drug-loaded polymer formulation was n = 3.

2.2.14 SANS analysis of hydrated polycarbonates with and without API

Compression molded films (placebo and API) were prepared according to Section 2.2.10 with the exception that the disks were punched at 11 mm diameter. Test specimens were incubated in deuterated PBS (PBS powder consisting of sodium chloride and potassium chloride dissolved in deuterium oxide to make a 0.01M solution at pH 7.4) for various times of 1, 2, 25 and 60 hours and temperatures of 22, 37 and 47 °C prior to SANS analysis. Each hydrated sample was stacked inside a custom made quartz cell (fused quartz discs, 1/2 inch diameter x 1/16 inch thick, Quartz Plus Inc., Brookline, NH) and neutron scattering data was collected at the SANS1 CNG2 beam line (Oak Ridge National Laboratories, ORNL, Oak Ridge, TN) at a wavelength of 4.766 Å and a sample-to-detector distance of 8.65 meters over a q-range of 0.007 to 0.154 $Å^{-1}$. Exposure time per sample for data collection ranged from 20-1200 seconds. An air blank (empty cell) was run for background subtraction.

2.2.15 SAXS/WAXS analysis of hydrated polymers with and without API

Compression molded films (placebo and API) were prepared according to Section 2.2.9 with the parameters ‘a’ = 7 parts, ‘b’ = 3 parts, ‘c’ = 0.5 mm and a processing temperature, T_p, as given in Table 2-3. Test articles were made by punching 6 mm disks from the compression molded film. Test specimens were incubated in PBS at pH 7.4 and 37 °C for 1, 4 and 7 weeks. Each hydrated sample was stacked inside a custom made aluminum holder (1 mm thick) with 0.3 mil (8 μm) thick Kapton® (cat.# 3511, Spex CertiPrep Inc., Metuchen, NJ) windows. X-ray scattering data was collected at the 5ID-D enclosure at the Advanced Photon Source (APS, Argonne National Laboratory, Argonne, IL) in transmission mode at room temperature with a wavelength of 1.0332 Å

and a beam size of 0.2 x 0.2 mm. WAXS data was collected by a 100 x 200 mm CCD camera (NTE/CCD-1340/1300E CCD module, Princeton Instruments, Inc., Trenton, NJ) with a sample-to-detector distance of 0.23 meters and q range of 0.43 to 3.21 $Å^{-1}$. SAXS data was simultaneously collected by a 100 x 100 mm CCD camera (NTE/CCD-1340/1300E CCD module, Princeton Instruments, Inc., Trenton, NJ) with a sample-to-detector distance of 2.897 meters and q range of 0.006 to 0.160 $Å^{-1}$. Dark frame, distortion and flat-field correction were performed at APS using FIT2D software (A. Hammersley, ESRF, France; (82)). Exposure time per sample for data collection ranged from 0.1 to 12 seconds. An air blank (empty cell) was run for background subtraction.

2.2.16 SAXS analysis of phase separated polycarbonates

Compression molded drug loaded films were prepared according to Section 2.2.10. Test articles were punched into 11 mm disks from the compression molded film, then individually placed into 20 ml of PBS at pH 7.4 in a glass vial and incubated at 37 °C for 2.5 and 25 days. The PBS solution was changed at regularly (at least every three days). At the desired time point, the buffer was decanted from the vial, and each sample was washed four times in deionized water. The wet polymer matrix was frozen at -20 °C in the freezer, then dried by lyophilization in a Labconco FreeZone 2.5 lyophilizer. All samples were stored under dry conditions in a moisture-proof sealable bag until analyzed by SAXS. The test samples were E0800(1K), E1200(1K), E0012(1K), E0018(1K), E0609(1K), E1206(1K), E1212(1K) and E1218(1K). The PEG-containing co- and terpolymers were chosen since their early-to-late stage transition for drug release was less than 25 days (refer to Table 8-4 in the Appendix). The DTE-co-DT copolymers were chosen as control samples. SAXS analysis was performed at the APS using a similar

setup as described in Section 2.2.15, using a wavelength of 0.7293 Å, a sample-to-detector distance of 4.575 meters, an exposure time of 2 seconds and a q range of 0.006 to 0.160 $Å^{-1}$.

2.2.17 WAXS analysis of dry E1818(1K) drug-loaded polymers

Compression molded films (placebo and API) were prepared according to Section 2.2.9 with the parameters given in Table 2-4. Dry films were cut and stacked to fit inside a custom aluminum holder (1 mm thick) with a 0.3 mil (8 μm) thick Kapton® (cat.# 3511, Spex CertiPrep Inc., Metuchen, NJ) windows. X-ray scans of the sample were performed at room temperature using a Rigaku Geigerflex and D/max-B diffractometer (Rigaku Denki Corp., Japan), in reflection mode using a CuKα source with wavelength of 1.5418 Å with a 2θ range of 5 to 55 degrees (corresponding q-range was 0.35 to 3.76 $Å^{-1}$). A parallel beam was produced from a focusing multilayer crystal with dimensions of 1 mm x 18 mm. Exposure time per sample for data collection was approximately two hours. An air blank (empty cell) was run for background subtraction.

Table 2-4. Process parameters for compression molding E1818(1K) film with and without API for WAXS analysis.

Polymer-drug composition	'a' parts of polymer	'b' parts of voclosporin	'c' shim thickness (mm)	T_p (°C)
E1818(1K)	1	0	0.5	70
E1818(1K) + 10 wt. % drug	9	1	0.2	60
E1818(1K) + 30 wt. % drug	7	3	0.5	70
E1818(1K) + 50 wt. % drug	1	1	0.2	60-70
E1818(1K) + 60 wt. % drug	6	4	0.2	60-70
E1818(1K) + 70 wt. % drug	7	3	0.2	70
E1818(1K) + 80 wt. % drug	8	2	0.2	70

2.2.18 Fabrication of test samples for rabbit subcutaneous study

Compression molded films (placebo and API) were prepared according to Section 2.2.9 with the parameters 'a' = 8.5 parts, 'b' = 1.5 parts, 'c' = 0.36 mm and a processing temperature, T_p, as given in Table 2-5. Test articles were made by punching 6 mm disks from the molded film. The thickness and weight of each sample was recorded.

Table 2-5. Process temperatures for compression molding film with and without API for rabbit subcutaneous study.

Polymer composition	Processing temperature, T_p (°C)
M1218(1K)	70
M1420(1K)	80
M1224(1K)	80
E1218(1K)	70
E1420(1K)	70
E1224(1K)	70
1:1 blend of E1224(1K)+PLGA 50:50	80
PLGA 75:25	90

2.2.19 Fabrication of test samples for rabbit episcleral study

Compression molded films (API only) were prepared according to Section 2.2.9 with the parameters 'a' = 8.5 parts, 'b' = 1.5 parts, 'c' = 0.36 mm and a T_p of 70 °C, and the following exceptions: (i) Vitamin E was added to the mixture at 1 wt. % (per weight of polymer) and (ii) two polymer formulations were used: E1218(1K) and a 1:2 blend (wt./wt.) of E1224(1K)+PLGA 50:50. Test articles were made by punching with an oblong-shaped custom die with dimensions of 2 mm wide x 15 mm long. The thickness and weight of each sample was recorded.

2.2.20 Packaging and sterilization of test samples for animal studies

Individual test samples were placed inside a 0.5 ml Eppendorf amber tube and purged with nitrogen prior to capping. Each tube was sealed inside a labeled tyvek pouch. All samples were sent to Sterigenics Inc. (Charlotte, NC) for gamma sterilization. A sterilization dose of 22 kGy ± 10 % was determined by Sterigenics Inc. from bioburden (aerobes and fungi) testing. Minimum and maximum gamma radiation doses were recorded at 20.8 and 21.8 kGy, respectively, for devices used in the rabbit subcutaneous study. Minimum and maximum gamma radiation doses were recorded at 21.0 and 21.5 kGy, respectively, for devices used in the rabbit episcleral study.

2.2.21 Rabbit subcutaneous implantation and explantation of test articles

Subcutaneous sample implantation, animal husbandry, sample explantation, and histopathology were performed at the Ophthalmic Research Laboratory, College of Veterinary Medicine at North Carolina State University (NCSU), in the laboratory of Professor Brian Gilger. A total of 18 healthy female New Zealand White (NZW) rabbits were used to implant sterile samples subcutaneously between the shoulder blades of the animals. Each animal received 12 implants where each of four replicate test samples were placed within individual pockets along a row in the back of the animal, as shown in Figure 2.1. The forth row was used as a control site having an incision only but no implant. Test samples consisted of the eight polymers listed previously in Section 2.2.18 without drug (placebo) and containing 15 wt. % voclosporin.

Samples were explanted at 4, 10 and 20 weeks. Polymer resorption was evaluated by visual observation of the explanted device. For each polymer set, the excised tissue containing each sample (three replicates) was individually placed into an eppendorf tube

and frozen at -20 °C, then shipped in dry ice to the NJCBM at Rutgers University for analysis of drug content. The fourth replicate was submitted for histopathology work (H&E staining) at NCSU.

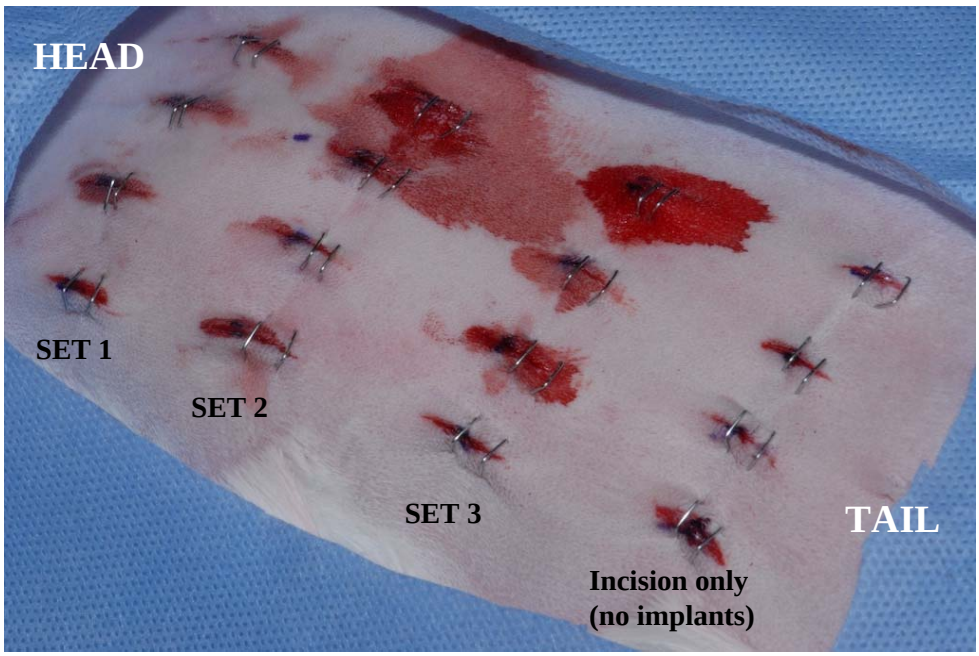

Figure 2.1. Layout for subcutaneous implantation of test samples in rabbit. Photo courtesy of Professor Brian Gilger, College of Veterinary Medicine, NCSU.

Frozen explanted samples (both drug-loaded and placebo polymers) were thawed and each polymeric sample was exposed by cutting open the surrounding tissue with a sharp razor blade. Each sample (tissue and polymer) was placed into individual amber glass vials. To each sample, 0.5 ml of DCM was added to dissolve the polymer for at least one hour. A volume of 3.25 ml of MeOH was then added to each vial at room temperature to extract drug from the excised tissue and polymer.

For HPLC analysis, a 200 µl aliquot of the extract was mixed with 1800 µl of ACN:water (50:50, by vol.), then filtered using a 0.45 µm Teflon® filter. All parameters

for the HPLC were the same as given in Section 2.2.12, with the exception of the linear gradient of mobile phases A and B. The gradient was changed to minimize the overlap of the retention times for proteins from the tissue and the peptide voclosporin. The linear gradient of A and B was 0 min: 50 % A and 50 % B; 1 min: 50 % A and 50 % B; 3 min: 39 % A and 61 % B; 8 min: 38 % A and 62 % B; 9 min: 25 % A and 75 % B; 10 min: 0 % A and 100 % B; 11 min: 50 % A and 50 % B.

2.2.22 Rabbit episcleral implantation and explantation of test articles

Episcleral device implantation, animal husbandry, test article explantation and histopathology were performed at the Ophthalmic Research Laboratory, College of Veterinary Medicine at NCSU, in the laboratory of Professor Brian Gilger. A total of 24 healthy female NZW rabbits were used to implant sterile devices under the superior conjunctiva approximately 5 mm proximal to the limbus in both eyes (refer to Figure 2.2(B)). Each animal received 1 implant (single dose) in the left eye and 3 implants (3X dose) in the right eye. Four animal replicates were used per polymer configuration and animals were euthanized at two time points. Test devices consisted of the two formulations: (a) E1218(1K) containing 15 wt.% voclosporin and 1 wt. % (per weight of polymer) of Vitamin E and (b) a 1:2 blend of E1224(1K)+PLGA 50:50 containing 15 wt. % voclosporin and 1 wt. % (per weight of polymer) of Vitamin E.

Excised tissue containing explanted devices at 4 and 11 weeks were individually placed into an eppendorf tube and frozen at -20 °C, then shipped in dry ice to the NJCBM at Rutgers University for analysis of drug content. Ocular tissue samples containing released voclosporin were sent to Virginia Tech for analysis of drug content. Histopathology work (H&E staining) was performed at NCSU.

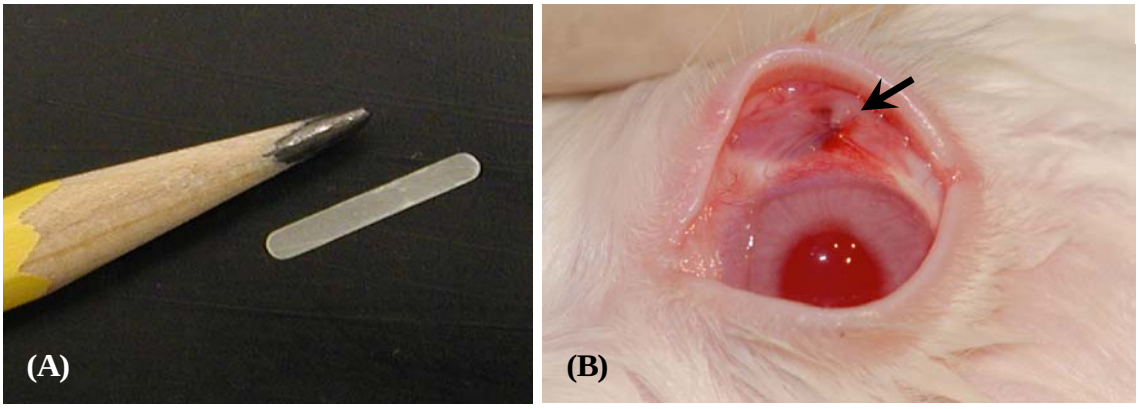

Figure 2.2. Episcleral implantation of drug-loaded polymeric devices in rabbit: (A) Tyrosine-based polycarbonate terpolymer carrier: 2 mm wide x 15 mm long x 0.5 mm thick and (B) Location of implant in dorsal conjunctival region; photo courtesy of Professor Brian Gilger, College of Veterinary Medicine, NCSU.

For drug content analysis in the explanted device, the frozen samples were lyophilized for a minimum of 24 hours. Each dried sample was individually placed into an amber glass vial and was grounded as much as possible using a glass stirring rod. A volume of 0.5 ml of DCM was added to each vial and was left for eight hours at room temperature to dissolve the polymer in tissue. A volume of 4.5 ml of MeOH was then added to each vial, and the drug was extracted overnight at room temperature.

For HPLC analysis, a 200 µl aliquot of the extract was mixed with 1800 µl of ACN:water (50:50, by vol.), then filtered using a 0.45 µm Teflon® filter. All parameters for the HPLC were the same as given in Section 2.2.12, with the exception of the linear gradient of mobile phases A and B. The gradient was changed to minimize the overlap of the retention times for proteins from the tissue and the peptide voclosporin. The linear gradient of A and B was 0 min: 50 % A and 50 % B; 1 min: 50 % A and 50 % B; 15 min: 38 % A and 62 % B; 16 min: 25 % A and 75 % B; 17 min: 0 % A and 100 % B; 20 min: 0 % A and 100 % B; 22 min: 50 % A and 50 % B.

2.3 Screening mixture design for polycarbonate polymers

Response surface methodology was used to select poly(DTE-co-y%DT-co-z%PEG_{1K} carbonate) compositions in a {3,3} d-optimal design space using Design Expert® software version 7.1.6 (Stat-Ease Inc., Minneapolis, MN). The compositional limits of 'y'=12 mole % and 'z'=18 mole % were determined from preliminary studies where it was observed that sample fragmentation occurred at higher compositional limits with samples containing 30 wt. % voclosporin. The designation {3,3} defined the restrictions imposed on the empirical model, where the first number '3' indicates the number of components in the "mixture" (i.e., DTE, DT and PEG_{1K}), and the second number '3' indicates the highest degree of the polynomial used to fit the data (i.e., full cubic). For example, the canonical form of the full cubic polynomial, as shown in Eq. 2.1, is (83, 84):

Eq. 2.1: $$\eta = \sum_{i=1} \beta_i^* x_i + \sum_{i<j} \sum \beta_{ij}^* x_i x_j + \sum_{i<j} \sum \delta_{ij} x_i x_j (x_i - x_j) + \sum_{i<j<k} \sum \sum \beta_{ijk}^* x_i x_j x_k$$

where η is the response (or dependant) variable, x_i, x_j and x_k are the mixture component terms with i, j and k representing the three components DTE, DT and PEG_{1K}, and β_i^*, β_{ij}^*, β_{ijk}^* and δ_{ij} are the partial regression coefficients of the polynomial model. The multiple regression coefficients were estimated using the method of least squares, and analysis of variance (ANOVA) was used to select the statistically significant terms in the model. The polynomial was subjected to the following constraints:

Eq. 2.2: $$x_i, x_j, x_k \geq 0$$

indicating that no mixture component can be negative, and

Eq. 2.3: $$\sum_{i,j,k} x = 1$$

indicating the sum of all components must equal to 100 %. Design Expert® software was used to produce empirical models and for generating contour plots of the response variable as a function of the polymer components.

Figure 2.3 contains a listing of the chemical composition of the polymers used in this study for generating the contour plots. The apexes of the triangle in the figure give homopolymer compositions, the sides of the triangle give the copolymer compositions and the interior of the triangle gives the terpolymer compositions. Compositional points were equally spaced along the border of the shaded region in the triangle; this region corresponded to the limits of 'y' and 'z' previously mentioned. The only homopolymer used in this design, poly(DTE carbonate), was designated as '1'. Copolymers of poly(DTE-co-DT carbonate) were designated as '5', '6' and '2'. Copolymers of poly(DTE-co-PEG_{1K} carbonate) were designated as '7', '8' and '3'. All other compositions were terpolymers. Points '13', '14', '15' and '16', typically used for model validation, were used to fit the model instead. The center point '17' was used to detect curvature in and out of the plane of the response map. Points along the edges of the shaded region were used to detect curvature in these regions.

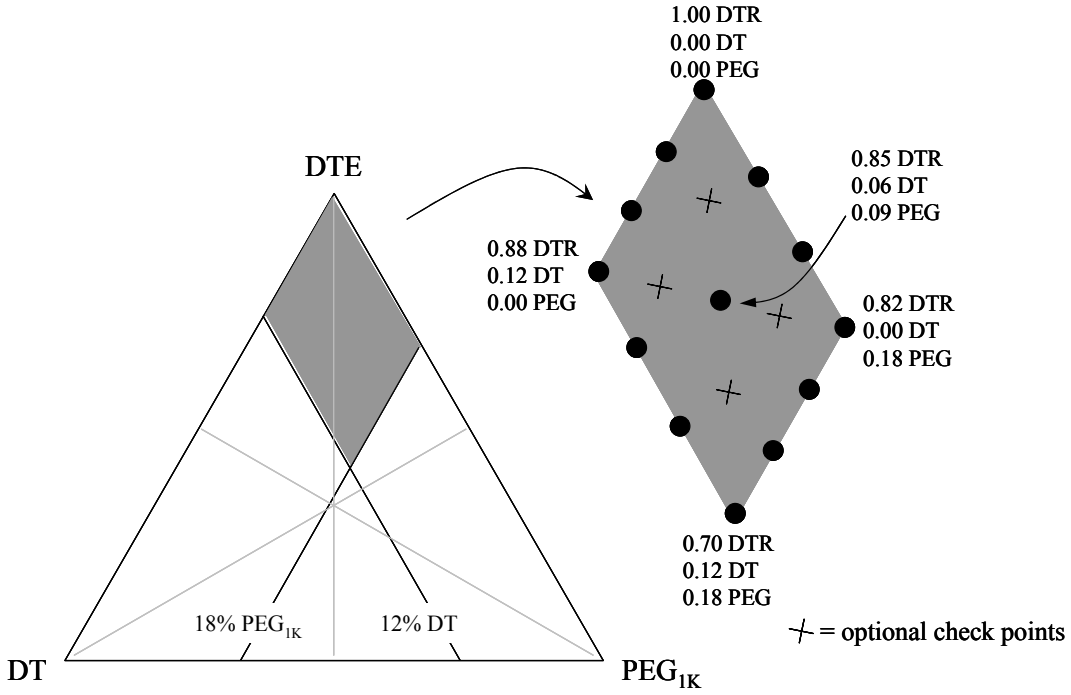

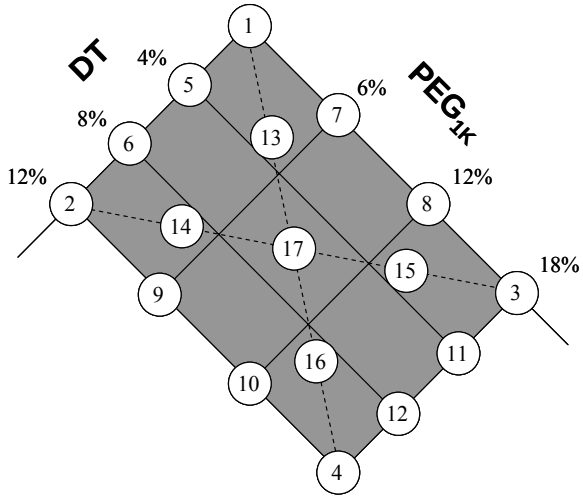

		%DTE	%DT	%PEG$_{1K}$
Vertex	1	100	0	0
Vertex	2	88	12	0
Vertex	3	82	0	18
Vertex	4	70	12	18
Third-edge	5	96	4	0
Third-edge	6	92	8	0
Third-edge	7	94	0	6
Third-edge	8	88	0	12
Third-edge	9	82	12	6
Third-edge	10	76	12	12
Third-edge	11	78	4	18
Third-edge	12	74	8	18
Axial	13	92.5	3	4.5
Axial	14	86.5	9	4.5
Axial	15	83.5	3	13.5
Axial	16	77.5	9	13.5
Centroid	17	85	6	9

Figure 2.3. Limits and point assignment for {3,3} d-optimal experimental design for poly(DTE-co-y%DT-co-z%PEG$_{1K}$ carbonate) mixtures (shaded region) in Design Expert® software. All percentages are in mole percent.

2.4 Curve fitting techniques for analyzing scattering data

Small-angle scattering data was curve fitted with either the Zernike-Prins (ZP) model (85) or an extended ZP model to estimate the size and spacing of hydrophilic domains within the polymers. The extension of the ZP model was the addition of a Guinier term (86) of the form [I_{CDS} $\exp(-q^2R_g^2/3)$] that mathematically described the decaying exponential signal at very low q values (< 0.015 $Å^{-1}$) and physically described a central diffuse scattering (CDS) from a monodispersed spherical particulate system. The extended ZP model is given in Eq.2.4**,** where q is scattering vector, I(q) is the measured scattering intensity as a function of q, I_{CDS} and I_0 are the intensities at q = 0, R_g is the radius of gyration of the CDS domains, R is the radius of phase separated or hydrated domains, d is the interdomain spacing of these phase separated or hydrated domains, A = $\exp(-q^2\sigma^2/2)$ and σ is the distribution of the interdomain spacing.

Eq.2.4: $$I(q) = \left[I_{CDS} \exp\left(-q^2 \frac{R_g^2}{3} \right) \right] + I_0 \left[\frac{\sin(qR) - qR\cos(qR)}{(qR)^3} \right]^2 \left[\frac{1 - A^2}{1 - 2A\cos(qd) + A^2} \right]$$

Curve fitting of the experimental data was performed by coding Eq.2.4 in either MatLab® version 6.1 software or higher (The MathWorks Inc., Natick, MA) or Microsoft Excel® Solver (Microsoft Inc., Redmond, WA) with the following variable parameters of the mathematical model: I_{CDS}, I_0, R_g, R, d and σ. Initial values for these parameters were picked by trial and error until a best fit was obtained. Convergence was obtained by minimizing the root mean square difference between the computed (or predicted) values and the experimental values. The fit was performed on the portion of the data that exhibited a scattering signal.

Wide-angle scattering data was curve fitted with Gaussian peak profiling methods using Jade Plus software version 6.5.24 (Materials Data Inc., Livermore, CA). Peak position (q_{max}), peak area under the curve (AUC) and peak full width at half maximum (FWHM) were determined for the portion of the data that exhibited a scattering signal.

2.5 Optimization of the DTE-co-DT / voclosporin complex using MMFF94

The chemical structures of a single DTE-co-DT chain fragment and the voclosporin drug molecule were drawn in ChemBioDraw Ultra software version 11.0 (CambridgeSoft Inc., Cambridge, MA). Their three dimensional (3D) structures were imported into Molecular Operating Environment software package version 2008.09 (MOE; Chemical Computing Group Inc, Toronto, Quebec, Canada), and minimized using an all atom molecular mechanics force field, MMFF94x. A complex was assembled with the drug molecule sandwiched between two chain fragments of DTE-co-DT. The polymer fragments were arranged in close proximity (5.99 Å apart) in one of two possible configurations: head-to-head or head-to-tail. The complex was allow to relax to a minimal conformational state during the optimization process using the same molecular mechanics force field MMFF94x, in vacuum environment, with four restraints to preserve the sandwich geometry of the complex. Two distance restraints were assigned at the ends of the chain fragments and two other distance restraints were assigned close to the drug molecule in order to hold the drug in the desired geometrical position. Then the complex was allowed to relax under the same force field on a second optimization process to ensure the "stability" of the complex. Finally, distance measurements of the spacing between the chain fragments of the minimized complex were obtained. This

work was performed in collaboration with Dr. Aurora D. Costache at the Center for Computational Design at Rutgers University.

2.6 Statistical analysis

All statistical analysis of data was performed with SPSS version 16.0 software or higher (SPSS Inc., Chicago, IL) and Design Expert® version 7.1.6 software. Analysis using SPSS included the one-way ANOVA, post-hoc test for multiple comparisons consisting of Tukey's Honestly Significant Difference (HSD) and Least Significant Difference (LSD), independent two-sample t-test and paired t-test. Analysis using Design Expert® included ANOVA for full-factorial experimental designs. All statistical testing was performed at a significance level of alpha = 0.05.

3 *In vitro* performance of tyrosine-based polycarbonates as a drug delivery carrier

This chapter presents supporting data that demonstrates (1) a systematic compositional structure of the bioerodible tyrosine-based polycarbonate polymers that can modulate the release of the hydrophobic peptide molecule voclosporin in a predictive manner, (2) a potential hydrophobic interaction involving DT polymer sections and the voclosporin molecule that may play a role in an observed late-stage drug retention within the carrier, and (3) the utility of polycarbonate-PLGA blended matrices that extend the enhanced (or early-stage) drug release lifetime.

3.1 Characterization of tyrosine-based polycarbonates

Table 3-1 lists the basic physical properties of chemical structure identification, number average molecular weight and polydispersity, dry T_g and thermal decomposition temperature measurements for the tyrosine-based polycarbonate polymers used throughout this work. The chemical structures of these polymers were confirmed by ^{1}H-NMR at or near their designed compositions of DT and PEG_{1K} content in mole percent. All polymers were within ± 1 mole % of their theoretical composition, with the exception of E1818(1K) and E2418(1K) which were within ± 2 mole %. All polymers were high in molecular weight, ranging from 77 to 333 kDa, and their polydispersity of 1.2 to 1.7 were typical for a condensation-type reaction. The measured dry T_g values ranged from -17 to 139 °C, where in general, an increase in PEG_{1K} content lowered the dry T_g of the polymer

Table 3-1. Physical characterization of tyrosine-based polycarbonate polymers.

Polymer composition	Lot No. (MDL-)	Measured Chemical Structure DT	Measured Chemical Structure PEG_{1K}	M_n (kDa)	PD	Dry T_g (°C)	Decomp. Temp. (°C)
poly(DT carbonate)	111808n6p31	100	0	122	1.2	139	255
poly(PEG_{1K} carbonate)	111708n6p28	0	100	111	1.5	(*)	230
M1218(1K)	081308n5p90	12	18	237	1.3	13	284
M1420(1K)	092308n6p6	14	20	333	1.3	9	278
M1224(1K)	092308n6p8	12	24	252	1.3	-3	294
E0000(1K)	041807n2p73	0	0	153	1.7	93	337
E0400(1K)	042507n2p88	4	0	114	1.6	96	325
E0800(1K)	042607n2p92	8	0	98	1.6	97	317
E1200(1K)	042307n2p84	12	0	73	1.7	96	306
E0006(1K)	042407n2p86	0	6	128	1.6	55	328
E0012(1K)	043007n2p94	0	11	161	1.4	33	331
E0018(1K)	042607n2p90	0	18	93	1.6	5	326
E0304.5(1K)	050707n3p5	4	4	95	1.6	64	329
E0904.5(1K)	050807n3p7	10	4	77	1.5	66	317
E1206(1K)	043007n2p96	13	6	122	1.4	59	306
E0609(1K)	051407n3p15	6	10	116	1.5	42	317
E1212(1K)	050107n2p98	12	12	115	1.4	30	309
E0313.5(1K)	050907n3p9	3	13	105	1.6	22	330
E0913.5(1K)	051007n3p11	9	13	128	1.4	23	316
E0418(1K)	050207n3p1	4	17	99	1.4	9	323
E0818(1K)	050307n3p3	7	18	112	1.6	6	315
E1218(1K)	041707n2p71	11	18	107	1.6	8	311
E1818(1K)	101607n4p22	16	19	159	1.2	8	298
E2418(1K)	101907n4p27	22	18	166	1.2	10	299
E4018(1K)	013008n4p83	40	18	142	1.4	17	265
E6018(1K)	013108n4p85	61	18	147	1.3	21	265
E1420(1K)	093008n6p10	14	20	240	1.3	4	320
E1224(1K)	031908n5p3	12	23	228	1.3	-4	328
E1230(1K)	032008n5p6	12	30	220	1.3	-17	317

(*) Melting point (T_m) and recrystallization temperatures measured at 44 and 19 °C, respectively.

and an increase in DT content, in the absence of PEG, raised the dry T_g. Poly(PEG_{1K} carbonate) was the only polycarbonate that exhibited crystalline properties with a melting point temperature, T_m, of 44 °C and a recrystalization temperature of 19 °C. A relatively

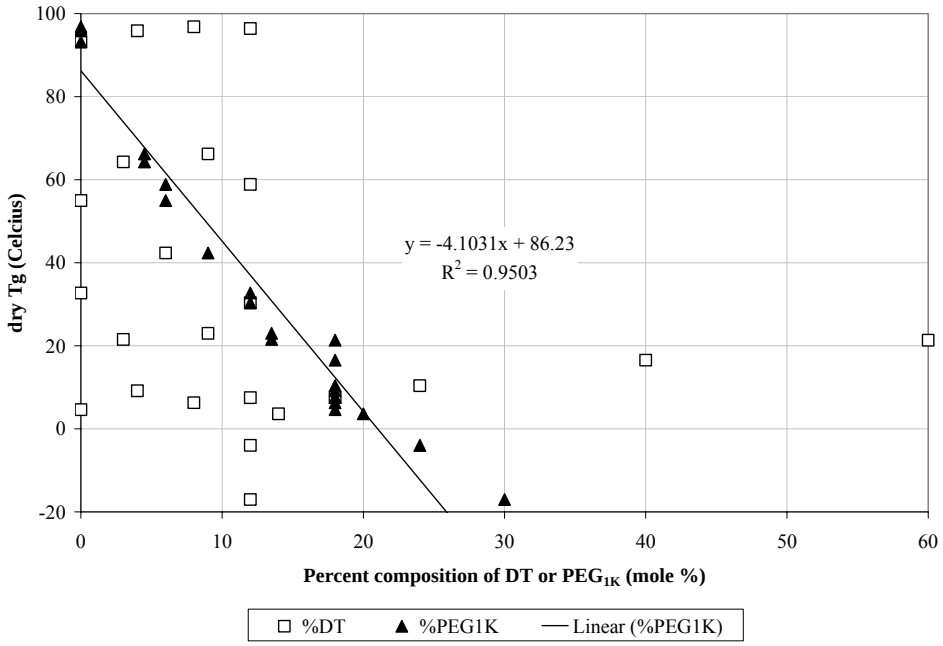

Figure 3.1. Effect of percent composition of DT and PEG_{1K} in poly(DTE-co-y % DT-co-z % PEG_{1K} carbonate) on dry T_g.

high thermal decomposition temperature range of 230 to 340 °C indicated that all polymers were heat stable during the compression molding operation of 60 to 130 °C used in fabricating samples for performance testing.

Figure 3.1 is a plot of the dry T_g of the DTE polycarbonates as a function of the mole percentage compositions of DT and PEG_{1K}, constructed using the data taken from Table 3-1. All samples were compression molded prior to testing as described in Section 2.2.10 and contained no drug. The data showed a strong inverse linear relationship between the dry T_g of the polymer and the % PEG_{1K} content in the composition (Pearson correlation coefficient, r = -0.975). On the other hand, there was considerable scatter in the data for dry T_g versus % DT content, resulting in a weak correlation (r = -0.266). An empirical equation for the calculation of the mole % PEG_{1K} content in these polymers was obtained from the linear fit,

Eq. 3.1:
$$\%\ PEG_{1K}\ content = \frac{dry\ T_g - 86.23}{-4.1031}$$

with the dry T_g measured in degrees Celsius.

3.2 Screening of poly(DTE-co-y%DT-co-z%PEG_{1K} carbonate)s as a degradable carrier for the controlled release of voclosporin

The *in vitro* performance of the tyrosine-based polycarbonate polymers was evaluated using the seventeen polymer compositions given in the mixture design of Figure 2.3. These polymer compositions provide a wealth of information regarding how the molecular weight degradation, drug release kinetics, polymer erosion and physical structure of the hydrated polymer change as a function of increasing DT and PEG_{1K} content. These characteristics will be described in this section, with the exception of the hydrated structure of the polymers which will be described later in Chapter 4.

3.2.1 Molecular weight degradation of polycarbonates

Figure 3.2 shows the fractional MW loss as a function of the seventeen DTE polycarbonate compositions over a period of five months incubation in PBS at 37 °C. No statistical analysis was performed on the data since the sample size, n, for each composition was ≤ 2. A substantial loss in molecular weight was shown to occur in the PEG-containing polycarbonates within the first month of hydration. There was no major difference in MW degradation between the control polymer E0000(1K) and the DTE-co-DT copolymers which suggested that chain scission in these hydrated solid matrices were not dependant on their DT content. Finally, there were no observable systematic synergistic relationships between DT and PEG_{1K} in reducing the molecular weight of the

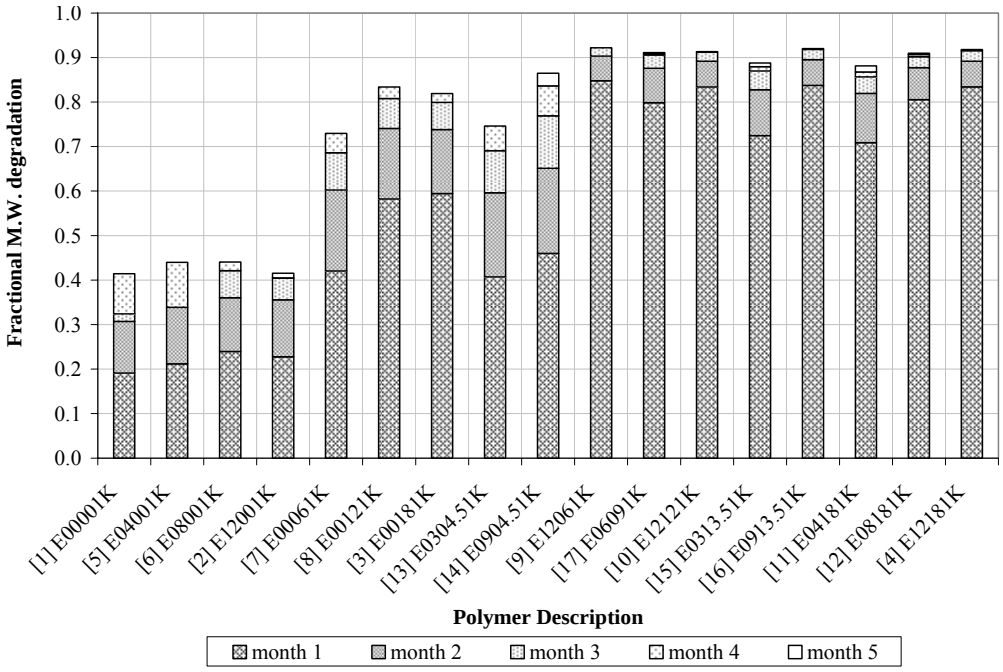

Figure 3.2. Fractional monthly change in molecular weight for poly(DTE-co-y %DT-co- z % PEG_{1K} carbonate) loaded with 30 wt. % voclosporin in PBS at 37 °C.

polycarbonates. In order to better characterize the MW degradation for the seventeen polycarbonates, each composition was assigned a relative classification of having either a low (Group A: $0 \leq$ value < 0.33), medium (Group B: $0.33 \leq$ value < 0.66) or high (Group C: $0.66 \leq$ value < 1) degradation based on the fractional loss of molecular weight within the first month. The homopolymer E0000(1K) and all the DTE-co-DT copolymers (Group A: '1', '2', '5' and '6') had approximately 20 to 25 % reduction in molecular weight by the end of the first month. All DTE-co-PEG_{1K} copolymers and all DTE-co-DT-co-PEG_{1K} terpolymers having a PEG_{1K} content $\leq$ 4.5 mole % had approximately 40 to 60 % reduction in molecular weight within the first month (Group B: '3', '7', '8', '13' and '14'). Terpolymers having both DT content $\geq$ 3 mole % and PEG_{1K} content $\geq$ 6 mole % showed approximately 70 to 85 % reduction in molecular weight in the first month

(Group C: ‘4, ‘9’ to ‘12’ and ’15 to ‘17’). The raw molecular weight data is given in Table 8-1 of the Appendix.

The increase in hydrolysis of carbonate bonds within the matrix was attributed to the greater water uptake as demonstrated by the relatively high PEG-containing polycarbonates. In fact, the terpolymers in group C lost more than 60 % of their initial molecular weight after the first 2 weeks of immersion in PBS at 37 °C. Hydrolytic degradation of the polycarbonate co- and terpolymers were complicated by the various rates of scission of the carbonate bond types present in the polymer backbone, namely, DTE-DTE, DTE-DT, DTE-PEG, DT-DT, DT-PEG and PEG-PEG, and by the access of water into these polymers over time. In order to simplify the comparison between the hydrolysis kinetics of the seventeen polymer compositions, the initial rates during the first seven days of *in vitro* hydration of the matrices were evaluated. Figure 3.3 shows an example of the fractional MW degradation profiles versus time for the low and high degrading polymer E0000(1K) and E1218(1K), respectively. Polymer chain scission for the wet E0000(1K) proceeded at a linear rate of 0.014 day^{-1}, whereas the rate of chain scission for the wet E1218(1K) was measured at 0.072 day^{-1}, which represented a five-fold increase in the loss of molecular weight. The raw molecular weight data for all 17 polycarbonates are given in Table 8-2 of the Appendix.

The initial MW degradation rates for all polycarbonates were determined from the slope of a linear fit of the data. The following grouping for the initial degradation rates based on the classification scheme given earlier in this section is: (1) Group A (low): ‘1’, ‘5’ to ‘7’ and ‘13’, (2) Group B (medium): ‘2’, ‘3’, ‘8’, ‘9’, ‘14’, ‘15’ and ‘17’ and (3)

Group C (high): ‘4’, ‘10’ to ‘12’ and ‘16’. Most of the polymers in each set were identical to the previous groups, with a few exceptions.

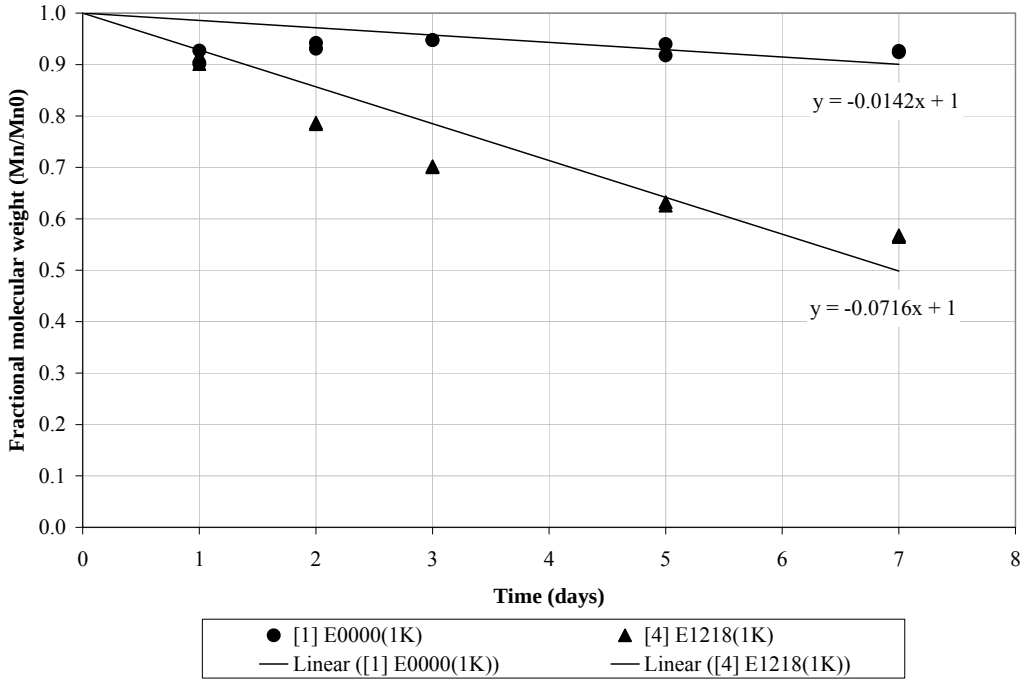

Figure 3.3. Fractional molecular weight degradation of E0000(1K) and E1218(1K) polymers during the first week of incubation in PBS at 37 °C. Slope of the linear fit gives the initial rate of polymer degradation.

The 7-day initial MW degradation rates were entered into a historical d-optimal mixture design (Design Expert® software; no replicates) for analysis and modeling of the data to generate an empirical response surface map. Backwards elimination regression and ANOVA in Design Expert® software was used to select a linear polynomial model that best fitted the experimental data (adjusted $R^2 = 0.6701$; predicted $R^2 = 0.6036$; $p = 0.0002$). Figure 3.4 shows the contour plot generated by Design Expert® software for the initial degradation rates as a function of the polymer components of DTE, DT and PEG_{1K}. Blue and red regions indicate the lowest and highest rates achieved, respectively,

and the gradient of colors in between is marked by contour lines that indicate the gradual change in the initial rates of degradation. The linear relationship between DTE, DT and PEG_{1K} (as illustrated in the contour map) indicated that there was no strong synergy between these components to accelerate polymer degradation. The empirical model did show a gradual increase in MW loss in DTE-co-DT copolymers which was not apparent in the bar graph in Figure 3.2. In addition, there was a gradual predicted increase in the MW degradation of the terpolymer as both the DT and PEG_{1K} content were increased.

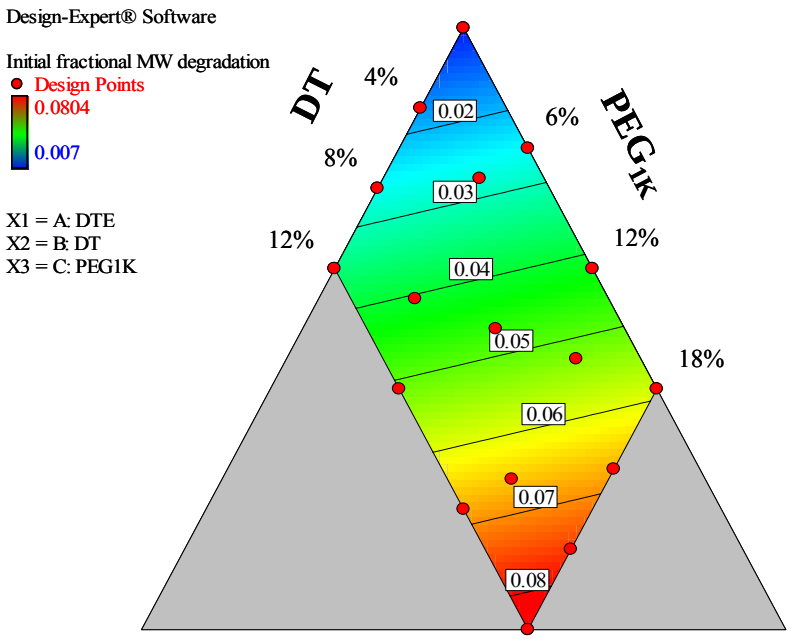

Figure 3.4. Response surface map for initial rate (7-day period) of molecular weight degradation of poly(DTE-co-y %DT-co-z %-PEG_{1K} carbonate) in PBS at 37 °C. Data is fit to a linear model. Values at contour lines indicate the initial rates for molecular weight degradation. Plot generated by Design-Expert® software.

3.2.2 *In vitro* kinetic drug release of voclosporin from polycarbonates

In vitro drug release profiles for the seventeen tyrosine-based polycarbonates, compression molded in the shape of 6 mm flat disks containing 30 wt. % voclosporin, were collected over a period of 35 weeks in PBS at 37 °C. The average daily drug release in μg/day versus time for these compositions is shown in Figure 3.5. This overall view of drug release, given in Figure 3.5(A), reveals two potential grouping for the polycarbonate compositions. Each polymer was therefore assigned a relative classification of being either a low (Group D: normalized average daily release ≤ 0.5) or high (Group E: normalized average daily release > 0.5) drug release carrier based on the first week of data. The homopolymer E0000(1K), all DTE-co-DT copolymers and all DTE-co-DT-co-PEG_{1K} terpolymers having a PEG_{1K} content ≤ 4.5 mole % were classified as group D polymers (‘1’, ‘2’, ‘5’ to ‘7’, ‘13’ and ‘14’). All other compositions were classified as group E polymers. Statistical analysis using a one-way ANOVA and the Tukey test indicated that there was a statistical difference between polymer groups D and E for the average daily drug release during the first week of hydration ($p < 0.001$). These values for group D and group E polymers were 12 ± 3 and 2 ± 2 μg/day, respectively. After approximately 4.5 weeks, the average daily release of voclosporin from all compositions fell below 3 μg/day, however the Group E polymers continued to release relatively higher amounts of drug per day. The corresponding profiles of the average cumulative fractional drug release versus time for the seventeen polycarbonates are given in Figure 3.6. In 35 weeks, group D polymers released 0.9 % to 10.5 % of the loaded drug, with the exception of the homopolymer E0000(1K) which released 16.3 % of its loaded drug. E0000(1K) was observed to behave differently from other polycarbonates,

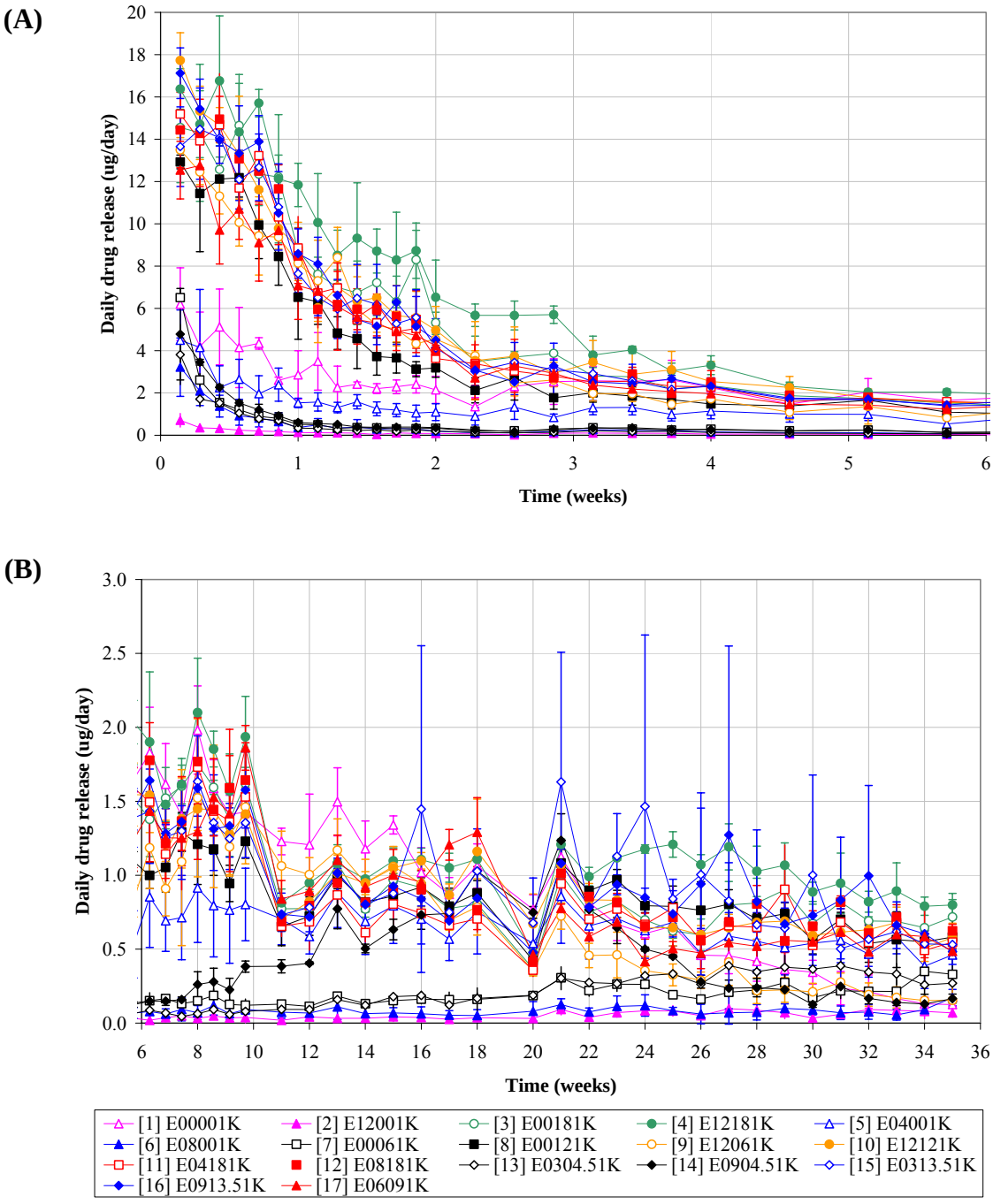

Figure 3.5. Average daily drug release from 6 mm diameter x 200 μm thick (nominal) disks of poly(DTE-co-y % DT-co-z % PEG_{1K} carbonate) loaded with 30 wt. % voclosporin in PBS at 37 °C for (A) 0 to 6 weeks and (B) 6 to 35 weeks. Error bars represent standard deviation of n = 3 samples. Lines connecting data points are for visual purposes only.

where it had a single-stage diffusion mechanism for drug release during 27 weeks of hydration. Group E polymers released 15.1 % to 23.2 % of their drug capacity during the time period of 35 weeks of hydration. The measured average cumulative fractional drug release from the 17 polycarbonates is given in Table 8-3 of the Appendix.

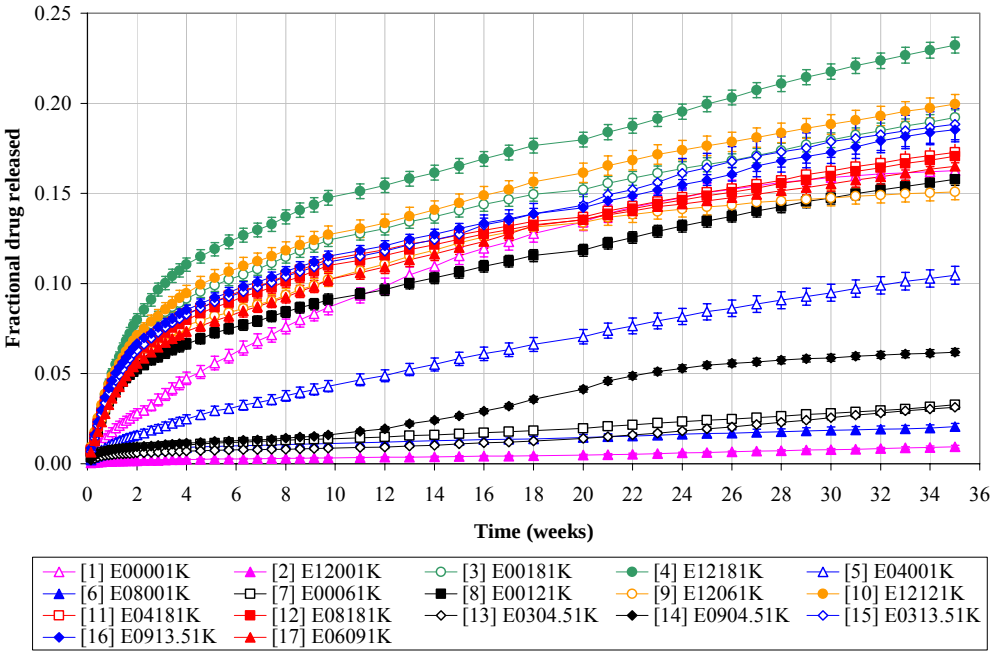

Figure 3.6. Average 35-week cumulative fractional drug release from 6 mm diameter x 200 μm thick (nominal) disks of poly(DTE-co-y % DT-co-z % PEG_{1K} carbonate) loaded with 30 wt. % voclosporin in PBS at 37 °C. Error bars indicate cumulative error. Lines connecting data points are for visual purposes only.

A linear plot of the fractional cumulative release as a function of the square root of time is indicative of a diffusion-controlled mechanism for drug release from the polymeric carrier. The slope of the line gives an empirical coefficient that describes the rate of release of drug (units of $day^{-1/2}$). Figure 3.7 shows the cumulative fractional drug release versus the square root of time for the seventeen polycarbonate disks loaded with 30 wt. % voclosporin and incubated in PBS at 37 °C. A linear fit of the data for each polymer composition was used to obtain the rate coefficients for two apparent stages of

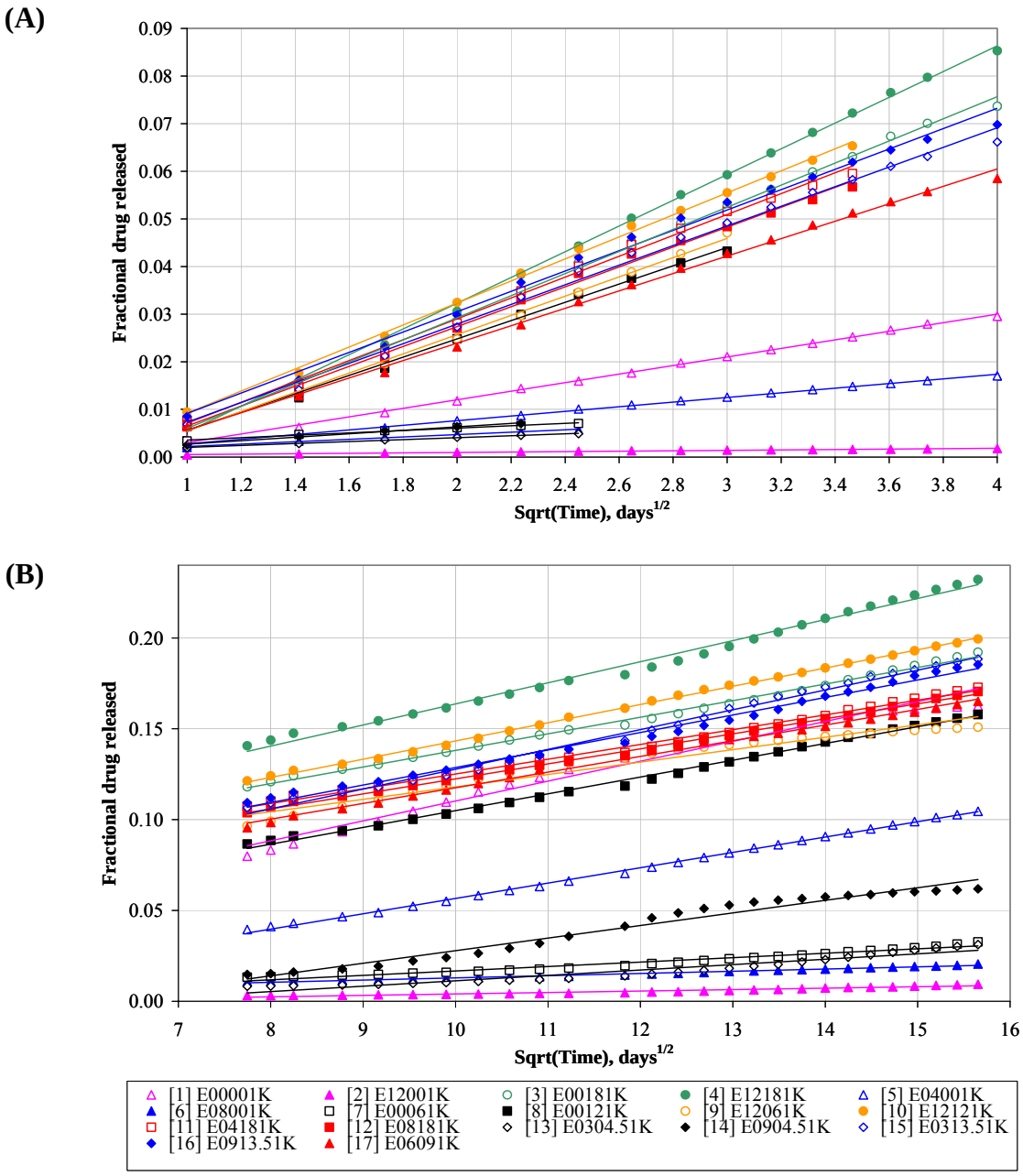

Figure 3.7. Plot of average cumulative fractional drug release versus square root of time for 6 mm diameter x 200 μm thick (nominal) disks of poly(DTE-co-y % DT-co-z % PEG_{1K} carbonate) loaded with 30 wt. % voclosporin in PBS at 37 °C showing (A) early-stage (≤ 16 days) and (B) late-stage (> 60 days) diffusion-controlled release (indicated by lines).

drug release, namely, an early-stage fractional drug release having a rate coefficient of k_1, followed by a late-stage fractional drug release having a different rate coefficient of k_2.

The extent of the deviation from early-stage fractional release was described using a term called the persistence factor, η_p, where,

Eq. 3.2:
$$\eta_p = \frac{k_2}{k_1}$$

In cases where $k_2 = k_1$, the value of η_p is unity, and release persisted without drug retention within the polymer matrix via a single-stage diffusion-controlled mechanism. If $k_2 = 0$, then η_p is equal to zero, and a condition of complete drug retention occurred within the carrier. Values of η_p between 0 and 1 described the various degrees of drug retention within the matrix, and values of $\eta_p > 1$ described an augmentation of pure diffusion either by (i) polymer erosion which can break the matrix apart and expose drug particles for dissolution, (ii) polymer swelling which can open the free volume of the matrix, (iii) slowly developing microphase separation which can cause local mixing from the polymer chain mobility, or (iv) some combination thereof. The measured values for early and late stage average daily drug release, values for k_1 and k_2, the transition time for early to late stage release and the calculated persistence factors for all seventeen polycarbonates are listed in Table 8-4 of the Appendix. Group D polymers had $\eta_p > 1$, with the exception of E0000(1K) and E0800(1K) polymers which had η_p values of 0.3 and 0.5, respectively. All of the relatively high releasing group E polymers had $\eta_p \leq 0.5$.

Figure 3.8 shows the 35-week *in vitro* cumulative fractional drug release from polycarbonate disks composed of 0 and 18 mole % PEG_{1K} as a function of the mole percentages of DT. Statistical analysis using a one-way ANOVA and the Tukey's HSD test indicated that there was a statistical difference in drug release between DTE-co-DT copolymers ($p < 0.001$) as the DT content was increased from 0 to 12 mole %. This

corresponded to approximately 91 % decrease in fractional drug release with a slope of 0.014 units per mole % as the DT content was increased from 0 to 12 mole %. For the DTE-co-DT-co-PEG_{1K} terpolymers there was no statistical difference in cumulative fractional drug release between polymers containing 18 mole % PEG_{1K} and increasing amounts of DT from 0 to 8 mole %. Additionally, there was no statistical difference between the cumulative fractional drug release from E0018(1K) and E1218(1K) polymers. The overall data shown in this figure indicated that polymer compositions containing sufficient quantities of PEG_{1K} was able to overwhelm the retention behavior that was manifested in their counterpart compositions that contained no PEG_{1K} in the polymer.

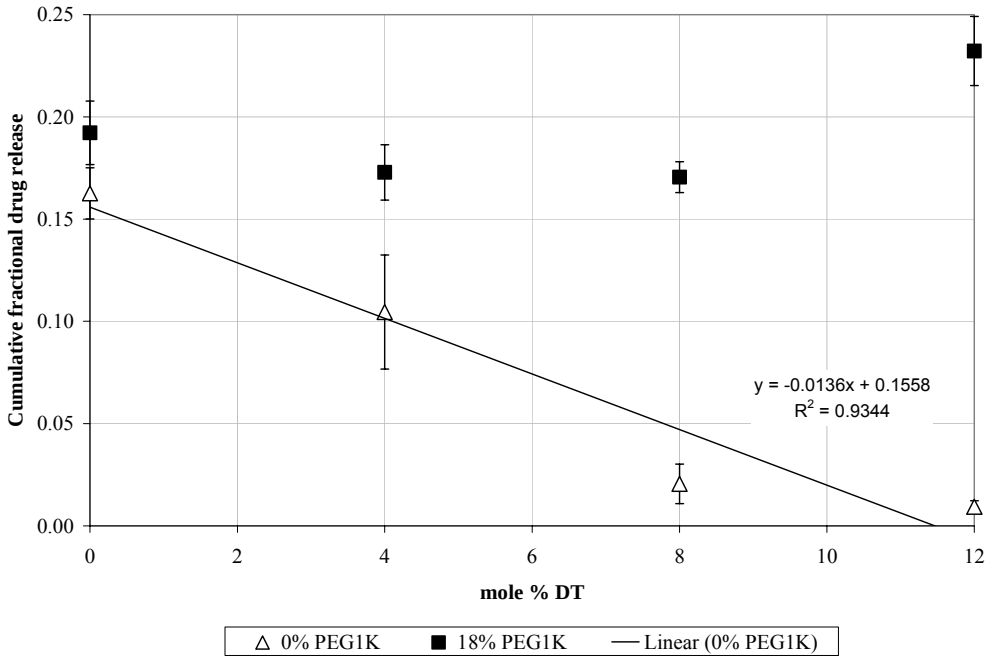

Figure 3.8. Effect of polymer composition on 35-week cumulative fractional of drug release for 6 mm diameter x 200 μm thick (nominal) disks of poly(DTE-co-y % DT-co-z % PEG_{1K} carbonate) loaded with 30 wt. % voclosporin in PBS at 37 °C. Error bars represent standard deviation of n = 3 samples.

Figure 3.9 shows the contour plot generated by Design Expert® software for the 35-week *in vitro* cumulative fractional release of voclosporin in PBS at 37 °C as a function of the polycarbonate compositions of DTE, DT and PEG_{1K}. Backwards elimination regression and ANOVA in Design Expert® software was used to select a reduced cubic polynomial model that best fitted the experimental data (adjusted R^2 = 0.8451; predicted R^2 = 0.8138; $p < 0.0001$). Blue and red regions indicate the lowest and highest amount of drug released, respectively, and the gradient of colors in between is marked by contour lines that indicate the gradual change in drug release. Lack of fit of the model was significant ($p < 0.0001$) due to all data points at low drug release lying at

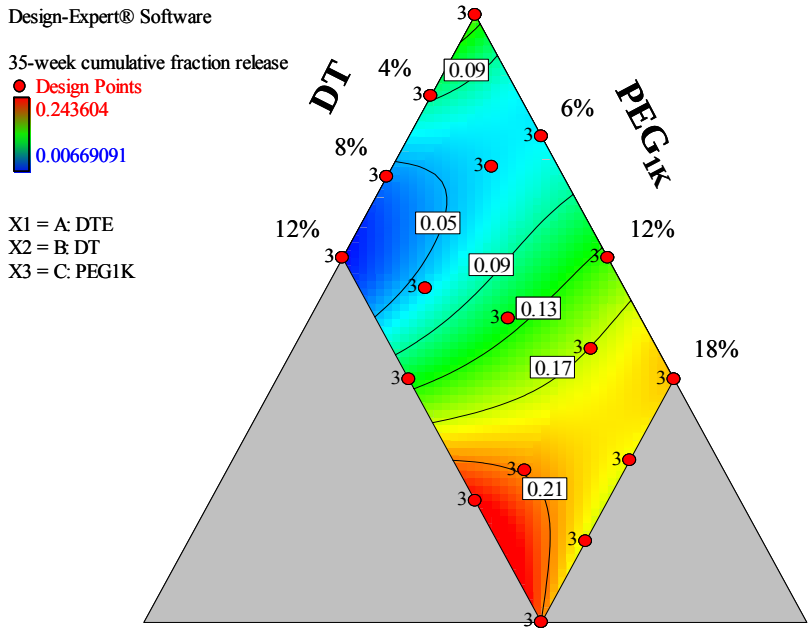

Figure 3.9. Response surface map for 35-week cumulative fractional drug release from 6 mm diameter x 200 μm thick (nominal) disks of poly(DTE-co-y % DT-co-z % PEG_{1K} carbonate) loaded with 30 wt. % voclosporin in PBS at 37 °C. Data is fit to a reduced cubic polynomial model. Values at contour lines indicate the cumulative fractional drug release. The number '3' at lattice points indicate triplicate runs. Plot generated by Design-Expert® software.

or above the model surface and many of the points at medium release lying below the model surface (refer to Figure 3.10). Data points for high drug release was more uniformly scattered above and below the model surface. This model was accepted since it provided the best representation of the drug release trends from the polycarbonates.

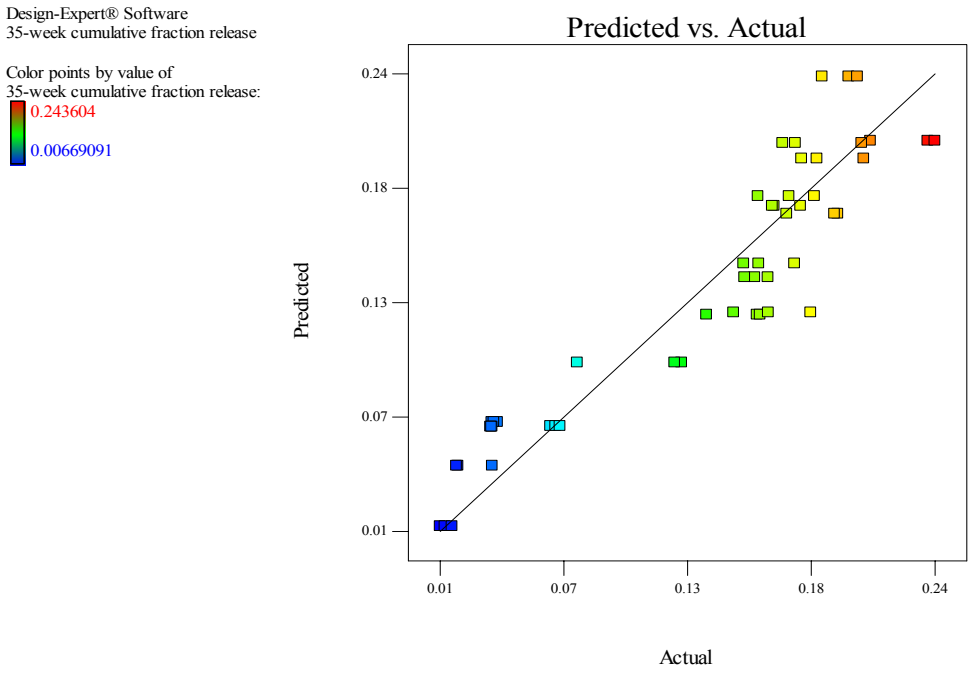

Figure 3.10. Predicted versus experimental data (actual) for 35-week cumulative fractional drug release from 6 mm diameter x 200 μm thick (nominal) disks of poly(DTE-co-y % DT-co-z % PEG_{1K} carbonate) loaded with 30 wt. % voclosporin in PBS at 37 °C. Line indicates reduced cubic model surface. Plot generated by Design-Expert® software.

Finally, a mass balance analysis on the seventeen *in vitro* polycarbonate test samples was performed by summing the cumulative percentage of drug released in PBS at 37 °C over 35 weeks (column 'A' in Table 3-2) with the percentage of drug remaining in the sample after 35 weeks (column 'B' in Table 3-2). Quantification of drug remaining within the test samples was performed by dissolving the sample in an organic

solvent mixture and analyzing by HPLC (refer to the Methods Section 2.2.12). A range of 42 to 84 wt. % of active drug was present in the hydrated test samples after 35 weeks incubation in PBS at 37 °C (column 'B'). The average mass balance for each of the seventeen polymer compositions is given in column 'C'. This data demonstrated that there were adequate amounts of drug remaining in the devices during the time of late-stage release (i.e., drug retention). The lack of summation to 100 % for the mass balance gave an indication of the accumulated errors encountered in performing the KDR study.

Table 3-2. Mass balance for *in vitro* drug release from polycarbonate polymers loaded with 30 wt. % voclosporin after 35 weeks incubation in PBS at 37 °C. Reported error for percent drug released from disk is cumulative error (column A).

Lattice point	Polymer composition	(A) Percent released from disk (%)	(B) Percent retained in disk (%)	(C) Total percentage (%)
1	E0000(1K)	16.3 ± 0.5	75.9 ± 9.0	92.1 ± 9.1
2	E1200(1K)	0.9 ± 0.1	75.8 ± 7.0	76.7 ± 7.0
3	E0018(1K)	19.2 ± 0.4	54.4 ± 5.8	73.6 ± 5.8
4	E1218(1K)	23.2 ± 0.4	50.8 ± 6.7	74.0 ± 6.7
5	E0400(1K)	10.5 ± 0.5	74.2 ± 11.1	84.7 ± 11.1
6	E0800(1K)	2.1 ± 0.2	76.3 ± 10.8	78.3 ± 10.8
7	E0006(1K)	3.3 ± 0.1	74.8 ± 0.9	78.1 ± 0.9
8	E0012(1K)	15.8 ± 0.4	76.9 ± 5.0	92.7 ± 5.1
9	E1206(1K)	15.1 ± 0.4	73.4 ± 6.5	88.5 ± 6.6
10	E1212(1K)	20.0 ± 0.5	41.5 ± 14.2	61.5 ± 14.2
11	E0418(1K)	17.3 ± 0.4	65.3 ± 6.7	82.6 ± 6.7
12	E0818(1K)	17.1 ± 0.4	70.1 ± 5.5	87.1 ± 5.5
13	E0304.5(1K)	3.1 ± 0.1	85.3 ± 5.3	88.4 ± 5.3
14	E0904.5(1K)	6.2 ± 0.2	74.2 ± 5.9	80.3 ± 5.9
15	E0313.5(1K)	18.8 ± 0.9	58.9 ± 11.4	77.7 ± 11.4
16	E0913.5(1K)	18.5 ± 0.7	61.5 ± 15.3	80.0 ± 15.4
17	E0609(1K)	16.5 ± 0.4	69.7 ± 5.3	86.2 ± 5.3

3.2.3 *In vitro* erosion of polycarbonates containing voclosporin

Figure 3.11 shows the fractional polymer mass loss versus the seventeen polycarbonate compositions that were compression molded as 6 mm flat disks containing 30 wt. % voclosporin and hydrated in PBS at 37 °C over a period of 32 weeks. No detectable polymer erosion was obtained for E0000(1K) or for any of the DTE-co-DT copolymers. As before, each composition was assigned a relative classification of having either a low (Group F: $0 \leq x < 0.33$), medium (Group G: $0.33 \leq x < 0.66$) or high (Group H: $0.66 \leq x \leq 1$) normalized average polymer mass loss. The homopolymer E0000(1K), all DTE-co-DT copolymers, all DTE-co-PEG_{1K} copolymers having a PEG_{1K} content ≤ 12 mole % and all terpolymers having both DT content ≤ 3 mole % and PEG_{1K} content ≤ 4.5

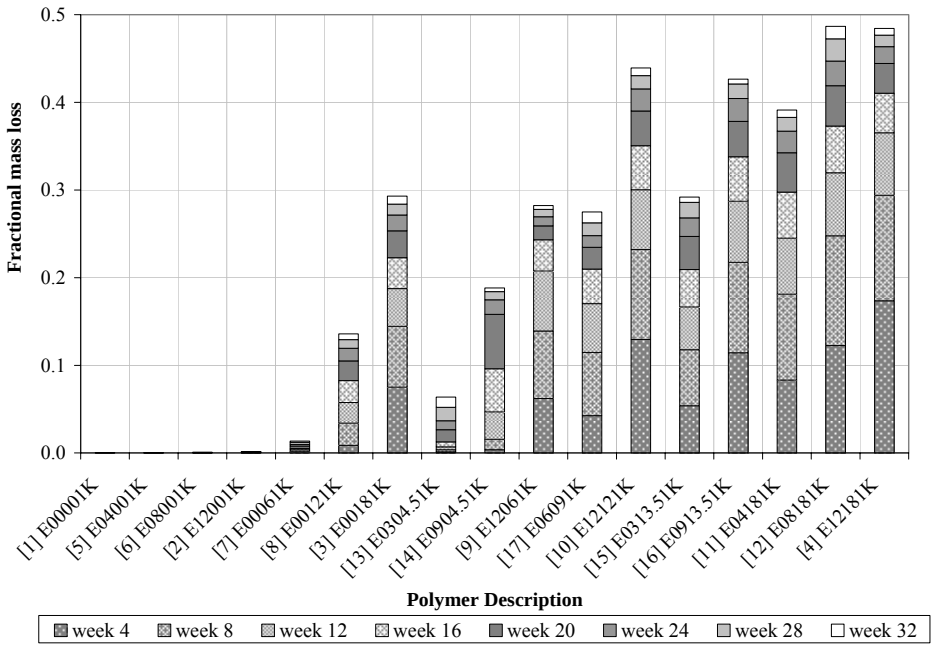

Figure 3.11. Average fractional polymer erosion of 6 mm diameter x 200 μm thick (nominal) disks of poly(DTE-co-y % DT-co-z % PEG_{1K} carbonate) loaded with 30 wt. % voclosporin in PBS at 37 °C. Numbers at the beginning of each polymer description is the point assignment of the {3,3} d-optimal mixture design.

mole % were classified as group F polymers ('1', '2', '5' to '8' and '13'). The DTE-co-PEG_{1K} copolymer E0018(1K) and the following terpolymers – E1201(1K), E0904.5(1K), E0313.5(1K) and E0609(1K) – were classified as group G polymers ('3', '9', '14', '15' and '17'). All remaining terpolymers were classified as group H ('4', '10' to '12' and '16').

Figure 3.12 shows the fractional amounts of both DT and PEG_{1K} components eroded from the seventeen hydrated polycarbonate disks containing 30 wt. % voclosporin over the period of 32 weeks. The data shows that PEG_{1K} segments of the polymers were resorbed 1.4 to 3.4 times faster than the DTR segments for all compositions at 32 weeks, with the exception of E0006(1K) which had a higher PEG_{1K}:DT resorption ratio of 9.6.

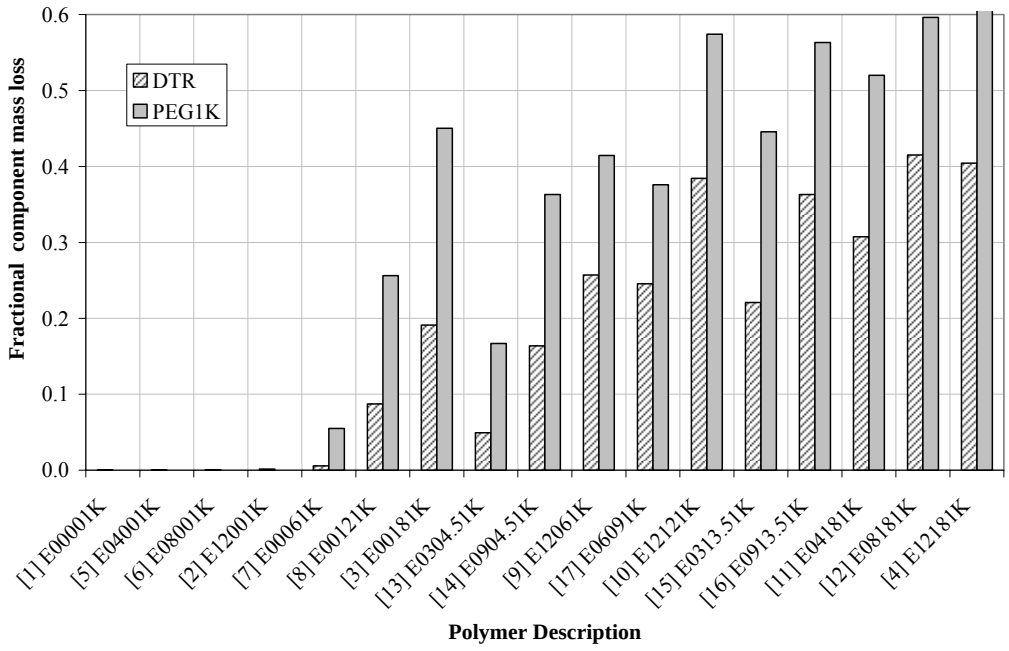

Figure 3.12. 32-week cumulative fractional erosion of DTR and PEG_{1K} components from 6 mm diameter x 200 μm thick (nominal) disks of poly(DTE-co-y % DT-co-z % PEG_{1K} carbonate) loaded with 30 wt. % voclosporin in PBS at 37 °C. Numbers at the beginning of each polymer description is the point assignment of the {3,3} d-optimal mixture design.

The amount of PEG_{1K} removed as a percentage of the total polymer mass loss after 32 weeks of hydration ranged from 24 to 64 % depending on the initial composition of the polycarbonate. The average mass loss of DTR and PEG_{1K} components are given in Table 8-5 and Table 8-6 of the Appendix.

Figure 3.13 shows the contour plot generated by Design Expert® software for the 32-week *in vitro* cumulative fractional polymer erosion of the drug loaded disks incubated in PBS at 37 °C as a function of the polycarbonate compositions of DTE, DT and PEG_{1K}. Backwards elimination regression and ANOVA in Design Expert® software

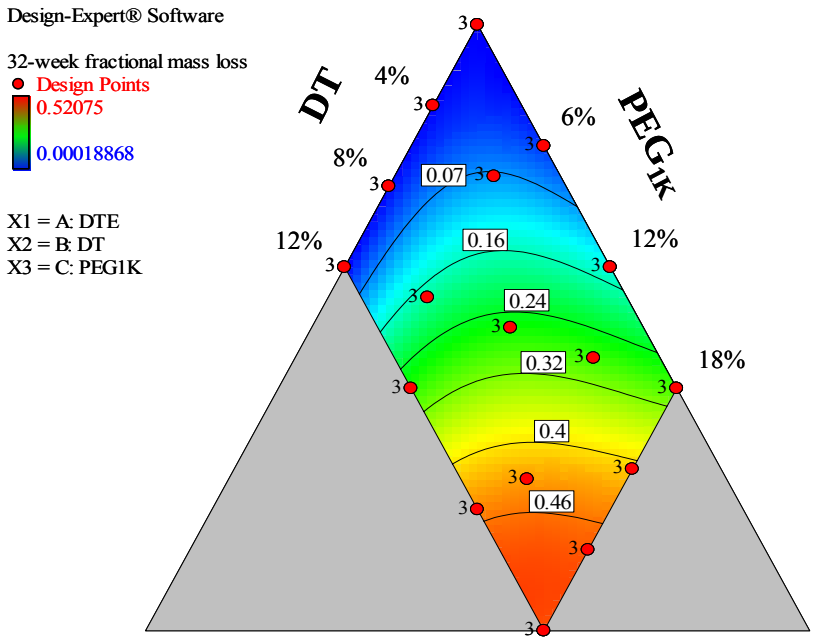

Figure 3.13. Response surface map for 32-week cumulative fractional polymer erosion of 6 mm diameter x 200 μm thick (nominal) disks of poly(DTE-co-y % DT-co-z % PEG_{1K} carbonate) loaded with 30 wt. % voclosporin in PBS at 37 °C. Weight of polymer sample adjusted for drug content. Data is fit to a reduced cubic polynomial model. Values at contour lines indicate the cumulative fractional polymer erosion. The number '3' at lattice points indicate triplicate runs. Plot generated by Design-Expert® software.

was used to select a reduced cubic polynomial model that best fitted the experimental data (adjusted R^2 = 0.9856; predicted R^2 = 0.9827; $p < 0.0001$). Blue and red regions indicate the lowest and highest cumulative fractional polymer mass loss, respectively, and the gradient of colors in between are marked by contour lines that indicate the gradual change in the fractional mass loss. Lack of fit of the model was insignificant ($p = 0.3817$) indicating that the model was adequate. The surface map in the figure is a good way to represent the trends in the data for the polycarbonate compositions as it relates to *in vitro* polymer resorption. The lack of water uptake in both the homopolymer E0000(1K) and the DTE-co-DT copolymers resulted in negligible mass loss as indicated by the dark blue regions. The extension of this dark blue region to low PEG-containing co- and terpolymers indicated that the PEG in these compositions may not be accessible to large amounts of water. The curvature in the map demonstrated some level of synergy between DT and PEG_{1K} components in terms of erosion. Finally, the contour map pointed in a direction where polycarbonate terpolymer compositions could have a higher theoretical level of mass loss during hydration.

A striking feature of all the response surface maps shown in this chapter was their diversity in topography. Polymer degradation is a prerequisite for mass loss since the polymer chains must first be broken down into monomers and oligomers, then solubilized in water and transported out of the matrix. The polymer erosion color map demonstrated that the oligomeric byproducts of degradation from the E0000(1K) and DTE-co-DT copolymers were either not short enough for solubilization or there was inadequate water present for significant mass transport out of the matrix. This lag in mass transport is evident when the response surfaces for MW degradation rate and polymer erosion are

compared side by side. The color map for cumulative drug release is expected to be different since drug diffusion is immediate in the polycarbonates upon hydration in PBS.

Figure 3.14 is a plot of the measured dry T_g for two polymers, E0000(1K) and E1218(1K), as a function of the time of incubation in PBS at 37 °C. The polymer samples (no API present) were hydrated at various times, dried by lyophilization, then analyzed by DSC to determine the polymer dry T_g. All samples were measured in triplicate. The polymer E0000(1K) did not show any statistically significant change in its dry T_g indicating that there was no change in composition for up to 20 weeks of hydration at 37 °C. However, E1218(1K) showed a significant increase in the dry T_g indicating that percentage of PEG_{1K} content in the polymer composition could be decreasing over time.

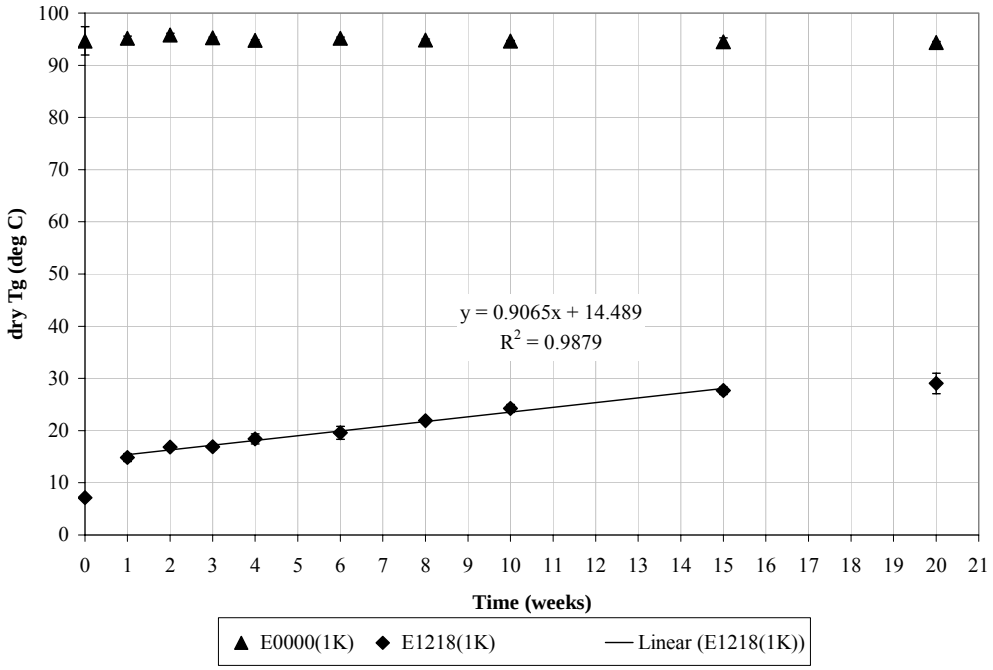

Figure 3.14. Measurement of dry T_g for E0000(1K) and E1218(1K) polymers during a 20 week incubation period in PBS at 37 °C.

The E1218(1K) terpolymer measured a two-fold change in the dry T_g within the first week of incubation, then settled into a constant rate of T_g increase of approximately 0.14 °C per day for the next 14 weeks. There was no substantial change in Tg from week 15 to week 20. The non-linearity within the first week was attributed to the rapid loss of PEG from the matrix. In the literature, T_g is reported as a function of the MW of semicrystalline polymers such as PLGA (87). However, this relationship is not relevant for the amorphous polycarbonates used in this work. An empirical equation relating the change in dry T_g with the time of hydration for the E1218(1K) terpolymer is given as,

Eq. 3.3: $$\text{dry } T_g = 0.9065 * \text{time in weeks} + 14.489$$

Using Eq. 3.1 and Eq. 3.3, the PEG_{1K} content of the eroding polymer E1218(1K) was calculated at the time points given in Figure 3.14, and the rate of decrease of PEG_{1K} content in E1218(1K) was estimated at 0.034 mole % per day during the period of 1 to 15 weeks. For comparison, the rate of decrease of PEG_{1K} in E1218(1K) as measured by the ELSD method (refer to Section 2.2.13) for the same period was 0.028 mole % per day.

3.2.4 Correlation between *in vitro* drug release and *in vitro* polymer erosion

Figure 3.15 shows a scatterplot of the *in vitro* cumulative fractional voclosporin release versus the *in vitro* cumulative fractional polymer erosion for the seventeen polycarbonates. The correlation coefficient, r, for drug release versus polymer erosion was 0.782. Most of the polymers in the figure were categorized as low eroders/low releasers (‘2’, ‘5’ to ‘7’, ‘13’ and ‘14’) and high eroders/high releasers (‘3’, ‘4’, ‘9’ to ‘12’ and ‘15’ to ‘17’) based on their location in one of the four quadrants shown. This

classification was limited to polymer compositions within the d-optimal design space ('y' = 0 to 12 mole % DT and 'z' = 0 to 18 mole % PEG_{1K}). Polymers falling into the low eroder/low releaser group had a PEG_{1K} content ≤ 4.5 mole %. Polymers falling into the high eroder/high releaser group had a PEG_{1K} content ≥ 6 mole %. The two polymers '1' and '8' representing the E0000(1K) and E0012(1K), respectively, did not fall into the two categories given above. Instead, these polymers had low erosion/high release characteristics. There were no polymers that fell into the bottom right quadrant, since high eroding polymers have a tendency to "dump" their drug content.

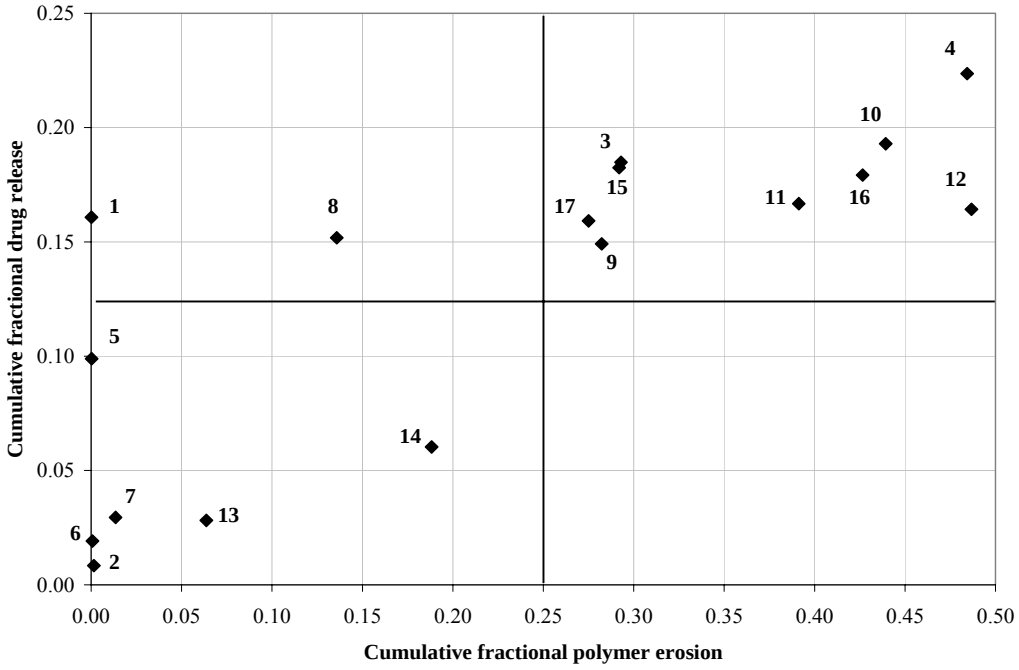

Figure 3.15. Scatterplot of 32-week *in vitro* cumulative fractional drug release versus polymer erosion for 6 mm diameter x 200 μm thick (nominal) poly(DTE-co-y % DT-co-z % PEG_{1K} carbonate) disks loaded with 30 wt. % voclosporin in PBS at 37 °C. Numbers represent the polymer compositions given in Figure 2.3.

Figure 3.16 is a comparison of the polymer erosion and drug release profiles of E1218(1K) loaded with 30 wt.% voclosporin and hydrated in PBS at 37 °C over an 8 month period. The shapes of both profiles were remarkably similar. With proper scaling of the x and y axes[3], both curves for erosion and release could be superimposed, indicating that the mechanism for species erosion and drug release might be similar. The same strong relationship between polymer erosion and drug release was obtained for polycarbonate terpolymers '10', '12' and '16'. The scaling values for polymers '4', '10', '12' and '16' were 0.30, 0.28, 0.18 and 0.25, respectively. These polymers are located in

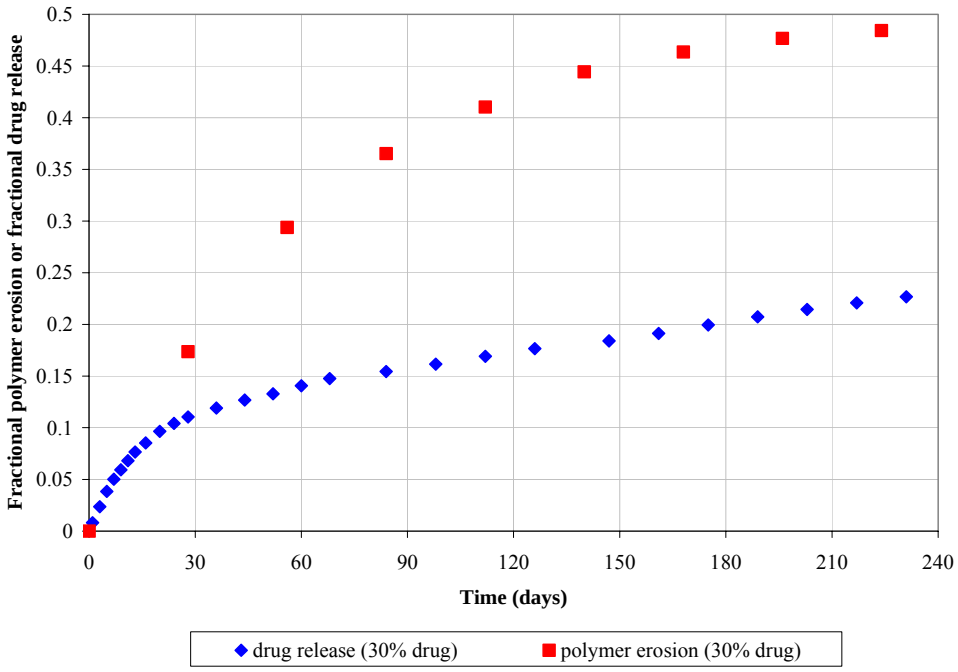

Figure 3.16. Comparison of the average fractional polymer erosion and average fractional drug release profiles of E1218(1K) loaded with 30 wt. % voclosporin in PBS at 37 °. Error bars removed for convenience.

[3] Both axes must be scaled by the same factor in order to prevent the slopes from changing. Scaling is not shown in the figure.

the uppermost region of the top right quadrant in Figure 3.15. Weaker relationships were obtained for the co- and terpolymers '3', '9', '11' and '17'. In all of these cases, drug release was observed to lag polymer erosion. No similarity between polymer erosion and drug release was obtained for the remaining polycarbonates, which included E0000(1K) and the DTE-co-DT copolymers.

3.3 Comparison of DTM versus DTE polycarbonates as a drug delivery carrier for voclosporin

The previous sections demonstrate the advantages of having adequate PEG_{1K} content in the polycarbonate compositions to enable satisfactory performance of drug release and polymer erosion. In this section, a comparison between the drug release performance of DTM and DTE polycarbonate terpolymer carriers is presented, mainly to judge whether the more soluble DTM can significantly enhance drug release from the matrix.

Figure 3.17 shows the fractional decrease in molecular weight versus time for three DTM polymers – M1218(1K), M1420(1K) and M1224(1K), and the corresponding three DTE polymers – E1218(1K), E1420(1K) and E1224(1K), incubated in PBS at 37 °C for approximately three months. The overall degradation profiles for these polymers were similar in nature. They all degraded rapidly to approximately 10 to 30% of their initial molecular weight within the first two weeks of hydration. The raw molecular weight data are given in Table 8-12 of the Appendix. The initial rates of MW degradation were obtained from a linear fit of the first seven days of hydration. The results are presented in Table 3-3 where the negative values indicate the decreasing rate of molecular weight with time. No statistical analysis was performed on the data since

the sample size, n, for each composition was 2. Qualitatively, the data showed that the initial decline in molecular weight appeared faster for the DTM terpolymer group compared DTE group as observed in Figure 3.17.

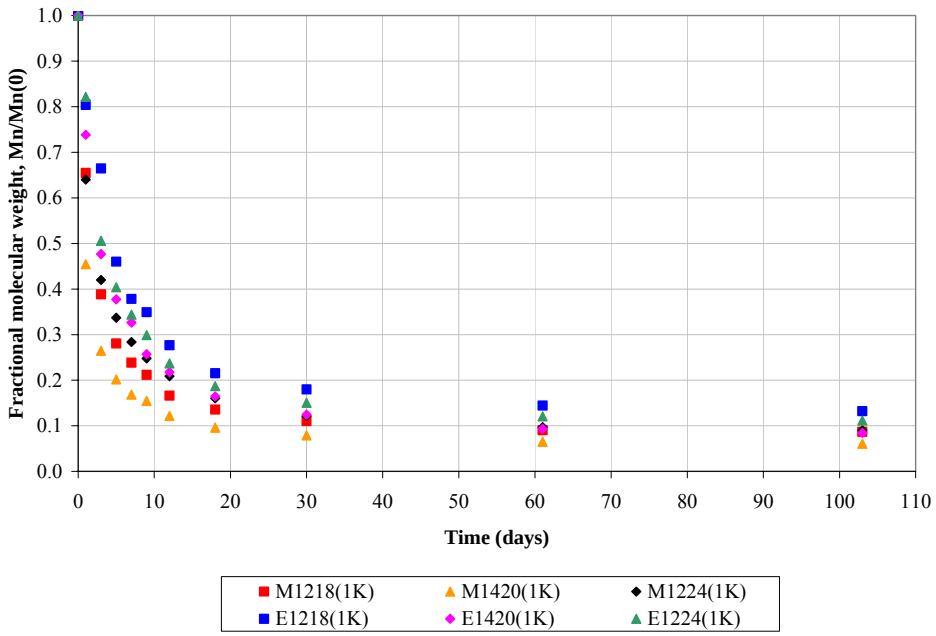

Figure 3.17. Fractional change in molecular weight for DTM and DTE polycarbonate terpolymers in PBS at 37 °C. Sample size, n = 2.

Table 3-3. In vitro initial rates of number average molecular weight (Mn) degradation of DTM and DTE polycarbonate terpolymers in PBS at 37 °C.

Polymer composition	Initial rate of M_n degradation (day^{-1})
M1218(1K)	-0.17
M1420(1K)	-0.13
M1224(1K)	-0.16
E1218(1K)	-0.13
E1420(1K)	-0.13
E1224(1K)	-0.14

Table 3-4 shows the average daily drug release from the DTM and DTE polycarbonates loaded with 15 wt.% voclosporin incubated in PBS at 37 °C. There was no statistical difference between the pairs of polymers M1218(1K) and E1218(1K),

M1420(1K) and E1420(1K), and M1224(1K) and E1224(1K) for the average daily release at time intervals of 1 to 4 weeks, 5 to 10 and 11 to 20 weeks. The shapes of the cumulative fractional drug release profiles for all these polycarbonates were similar to those given in Section 3.2.2 for the high releasing polymers. Based on *in vitro* data, there did not seem to be a substantial benefit to using DTM polycarbonate terpolymers for enhancing the drug delivery (and possibly polymer erosion) performance.

Table 3-4. Average *in vitro* daily drug release from DTM and DTE polycarbonate terpolymers loaded with 15 wt.% voclosporin incubated in PBS at 37°C.

Polymer composition	Avg. daily release during 1-4 weeks (μg/day)	Avg. daily release during 5-10 weeks (μg/day)	Avg. daily release during 11-20 weeks (μg/day)
M1218(1K)	19 ± 3	8 ± 2	3 ± 0
M1420(1K)	25 ± 3	13 ± 1	2 ± 0
M1224(1K)	26 ± 3	11 ± 1	1 ± 0
E1218(1K)	16 ± 3	5 ± 2	1 ± 0
E1420(1K)	21 ± 4	8 ± 1	1 ± 0
E1224(1K)	22 ± 3	7 ± 1	1 ± 0

3.4 PLGA as a degradable carrier for the controlled release of voclosporin

This section covers the drug release characteristics of three compositions of the commonly used biomaterial PLGA, as well as the release characteristics from blends of PLGA with polycarbonate terpolymers. Structural information of phase separated domains and polymer interchain spacing of the dry and hydrated states of the drug loaded PLGA is presented in Chapter 4. The performance data of PLGA as a controlled-release degradable matrix for voclosporin is intended to serve as a comparison to the work previously outlined for the tyrosine-based polycarbonates.

3.4.1 *In vitro* kinetic drug release of voclosporin from PLGA polymers.

Figure 3.18 is a plot of the *in vitro* cumulative fractional drug release versus time for three PLGA compositions – PLGA 50:50, PLGA 75:25 and PLGA 85:15, formed as compression molded 6 mm flat disks containing 5 wt.% voclosporin and incubated for approximately 30 weeks in PBS at 37 °C. Figure 3.19 is the corresponding plot of the *in vitro* average daily voclosporin release as a function of time for the PLGA compositions listed above. Three stages of drug release from the PLGA samples were evident. First, there was a lag time for drug release of approximately 4, 12 and 21 weeks for PLGA 50:50, 75:25 and 85:15, respectively. Second, a burst of drug occurred as the polymer disintegrated that lasted for approximately 4 to 6 weeks. The third and final stage of drug release was a low rate of release that occurred after the cessation of the burst. This sigmoidal shape of drug release is characteristic of the PLGA family of polymers (46). A comparison of the drug release profiles of the PLGA carriers versus the E1218(1K) is given in Figure 8.1 of the Appendix.

Figure 3.20 is a plot of the average cumulative fractional release of drug versus time for two polymers – E1224(1K) and a 1:1 (wt./wt.) blend of E1224(1K)+PLGA 50:50, loaded with 15 wt.% voclosporin and incubated in PBS at 37 °C for 30 weeks. The main distinction between the two formulations was the onset time for drug retention. The polymer E1224(1K) had an onset time of approximately 30 days, whereas the E1224(1K)/PLGA blend had an onset time of approximately 60 days. Both polymers attained similar steady state drug release after 90 days of hydration as indicated by the near-parallel curves. No drug burst was observed from the polycarbonate/PLGA blended matrix. Figure 3.21 is a plot of the cumulative fractional drug release versus the square

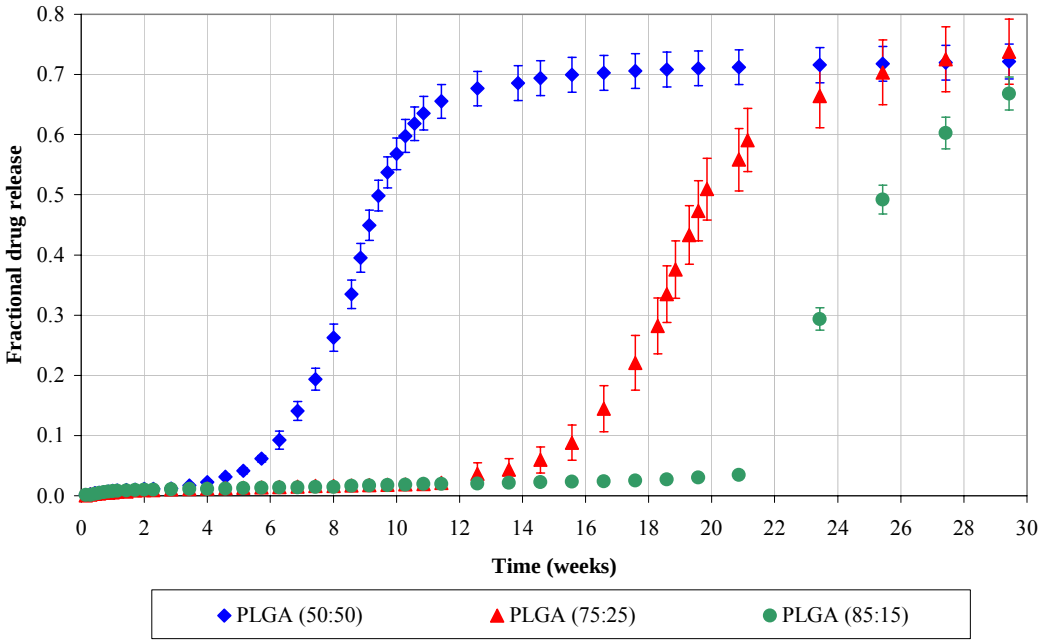

Figure 3.18. Average cumulative fractional release of 5 wt. % voclosporin from 6mm diameter x 160 μm thick (nominal) PLGA disks in PBS at 37 °C. Error bars indicate cumulative error.

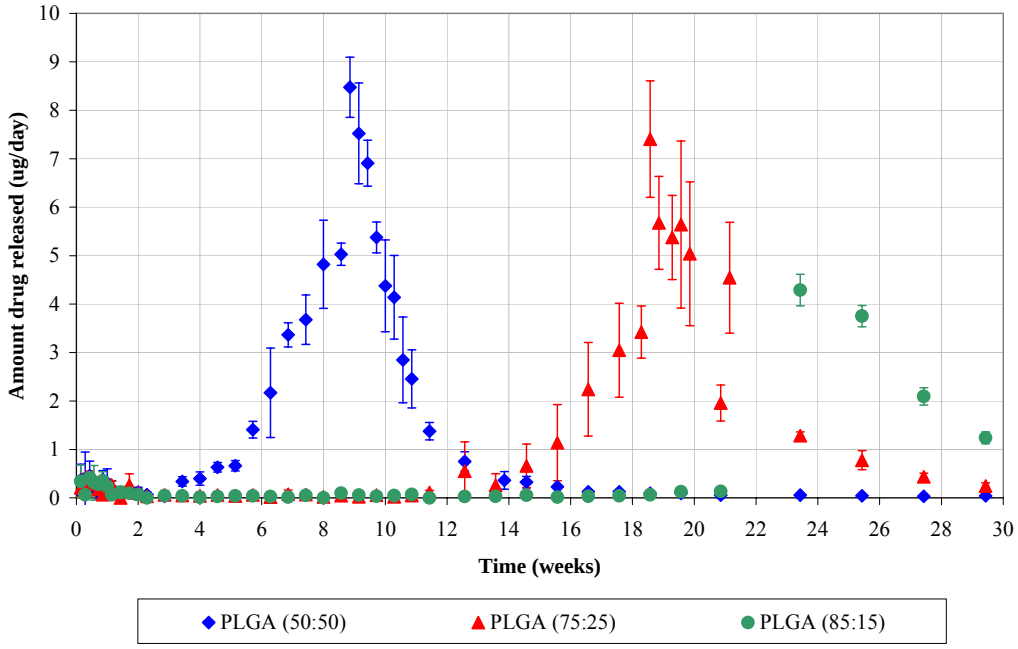

Figure 3.19. Average daily release of 5 wt. % voclosporin from 6mm diameter x 160 μm thick (nominal) PLGA disks in PBS at 37 °C. Error bars indicate standard deviation of n = 3 samples.

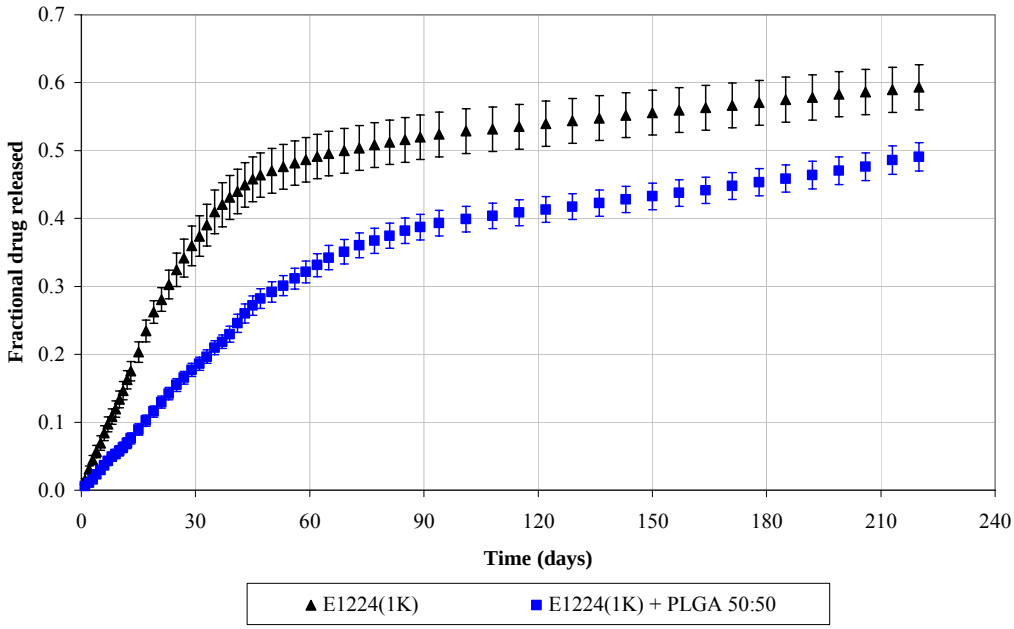

Figure 3.20. Average cumulative fractional release versus time for 6mm diameter x 360 μm thick (nominal) polymer disks containing 15 wt. % voclosporin in PBS at 37 °C. Error bars indicate cumulative error.

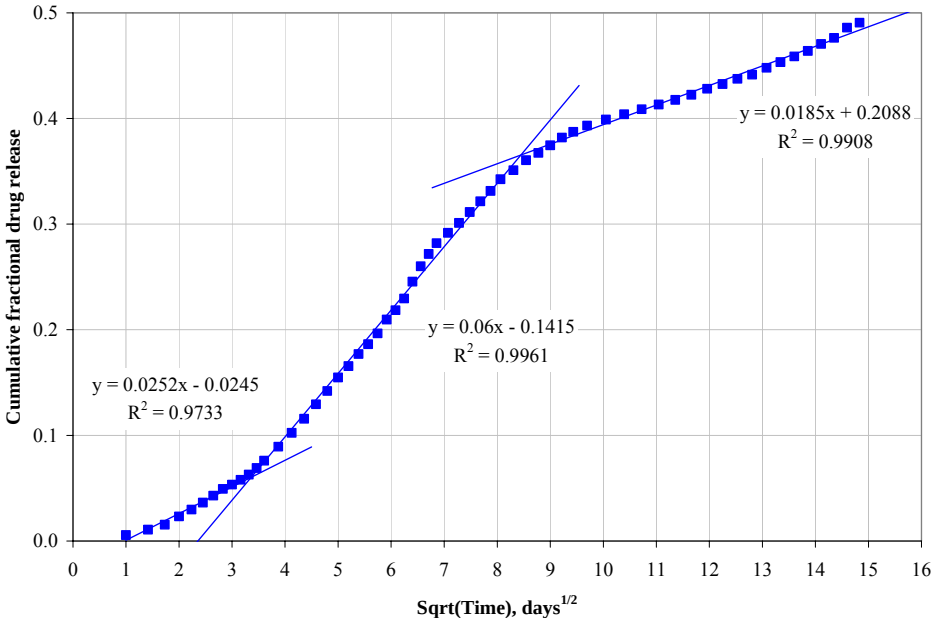

Figure 3.21. Average cumulative fractional drug release versus square root of time for 6 mm diameter x 360 μm thick (nominal) disks of 1:1 (wt./wt.) blend of E1224(1K) and PLGA 50:50 containing 15 wt.% voclosporin in PBS at 37 °C. Error bars removed for convenience.

root of time for the 1:1 blend of E1224(1K)+PLGA 50:50 mentioned above. The figure shows three apparent stages of drug release, indicated by the linear fitted regions of the curve, where the first and third stages had similar rates of release and the middle stage had a release rate of approximately two to three times faster.

3.5 Discussion

The tyrosine-derived polycarbonates used in this work demonstrate the versatility of this library of polymers for the customization of their physical and chemical properties. In the hydrated state, PEG-containing polymers were conformable, slowly taking the shape of any container in which they were placed. An increase in the PEG_{1K} content of the polymers exhibited a linear reduction of its dry T_g. A lower T_g meant that these drug-loaded materials could be thermally processed at temperatures that did not destroy the drug molecule. The use of PEG in the composition was important since it increased the water capacity of the matrix. Higher water uptake resulted in an acceleration of molecular weight degradation, mass transport of polymer degradation byproducts, and early-stage drug release from the eroding matrix. The main disadvantage of PEG incorporation into the polymer composition was its potential to form hydroperoxides when activated by heat or radiation, causing instability in the neighboring drug molecule, as discussed in Chapter 5.

In order to understand the utility of the polycarbonate library of polymers as a drug delivery carrier for the hydrophobic drug voclosporin, a series of seventeen polymers with varying amounts of DT and PEG_{1K} were studied. Three questions were posed: (a) how does the variation of DT and PEG_{1K} affect drug release, and how can these compositions be optimized to provide a dosage of 5 to 10 μg/day during the lifetime

of formed devices that are placed into aqueous media, (b) how does variation in the DT and PEG_{1K} affect the resorption of the polymer and how can the composition be formulated to prevent matrix fragmentation, and (c) how does polymer morphology change during hydration and how can this changing structure be correlated to the stages of drug release and polymer erosion. The first two questions were addressed in this chapter, and the last question was addressed in Chapter 4.

3.5.1 General grouping of polycarbonates based on *in vitro* test data

Three group for the polycarbonate polymers were assigned based on *in vitro* performance data of MW degradation, polymer erosion and drug release: (i) low eroders/low releasers – E0400(1K), E0800(1K), E1200(1K), E0006(1K), E034.5(1K) and E094.5(1K), (ii) low eroders/high releasers – E0000(1K) and E0012(1K), and (iii) high eroders/high releasers – E0018(1K), E0313.5(1K), E0418(1K), E0609(1K), E0818(1K), E0913.5(1K), E1206(1K), E1212(1K) and E1218(1K). All DTM polycarbonate terpolymers and PLGA/polycarbonate blends tested in this study were also placed into the category of high eroders/high releasers.

3.5.2 MW degradation of polycarbonates

Zhu, et al., demonstrated that polymer degradation in the hydrated solid form of the amorphous homopolymer poly(1,3-trimethylene carbonate) was different when compared to its degradation in aqueous solution (88). The same result is expected for the tyrosine-based polycarbonates. Random bulk hydrolysis in degradable polymeric systems occurs when the rate of water uptake is greater than both the rate of chain scission of hydrolysable bonds and the rate of byproduct solubilization (89, 90). Bulk

degradation and erosion of monomers and oligomers with molecular weights ≤ 10 kDa was observed in the hydrated solid forms of the polycarbonate terpolymers.

The expected rate of hydrolysis from general organic chemistry theory for the six carbonate bonds present in polycarbonate homo-, co- and terpolymers are: the aromatic-aromatic carbonate bonds (e.g., DT-DT, DTE-DT, DTE-DTE) > aromatic-aliphatic carbonate bonds (e.g., DT-PEG, DTE-PEG) > aliphatic-aliphatic carbonate bonds (e.g., PEG-PEG). In spite of this expected ranking, Figure 3.12 and Figure 3.14 demonstrated that PEG_{1K} was preferentially eroded within the hydrated matrix during *in vitro* studies, indicating that PEG carbonate bonds were being preferentially broken. The finding is not surprising if the local water environment of these bonds is taken into account. There is a greater statistical likelihood that PEG carbonate bonds were located in the vicinity occupied by most of the water present within the hydrated matrix, as demonstrated by the SANS and SAXS data shown in Chapter 4. It is important to mention that the incorporation of the hydrophobic drug, with its tendency to repel water, did not change the water capacity of the polymer. For a given polymer mass, in the presence or absence of the drug, the water capacity remained approximately the same (refer to Table 8-8 in the Appendix). Measurements of the fractional molecular weight degradation of poly(DT carbonate) and poly(PEG_{1K} carbonate) indicated that the degradation rates for these two polymers were similar, as shown in Figure 3.22, and were much faster than the degradation of poly(DTE carbonate) (refer to Figure 3.3). The proposed order for polymer degradation in terms of the hydrolysis rate of the carbonate bonds in the <u>solid</u> hydrated form is PEG-PEG, DT-PEG, DT-DT > DTE-PEG > DTE-DT, DTE-DTE. This ranking was based on the results in Figure 3.2 and Figure 3.22 that showed the high PEG

containing terpolymers, poly(DT carbonate) and poly(PEG_{1K} carbonate) all degrading faster than DTE-co-PEG_{1K} copolymers, which in turn degraded faster than DTE-co-DT copolymers and poly(DTE carbonate). Background information on the hydrolysis and degradation of the polycarbonates containing PEG or DT is given by past researchers of the Kohn laboratory (32-34, 42). Cleavage of PEG-PEG, DT-PEG and DTE-PEG carbonate bonds was more likely to produce low molecular weight oligomers that could be readily solubilized and transported out of the bulk polymer.

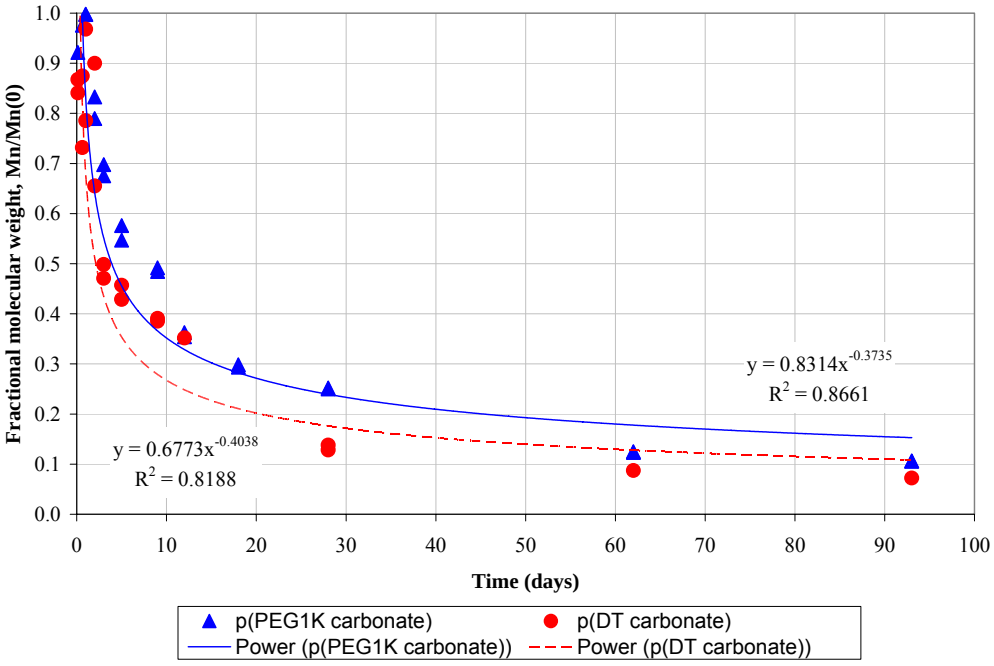

Figure 3.22. Fractional molecular weight degradation of poly(DT carbonate) and poly(PEG_{1K} carbonate) polymers during a 13 week incubation period in PBS at 37 °C. Sample size, n =2.

Modeling of the kinetics of random chain hydrolysis of degradable polymers was not attempted in this work due to insufficient data available on the actual rate of hydrolysis of the six carbonate bonds present in the hydrated solid form of the poly(DTR-

co- y% DT-co- z% PEG_{1K} carbonate). Excellent articles can be found in the scientific literature on hydrolytic degradation mechanisms that can assist future researchers on simulating the mechanism of degradation of the tyrosine-based polycarbonate homo-, co- and terpolymers (89, 91-95) once this data becomes available.

3.5.3 KDR from polycarbonates

Drug profiles of voclosporin delivery from the majority of polycarbonate copolymers were observed with at least two stages of release. The typical 24-hour burst of drug, often seen in other polymeric systems, did not occur in these systems. Instead, drug discharged from the polycarbonates followed sequential phases, where an early-stage release was characterized by an augmented diffusion mechanism, and a late-stage release was characterized by a steady state pure diffusion mechanism occurring at a lesser rate. Both stages of drug release could be mathematically described using classical Fickian diffusion, albeit having different coefficients for diffusion.

Early-stage drug release corresponded to a time associated with phase separation and relatively rapid removal of PEG_{1K} from the matrix for periods up to 4 weeks. The data collected during *in vitro* bench testing of these carriers indicated that this first stage had a complicated transport mechanism with contributions from polymer erosion, polymer swelling and polymer chain mobility during the phase separation of PEG_{1K} segments that was brought about by hydration. The second stage presented a simpler mechanism whereby the hydrophobic drug, sequestered within the DTE-co-DT hydrophobic segments of the matrix, slowly diffused out at a rate proportional to the low water content present in these local regions. The drug release characteristics for the polycarbonate terpolymers, classified as Group E polymers in Section 3.2.2, were

consistent with the proposed mechanisms. These polymers – E00012(1K), E0018(1K), E1206(1K), E0609(1K), E1212(1K), E0313.5(1K), E0913.5(1K), E0418(1K), E0818(1K), E1218(1K) – comprised of DTE-co-PEG_{1K} copolymers with a PEG_{1K} content ≥ 12 mole %, and DTE-co-DT-co-PEG_{1K} terpolymers with a PEG_{1K} content ≥ 6 mole %, all had persistence factors ranging from 0.40 to 0.49 (refer to Table 8-4 in the Appendix) that demonstrated the dual stage of drug release. The remaining polycarbonates in the set of seventeen polymers were either too low in PEG_{1K} content or contained no PEG, and therefore did not have sufficient water uptake capacity to enhance drug diffusion. Two polycarbonates from the remaining set were noteworthy, even though they were not ideal long-term degradable carriers for voclosporin. The first is the homopolymer E0000(1K) which displayed different characteristics compared to the other polymers. This polymer had a single-stage diffusion-controlled drug release profile (linear relationship with the square root of time) for 27 weeks. During this time, the water uptake within the matrix was low, the sample dimensions remained constant (visual observation), the polymer molecular weight rate of change was relatively small compared to the terpolymers (refer to Figure 3.3), and the polymer erosion was negligible (refer to Figure 3.11). Voclosporin mobility was limited by the drug solubility in the low amount of free water present throughout this matrix. A slowdown in drug transport (i.e., drug retention) was only observed after a 27 week period, possibly due to the conversion of a number of DTE segments to DT. The second noteworthy set of polymers to mention is the DTE-co-DT polycarbonates. These materials also had low water uptake (due to the lack of PEG content) and negligible polymer erosion, but showed a significant reduction in their ability to release voclosporin as the percentage of DT within these compositions

was increased from 4 to 12 mole %. This observation was the first indication of a possible interaction between the drug molecule and the DT chain segments of the polymer.

Computer simulations of the drug release data using semi-empirical models from the literature were not performed since test samples did not retain constant dimensions during prolonged hydration in PBS at 37 °C. The lack of dimensional stability was especially noticeable in PEG-containing polycarbonate co- and terpolymers, where swelling and flowing of the solid hydrated mass occurred. Distortion in the homopolymer poly(DTE carbonate) and the DTE-co-DT copolymers matrices were less apparent due to lower water uptake, however these polymers were not good carriers for voclosporin (very low rate of polymer erosion for E0000(1K) and retention behavior for DTE-co-DT copolymers). Drug release from poly(DT carbonate) was not tested since this composition dissolved within a few days in PBS, "dumping" all of its drug content into the release media.

3.5.4 Erosion behavior of polycarbonates

The removal of polymer degradation byproducts from the carrier was considered as an example of a reaction-diffusion system where the polymer chain was first broken down into low molecular weight oligomers and monomers, followed by species diffusional transport out of the matrix. A combination of polymer swelling and chain cleavage within the high-PEG containing terpolymers was responsible for removing dissolved drug and oligomers/monomers from the matrix within the first week of hydration. In high degrading polymers, this was manifested as the curved regions of the KDR profiles shown in Figure 3.23. Although not explicitly shown, the oligomers and

monomers formed during this time should also have similar profiles for mass loss. The access of water into these systems was necessary to enable both drug release and polymer resorption, where most of the water molecules were mainly associated with the oxygen atoms on the PEG chains. Water molecules do access hydrophobic polymers, but in very low amounts (approximately 5 wt % uptake or less), and can hydrolyze the ester groups of the DTR and all carbonate bonds in the chain. The statistical likelihood of water being in the vicinity of the oxygen molecules on PEG, based on its quantity and association, favored the preferential cleavage of PEG.

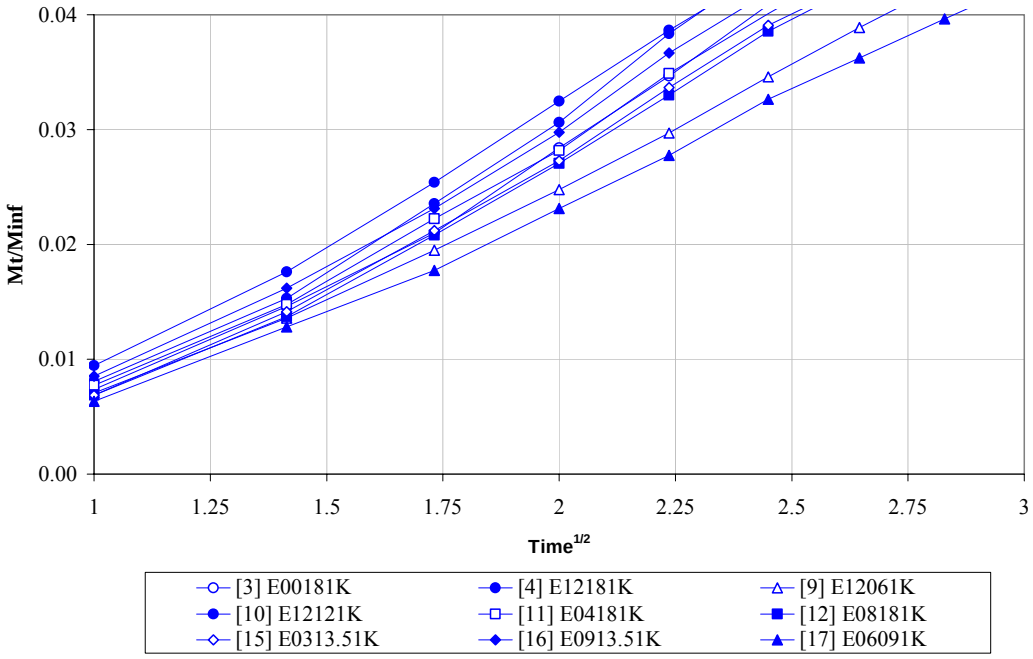

Figure 3.23. KDR profiles of high eroding/high releasing polycarbonate terpolymers loaded with 30 wt. % drug in PBS at 37 °C. Lines connecting data points are for visualizing curvature in profiles.

A linear relationship between the mole % of PEG_{1K} in the polycarbonate terpolymers and its dry T_g was an interesting finding that allowed the determination of

PEG_{1K} content in an unknown composition from the same family of polymers. Data from the dry T_g determination was used to calculate the PEG erosion rate from E1218(1K) during hydration (loss of PEG_{1K} = 0.034 mole % per day) and was compared to the PEG erosion rate as measured by ELSD in Section 2.2.13 (loss of PEG_{1K} = 0.028 mole % per day). The result indicated that the dry T_g method was adequate for estimating the changing PEG_{1K} content in the degrading polycarbonate terpolymer. For E1218(1K), a non-linearity in PEG_{1K} loss was confined only to the first week of hydration. During this time, there was a "burst" of PEG from the matrix, which then settled down to a constant erosion rate up to 15 weeks, followed by a slowdown in PEG removal (refer to Figure 3.14). The linear loss of PEG was a good indication of the polymer resorption stability during this time aiding in the controlled release of drug from its matrix. The slowdown in PEG loss after 15 weeks was attributed to the formation of a fully phase separated matrix system, where PEG domains became trapped within a hydrophobic exterior. Calculation of the PEG_{1K} content in E1218(1K) terpolymer using the dry T_g method showed that there was ~16.6 mole % of PEG remaining after 4 weeks of hydration. The 4 week time point corresponded to the transition time from early to late stage drug release for this polymer. This PEG content was insufficient to prevent drug retention onset due to its microphase separation within the matrix. Based on extrapolation of the latter portion of the E1218(1K) dry T_g curve from Figure 3.14, and using Eq. 3.1, the PEG_{1K} content of the terpolymer was estimated to be ~12.4 mole % after 32 weeks of hydration. At this time point the carrier was releasing very low daily amounts of drug at a steady rate. Initially at day zero, a terpolymer containing ~ 12 mole % PEG_{1K} would have been an average performer for both drug release and polymer

erosion, yet after 32 weeks of hydration the performance potential of this composition seemed to have changed. At 32 weeks, drug loading in E1218(1K) was estimated between 30 to 40 wt.% using the data given in Table 3-2, Table 8-3, Table 8-6 and Table 8-8, indicating that drug loading was high enough to be a driving force for diffusion.

There are several examples that demonstrated a synergistic relationship between DT and PEG_{1K} on polymer mass loss. Table 3-5 shows the average cumulative fractional erosion measurements taken from Figure 3.11 for DTE-co-DT copolymers (row labeled as 0 % DT), DTE-co-PEG_{1K} copolymers (column labeled as 0 % PEG_{1K}) and the polycarbonate terpolymers E1206(1K), E1212(1K), E0418(1K), E0818(1K) and E1218(1K). The total erosion measured for each terpolymer shown in the table was not equivalent to the summation of the total erosion of the corresponding DTE-co-DT + DTE-co-PEG_{1K} copolymers. For example, the fractional erosion of E1200(1K) + fractional erosion of E0018(1K) was 0.0016 + 0.2929 = 0.2945. The measured fractional erosion for E1218(1K) was 0.4843, which was 1.6 times larger. Similar calculations for other terpolymers yielded total erosion values for E1206(1K), E1212(1K), E0418(1K) and E0818(1K) that were 18.6, 3.2, 1.3 and 1.7 times larger than the sum of their corresponding copolymers.

Table 3-5. Average 32-week cumulative fractional polymer erosion of polycarbonates loaded with 30 wt.% voclosporin and incubated in PBS at 37 °C.

		PEG_{1K}			
		0 %	**6 %**	**12 %**	**18 %**
DT	**0 %**	--	0.0136	0.1358	0.2929
	4 %	0.0003	--	--	0.3912
	8 %	0.0008	--	--	0.4867
	12 %	0.0016	0.2823	0.4393	0.4843

3.5.5 Drug retention in polycarbonates

DT incorporation into the polymer composition had two main disadvantages. An increase in DT content of the polymer, in the absence of PEG_{1K}, resulted in an increased dry T_g. Higher processing temperatures up to 130 °C were required for compression molding. However, short exposure times ≤ 10 minutes at this higher temperature were utilized and did not have a significant effect on drug stability. Higher DT content, in the absence of PEG_{1K}, also had the undesirable effect of drug retention within the polymer matrix. An emerging hypothesis for retention of voclosporin in terpolymers was that an association between DTR-co-DT and drug, which forms during the reorganization of the polymer chains within the matrix during hydration-induced phase separation, may contribute to the immobilization of the drug (to be discussed in Chapter 4). It is important to remember that even if the DT monomer was not directly synthesized into the polymer composition, DTR would eventually hydrolyze to form random DT regions within the polymer chain. The presence of initial amounts of DT in terpolymers did not speed up the formation of these hypothesized polymer-drug interactions. This is evident from the fact that DTE-co-DT-co-PEG_{1K} terpolymers went into drug retention at times that were comparable to their corresponding DTE-co-PEG_{1K} copolymers. For example, the drug retention onset for terpolymers E1206(1K), E1212(1K), E0418(1K), E0818(1K) and E1218(K) were 18, 21, 16, 17 and 23 days, respectively, and the drug retention onset for the corresponding copolymers[4] E0012(1K) and E0018(1K) were 10 and 18 days, respectively (refer to Table 8-4 in the Appendix).

[4] The experimental data for the copolymer E0006(1K) did not show the expected drug retention behavior.

The retention of voclosporin in the polycarbonates was prominent in DTE-co-DT copolymers. It is now know that microphase separation occurred in these systems (refer to Chapter 4) during sample preparation and may have prevented drug release. However, an interesting speculation is that development of microphase separated structure might have occurred during late-stage release in PEG-containing co- and terpolymer carrier systems. Further discussion of this idea is presented in Chapter 4.

3.5.6 Correlation between KDR and erosion

Guidance for optimizing drug release as a function of the erodible nature of the polycarbonate composition was explored using response surface methodology. The empirically generated contour maps shown in Figure 3.9 and Figure 3.13 indicated a preferred direction to move for optimizing both voclosporin release and the concomitant polycarbonate terpolymer resorption. This information was tempered by the fact that higher levels of DT and PEG_{1K} within the composition led to rapid polymer fragmentation and drug burst. For example, polymers with composition limits greater than E1218(1K), such as E2418(1K), E4018(1K), E6018(1K) and E1230(1K), were unsuitable carriers that either broke into small pieces or quickly dissolved, dumping solid drug particles into the buffer solution that created erratic drug release profiles. Based on the response surface maps, the polycarbonate terpolymers having PEG_{1K} content between 9 and 24 mole % and DT content between 8 and 12 mole % were selected as the most useful and stable carrier systems.

3.5.7 Utility of PLGA in polycarbonate formulation

The degradation and bulk erosion characteristics of PLGA polymers are widely studied since these materials are often used as drug delivery vehicles (87, 90, 96). These PLGA matrices by themselves were unsuitable for the controlled delivery of voclosporin due to the presence of a lag phase for drug release and the ensuing drug burst caused by rapid polymer degradation. However, the controlled drug release at target levels was achievable when PLGA was blended with the tyrosine-based polycarbonate terpolymers. The degradation process of PLGA was observed to begin at a time when the PEG-containing polycarbonate was beginning to enter its drug retention phase. Blending of these two polymers had an interesting effect of lowering the maximum daily drug release rate from selected terpolymers from ~20 μg/day to ~10 μg/day and extending the effective release time for a total of ~ 60 to 90 days at the dose of 5 to 10 μg/day before drug retention settled in. In these hydrated blended carriers, there was no lag phase; instead, drug release was thought to occur predominantly from the mobility of PEG segments within the polycarbonate chains (refer to Chapter 4), albeit at a lower daily amounts. PLGA is known to autocatalyze its hydrolysis after a lag period from an increase in local pH (87, 96). The combination of these two polymers was revealed as the most promising candidate for use a controlled delivery platform. It is expected that further extension of drug release times can be attained by blending various compositions from the PLGA family with various combinations of the polycarbonate terpolymer family into a cocktail formulation of polymers in order to produce a zero order drug release system.

3.5.8 Other methods for enhancing drug release from polycarbonates

Other strategies for influencing drug release were investigated, such as (i) the use of high DT-containing polycarbonate terpolymers to create a highly porous matrix, (ii) the physical blending of PEG acting as a poragen within the polycarbonate, (iii) the physical blending of surfactants within the polycarbonate terpolymer to compatibilize the formulation, (iv) the use of newly synthesized polycarbonate terpolymers based on DTM, and (v) the use of newly synthesized polycarbonate terpolymers based on pendant PEG. For the first idea, higher DT content > 40 mole % within terpolymer compositions containing 18 mole % PEG_{1K} provided an excellent means for making highly porous hydrated solid structures (refer to Figure 3.24), however these matrices quickly dissolved within hours in PBS at 37 °C and were unsuitable for long-term drug delivery applications.

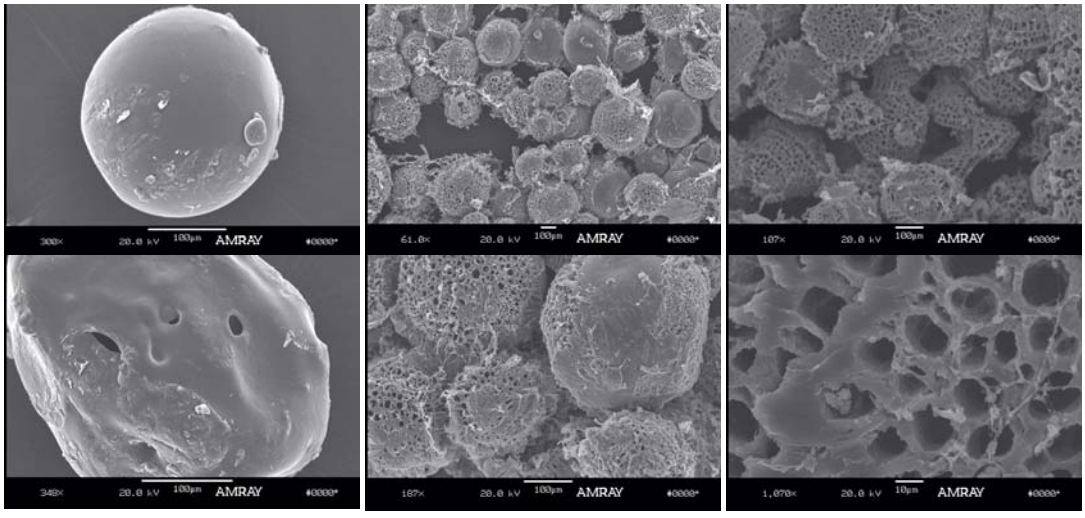

Control (no treatment) **10 min in PBS at 37°C** **20 min in PBS at 37°C**

Figure 3.24. SEM images of E4018(1K) microspheres loaded with 30 wt.% voclosporin incubated in PBS at 37 °C.

In the second idea, two PEG molecular weights, PEG_{35K} and PEG_{100K}, were physically mixed within E1200(1K) at a polycarbonate:PEG weight ratio of 7:3, containing a drug loading of 30 wt. % (per weight of total polymer) using the fabrication method outlined in Section 2.2.10. E1200(1K) was chosen since this carrier did not release voclosporin. Rapid dissolution of the high molecular weight PEG molecules during hydration of the test samples in PBS at 37 °C were used to create a porous network within the matrix to augment drug release. Drug release was enhanced, however the samples deteriorated after 2 to 3 weeks by fragmentation, releasing solid particulates of drug. For the third idea, three surfactants – Tween® 20, Tween® 80 and Span® 80 – were physically mixed into 30 wt. % drug loaded E1818(1K) at a weight ratio of 9:1 (polycarbonate:surfactant) using the fabrication method outlined in Section 2.2.10. There was no apparent benefit in voclosporin release from these formulations, and there was some indication of irregularity in the release profiles. For the fourth idea, DTM polycarbonates were synthesized, then loaded with 15 wt. % of drug using the fabrication method outlined in Section 2.2.10. The idea behind the use of DTM was to increase the resorption characteristics of the matrix and enhance the drug release property of these polycarbonates since DTM is approximately 10 times more water soluble than DTE. *In vitro* KDR studies revealed no statistically significant difference between drug release behavior of comparable DTM and DTE polycarbonates (refer to Section 3.3). For the final idea, M12-g-18(1K) polymer was synthesized. The symbol 'g' indicates that PEG was attached through an amide bond as a pendant group instead of being located within the backbone of the polymer chain. The polycarbonate was formulated with a drug loading of 15 wt. % using the fabrication method outlined in Section 2.2.10. The

innovation behind this composition was to impede the preferential loss of PEG during polymer erosion through the use of the more stable amide linkage (for *in vitro* studies), thereby preventing drug retention from occurring[5]. However, the polymer was rapidly dissolved within 48 hours in PBS at 37 °C and its drug cargo was completely released within the same time. The preliminary findings from these five ideas are considered useful methods for drug delivery but will require extensive investigations that are outside the scope of the present work.

The controlled release of drug from bulk eroding polymers is commonly modeled with an augmentation of species diffusion by the formation of a porous network within the polymer structure (97). This is not the case for the PEG-containing polycarbonate terpolymers used in this study. Lack of a stable porous network in these systems, the flowing nature of these hydrated solid polymers, the hydration-induced phase separation of PEG (refer to Chapter 4) and the possibility of an interaction between the drug and hydrophobic segments of the polymer chain make these modeling strategies obsolete. It is not yet possible to gain mechanistic insight of drug release through computational simulations for this complex system until a more fundamental understanding of the morphology of the tyrosine-based polycarbonates in dry and wet conditions, and in the presence and absence of voclosporin, is obtained. The next chapter in this thesis will begin to address this need.

---

[5] The assumption at the time was that the preferential loss of PEG made the matrix more hydrophobic, causing drug to be retained in the polymer.

4 Hydration behavior of PEG-containing polycarbonate terpolymers in the presence and absence of a hydrophobic peptide

The main goal of this chapter is to investigate the changes in the physical structure of the PEG-containing polycarbonate terpolymers during incubation in water. Knowledge of the dynamics of polymer morphology in the hydrated state will aid in explaining the release characteristics of the voclosporin molecule from the matrix. Background information pertinent to this effort relates to understanding the propensity for incompatible hydrophobic and hydrophilic polymeric domains to spontaneously phase separate, and how water might convert a miscible amorphous copolymer system, such as the tyrosine-based polycarbonates, into phase separated domains. General information and examples on hydration in PEG-containing polymers (98-101) and the theory of water clustering in polymers (102-108) are cited for additional reading.

The physical changes occurring within the tyrosine-based polycarbonates in their hydrated states were measured using neutron and x-ray scattering techniques. These methods provided information on the long-range ordering of the polymer chains and revealed a hydration-induced phase separation in PEG-rich polycarbonate terpolymers.

Examples from the literature on the determination of polymer morphology of biodegradable PEG-containing materials are given. Cohn and Salomon (109) used WAXS to measure the phase separation in a family of novel poly(ether-ester-urethane) multiblock copolymers containing PLLA-PEG-PLLA triblock segments. In the dry state, phase separated domains were manifested as crystalline peaks at q values of 1.22 and 1.67 $Å^{-1}$ for the PLLA and PEG blocks, respectively. Relatively long lengths of the

hydrophobic PLLA blocks were able to suppress PEG crystallinity in these copolymers, and a broad amorphous interference peak was obtained when the lengths of PLLA and PEG were both relatively low. Petrova, et al. (110), investigated WAXS profiles of multiblock copolymers containing poly(ε-caprolactone) and PEG, also showing spontaneous phase separation in the dry state. However, high PEG content, in this case, was able to prevent crystallization of the relatively hydrophobic polycaprolactone blocks. The effect of water on the apparent disruption of PEG crystallinity, that existed in the dry state for non-degradable hydrogels containing hydrophilic PEG blocks and hydrophobic blocks of either poly(tetramethylene oxide) or poly(dimethyl siloxane), was shown in DSC studies by Park and Bae (111). These examples demonstrate the delicate balance of polymer chain morphology in a set of seemingly simple polymeric systems that depended on their chemistry, processing history and environment. The underlying idea is that polymer chains have mobility that can be influenced by many factors, such as their molecular weight, the local hydrophobic-hydrophilic repulsion, or competitive hydrogen bonding with water molecules.

In Section 4.1 of this chapter, the development of water-rich domains was demonstrated by SANS in the series of seventeen polycarbonates composed of homo-, co- and terpolymers of DTE. Section 4.2 describes the morphological changes in these polymers over time during hydration at body temperature, by calculating the change in spacing between the hydration-induced phase-separated PEG domains obtained by SAXS and the polymer-polymer interchain distances obtained by WAXS. In addition, it is shown that the drug molecule was intercalated with the polymer chains during dry and wet conditions. Finally, preliminary evidence of microphase separation of DTE-co-DT

and drug, as well as the irreversible nature of hydration-induced phase separation within the PEG-containing polycarbonates, is presented. The formation of segregated domains was an important finding that explained voclosporin retention in the polycarbonates during late-stage *in vitro* drug release. Computer modeling of the conformation of DTE-co-DT/drug interaction is explored in Section 4.3 in order to determine if the polymer chain spacing measured by WAXS can be reproduced *in silico*. Section 4.4 describes the disadvantages of the established biomaterial PLGA to function as a carrier for the voclosporin molecule. The re-crystallization of drug was demonstrated from the degrading PLGA structures. This data, along with the drug release profiles for PLGA in Chapter 3, were used to support the argument that PLGA, when used alone, was not suitable for controlled release of the drug. A proposed theory for voclosporin release from the hydrated polycarbonate terpolymers is discussed in Section 4.5.

4.1 Examination of the short-term hydration behavior of polycarbonates with and without voclosporin using SANS

The data in this section cover SANS measurements of phase separated hydrophilic structural domains that occur during short-term hydration of DTE polycarbonate polymers in the presence and absence of drug. Figure 4.1 is a plot of the neutron scattering intensity, I(q), as a function of the scattering vector, q, for E1218(1K) hydrated in deuterated PBS at 37°C with and without 30 wt.% voclosporin at four times of incubation – 1, 2, 25 and 60 hours. The figure demonstrates two important features observed in polycarbonate copolymers that have PEG_{1K} content greater than 6 mole %. First, the presence of domains containing deuterated water was manifested as broad interference peaks, where the q values were related to the average spacing of clustered

spherical[6] water domains estimated to be 10 nm in diameter using the ZP model given by Laity, et al. (85). These clusters of water-rich spheres are believed to mobilize the PEG segments of the terpolymer, causing a hydration-induced phase separation of PEG from the surrounding hydrophobic chain sections of DTE and DT. The fact that the dry state of polycarbonate terpolymers, with or without drug, showed no indication of phase separation[7] supported this claim. Similar hydrated clusters and other complex behavior of water have been observed in other amorphous polymers (103, 105, 112).

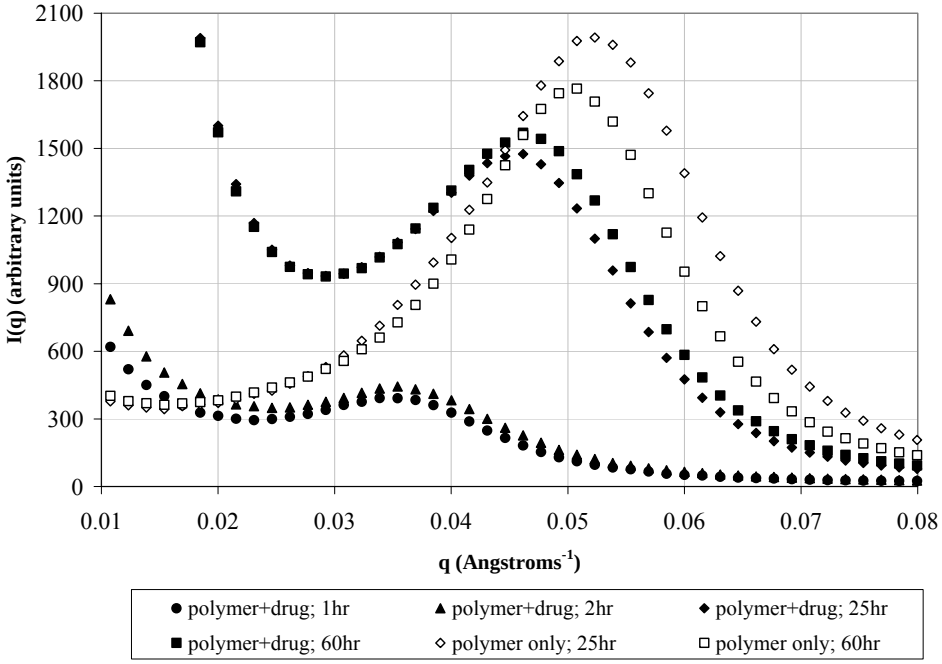

Figure 4.1. Plot of intensity, I(q), versus the scattering vector, q, for E1218(1K) with and without 30 wt.% voclosporin hydrated in deuterated PBS at 37°C. The q range for the data set was 0.007 to 0.154 Å^{-1}.

[6] Spherical shapes have the lowest surface to volume ratio that can minimize contact with the surrounding hydrophobic matrix.

[7] No interference peaks were obtained for any of the PEG-containing polycarbonates. These results are presented in Section 4.2.

Second, there was a central diffuse scattering (CDS) at very low q values which was much broader and more intense than what was observed in samples with less than 6 mole % PEG. This CDS[8] was only apparent in drug-loaded copolymers. The CDS was attributed to large isolated domains of water, referred to colloquially as "islands" of water, that were segregated within the matrix by the combined hydrophobicity of the drug molecules and the DTR regions of the polymer. The average size of these islands, assumed to be spherical[6] in shape, was estimated to be 100 nm in diameter using the extended ZP model described in Chapter 2 Section 2.4. The interference peaks attributed to the clusters of water domains, and their corresponding spacing in Å given in brackets, for the hydrated E1218(1K) polymer containing drug occurred at increasing q values of 0.034 [185], 0.035 [180], 0.046 [137] and 0.046 [137] $Å^{-1}$ for increasing incubation times of 1, 2, 25 and 60 hours, respectively. This unexpected trend[9] of smaller water domain separation within the clusters at the incubation times tested in the SANS study suggested that the water domains were being packed even though the polymer was continually swelling. The corresponding interference peaks for the hydrated E1218(1K) polymer samples in the absence of the drug occurred at relatively higher q values of 0.052 [121] and 0.051 [123] $Å^{-1}$ for incubation times of 25 and 60 hours, respectively, showing even tighter packing of the water domains. The presence of the hydrophobic drug molecule was shown to reduce the packing efficiency of water molecules in the matrix.

The q values and their equivalent interdomain spacing for interference peaks of the seventeen hydrated polycarbonates, with and without drug, are compiled in the

---

[8] The CDS peak is suppressed if a Lorentz correction is perfomed on the data. This correction was not performed on any sample in order to clearly demonstrate the presence of the CDS.

[9] SAXS measurements of these polycarbonates at extended times up to 7 weeks of hydration showed that the spacing within PEG domains increased with time.

Appendix in Table 8-7. The domain spacing, d (in Å), was calculated using the Bragg relationship:

Eq. 4.1: $$\text{Bragg spacing, } d = \frac{2\pi}{q_{max}}$$

The homopolymer E0000(1K), all DTE-co-DT copolymers, DTE-co-PEG_{1K} copolymers with a PEG content ≤ 6 mole % and DTE-co-DT-co-PEG_{1K} terpolymers with DT content ≤ 9 mole % and PEG_{1K} content ≤ 4.5 mole % exhibited no interference peak which indicated that their water content was either too low to cause phase separation or the water domain spacing was beyond the length scale of SANS. The only exception to this generalized statement was for the polymer E0006(1K). In the absence of the hydrophobic drug, this polymer has a detectable interference peak at relatively low q.

Figure 4.2 is the plot the neutron scattering intensity, I(q), versus the scattering vector, q, for the 25-hour hydrated E1218(1K) polymer loaded with 30 wt.% voclosporin, fitted with the extended ZP model to capture the CDS at low q (0.008 to 0.018 $Å^{-1}$) and the interference peak at q = 0.046 $Å^{-1}$. The Pearson correlation coefficient, r, for the fit was 0.9978. The fitted parameters from the extended ZP model provided an estimation of the radius of the spherical domains in water clusters (~ 54 Å), the spacing of these domains (~ 112 Å), the deviation of the interdomain spacing σ (~ 36 Å) and the R_g of the islands of water (~ 155 Å). The calculated Bragg spacing for drug loaded E1218(1K) polymer were close to the parameters calculated from the regular ZP model fit given in Table 8-8. However, these values were underestimated by 8 to 36 % when compared to the domain spacing calculated by the Bragg relationship. The distances obtained from

the Bragg relationship were considered to be a more accurate estimation of interdomain spacing since the ZP model is limited to one-dimension. This underestimation should be considered when evaluating all fitted values from the regular or extended ZP models.

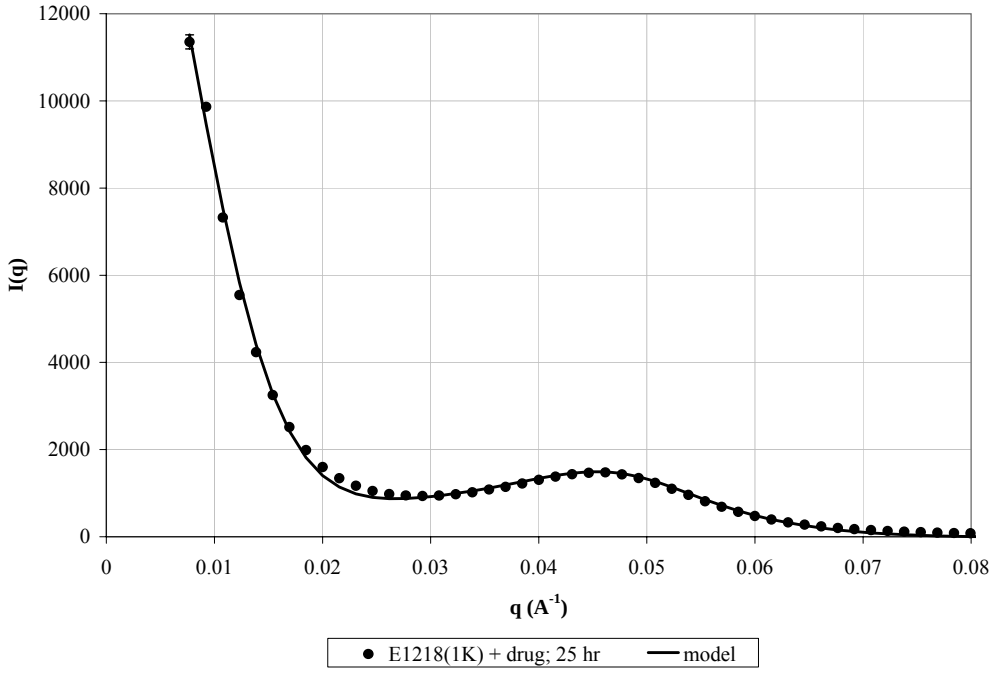

Figure 4.2. Extended ZP model fit (solid line) for E1218(1K) copolymer containing 30 wt.% voclosporin hydrated in deuterated PBS at 37°C for 25 hours. The q range for the data set was 0.007 to 0.154 $Å^{-1}$.

The size (approximated as average spherical domains of radius, R) and spacing of domains within water clusters obtained by curve fitting the SANS data to the ZP model were evaluated for general trends based on the PEG content within the polycarbonate compositions. PEG content was assumed to be proportional to the amount of water absorbed within these polymers. Figure 4.3 is the plot of the size of these hydrophilic domains within the seventeen hydrated polycarbonates versus the weight percent of water uptake during the short-term hydration of 25 and 60 hours in the presence and absence of

30 wt.% voclosporin. The percent water uptake in drug loaded polycarbonates was normalized to the actual weight of polymer in these samples. In general, all polycarbonates that exhibited interference peaks were approximated as having spherical hydrophilic domains with radii ranging from 40 to 65 Å (or with diameters ranging from 80 to 130 Å). The only exception was for the E0006(1K) samples which had radii of approximately 75 Å. No strong correlation (r = 0.316) was observed between water uptake and the size of the hydrophilic domains within the water clusters during the relatively short hydration times.

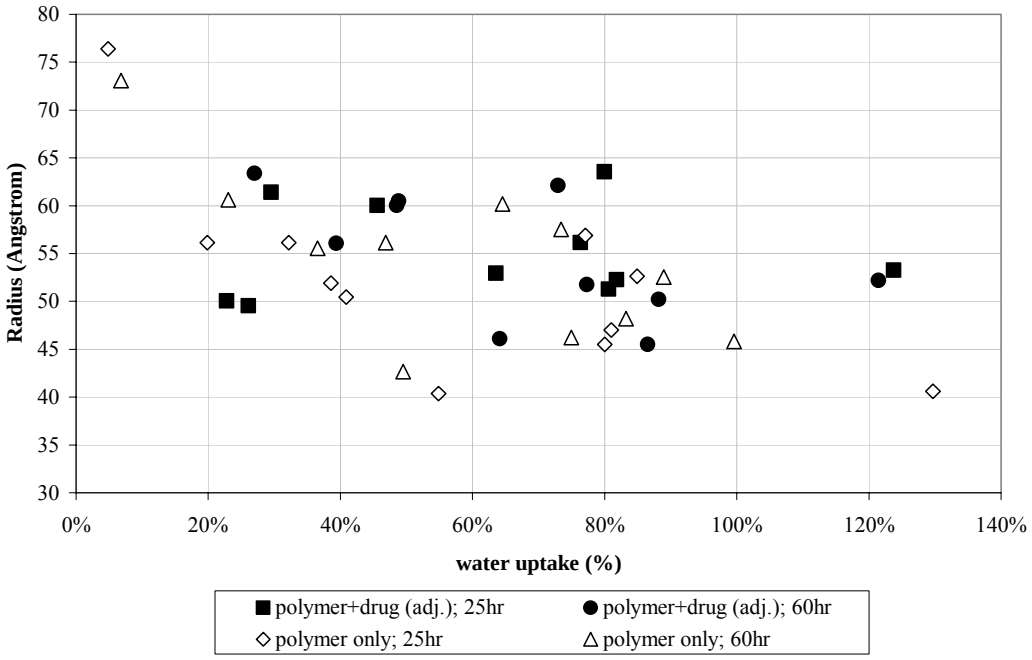

Figure 4.3. Radius of domains in water clusters at different percent water uptake for polycarbonates incubated in PBS for 25 and 60 hours at 37°C. Radius obtained from curve fitting experimental data to ZP model.

Similarly, Figure 4.4 shows the corresponding plot of the spacing of these hydrophilic domains within the seventeen hydrated polycarbonates versus the weight percent of water uptake during 25 and 60 hours of hydration, in the presence and absence of 30 wt.%

voclosporin. In general, all polycarbonates that exhibited interference peaks were approximated as having interdomain spacing ranging from 100 to 180 Å, with the exception of the E0006(1K) polymer which had a spacing of 223 to 244 Å. As before, no strong correlation (r = 0.196) was indicated between water uptake and interdomain spacing within the water clusters of the hydrated polycarbonates. These findings suggested that the water domains sequester in the same manner, regardless of their initial amount, in compositions with ≤ 18 mole % PEG_{1K}. In other words, during the short term incubation in water, there is continual nucleation of water domains within the clusters in PEG-containing polycarbonates. In the presence of the hydrophobic drug molecule, in addition this nucleation, growth or coalescence of these domains was observed. The values of the calculated parameters Io, R, d and σ for all polycarbonates, with and without drug during short-term hydration in PBS, is given in the Appendix in Table 8-8.

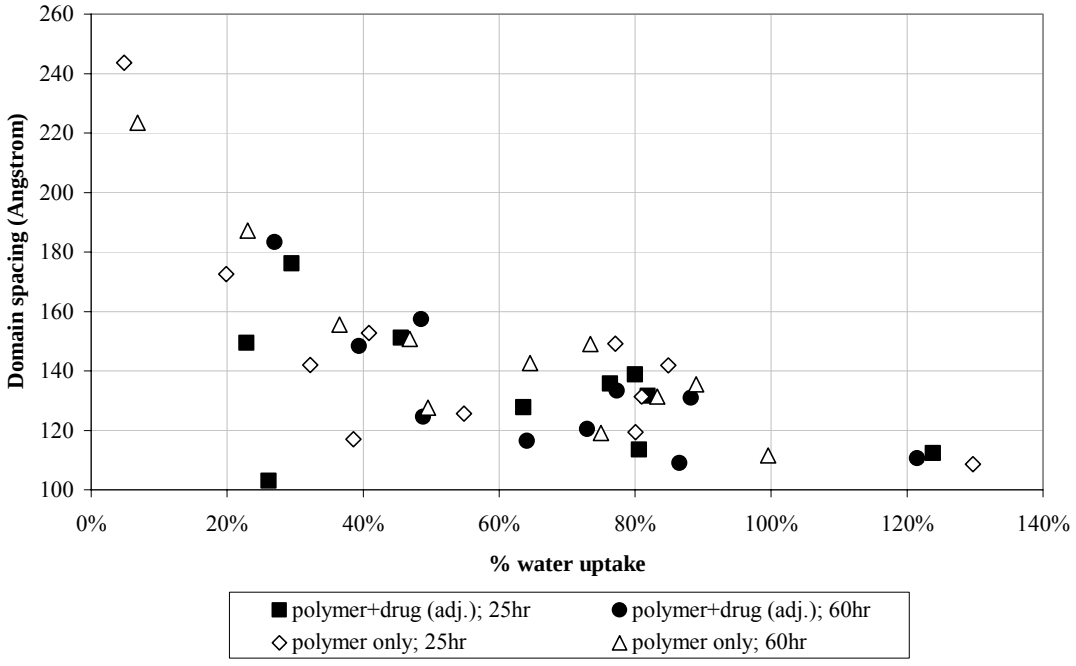

Figure 4.4. Spacing between domains in water clusters at different percent water uptake for polycarbonates incubated in PBS for 25 and 60 hours at 37°C. Spacing obtained from curve fitting experimental data to ZP model.

Lastly, it was discovered that the structural domains of water in the PEG-containing polycarbonates began to occur within minutes of incubation with water. Figure 4.5 is the plot the neutron scattering intensity, I(q), as a function of the scattering vector, q, for the time evolution of hydrated domains in the polymer E1218(1K) containing 30 wt.% voclosporin with SANS scans taken sequentially at time intervals of 30 to 120 seconds during a period of two hours in deuterated PBS at 37°C. The figure demonstrated the rapid penetration of water into the polymer and rapid mobility and redistribution of water molecules that initiated the formation of phase separated domains. Shortly after contact with water, the interference peaks and CDS became detectable and both continued to grow in intensity. The interference peak, initially developed at q ~ 0.039 $Å^{-1}$, first shifted towards a lower q (~ 0.035 $Å^{-1}$), then towards a higher q as shown

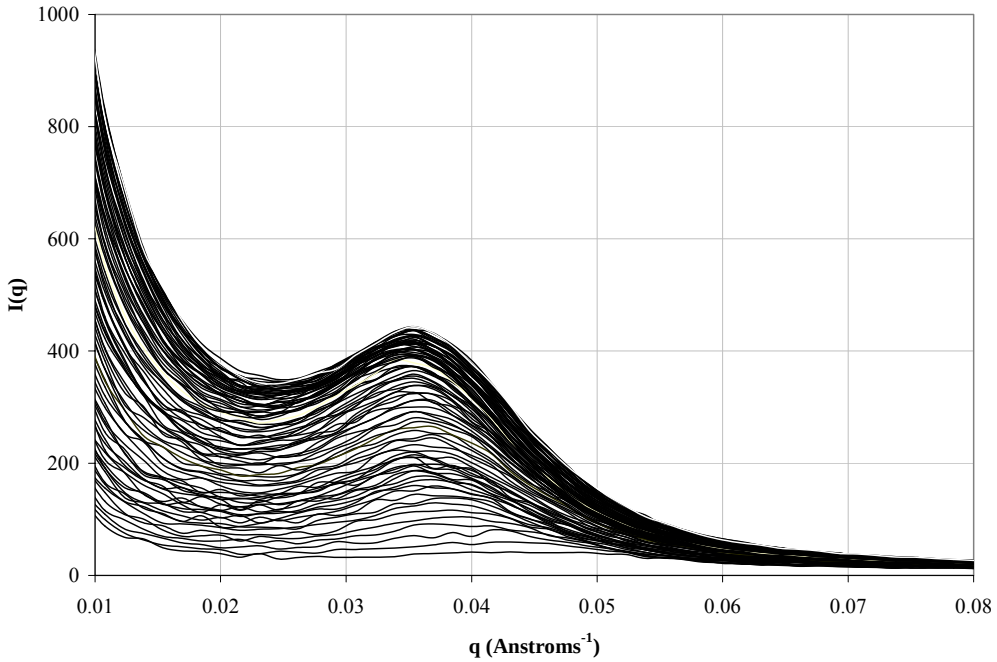

Figure 4.5. Time evolution for the hydration of E1218(1K) containing 30 wt.% voclosporin in deuterated PBS at 37°C. Each scan was taken at time intervals of 30 to 120 seconds during a two hour period.

in Figure 4.1. The formations were attributed to the random nucleation, growth and redistribution of PEG segments of the polymer chain, with the accompanying exclusion of the hydrophobic DTR segments from these water-rich regions.

4.2 Examination of physical structure of hydrated polycarbonates with and without voclosporin using SAXS/WAXS

Polymer morphology during long-term hydration studies of the DTR polycarbonate homo-, co- and terpolymers, in the presence and absence of drug, was examined using small and wide angle x-ray scattering measurements. Section 4.2.1 describes the results obtained from probing the phase separated interdomain size and spacing at a length scale of approximately 1000 Å down to 40 Å (q range ~ 0.006 to 0.157 $Å^{-1}$) by SAXS. The technique of SAXS is complementary to SANS, where the former is able to distinguish the higher electron density from PEG segments over the DTR regions in the polymer, and the latter uses deuterated water to provide contrast to distinguish it within the polymer matrix. The existence of an interference peak using both techniques is a confirmation that water molecules infiltrated the polymer matrix in the PEG regions, and caused mobility of PEG and the ensuing hydration-induced phase separation of PEG chain. The fact that there is no interference peak in the dry state of the polymers confirmed this phenomenon. Section 4.2.2 describes the results obtained from probing the polymer interchain spacing at a length scale of approximately 15 Å down to 2 Å (q range ~ 0.419 to 3.142 $Å^{-1}$) by WAXS. The data demonstrated that drug was intercalated within the hydrophobic regions of the polymer during fabrication and remained there, for the most part, during hydration of the matrix. Additionally, the

spacing between polymer chains with and without intercalated drug remained constant during incubation in PBS at 37 °C for the duration of the study.

4.2.1 SAXS analysis of hydrated structure of polycarbonates with and without voclosporin

Figure 4.6 is a plot of the x-ray scattering intensity, I(q), versus the scattering vector, q, for E1218(1K) loaded with 30 wt.% voclosporin and incubated in PBS at 37°C at three times – 1, 4, and 7 weeks. The figure is representative of the data gathered for polycarbonate co- and terpolymers having a PEG content ≥ 6 mole %, with or without the drug molecule. For the drug loaded E1218(1K), all wet samples had broad interference peaks, indicative of phase separated PEG regions, located at decreasing values of q of approximately 0.042 [150], 0.033 [193] and 0.017 [370] $Å^{-1}$ for increasing hydration

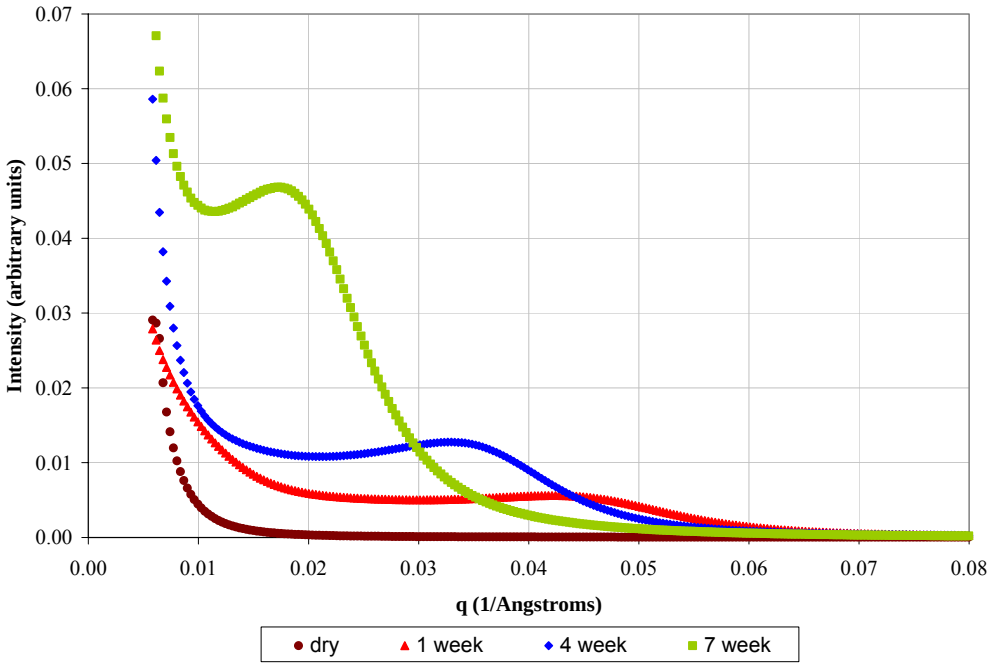

Figure 4.6. SAXS plot of intensity I(q) versus q for E1218(1K) containing 30 wt.% voclosporin, both dry and in wet conditions in PBS at 37 °C.

times of 1, 4 and 7 weeks, respectively. These q values can be converted into interdomain spacing in Å, as shown in square brackets, using the Bragg relationship given in Eq. 4.1. Included in the figure is the SAXS profile for the dry drug loaded polymer which did not show an interference peak.

The values of the interdomain distances for all polycarbonates, with and without drug, in dry and wet conditions are compiled in Table 8-9 of the Appendix. In the dry state, all polycarbonates lacked an interference peak, with the exception of poly(PEG_{1K} carbonate) and the drug loaded DTE-co-DT copolymers. The E0000(1K) did not manifest an interference peak during wet or dry conditions which was expected since this polymer is composed of a single hydrophobic monomer. By themselves, the DTE-co-DT copolymers did not produce interference peaks either in a dry or wet condition which was also not surprising since both monomers were similar in nature. However, these copolymers did show interference peaks in the dry and wet states only in the presence of the drug. This finding suggested that the DTE-co-DT regions of the polymer and the hydrophobic voclosporin molecule had undergone microphase separation. Figure 4.7 is a plot of the x-ray scattering intensity, I(q), versus the scattering vector, q, for the dry DTE-co-DT copolymers containing 30 wt.% voclosporin. The interference peaks were located at approximate q values of 0.012 [524], 0.010 [628] and 0.011 [571] $Å^{-1}$ for E0400(1K), E0800(1K) and E1200(1K), respectively. The corresponding spacing in Å is given in square brackets. No interference signal was obtained for the homopolymers, poly(DTE carbonate) and poly(DT carbonate), in the presence of the drug molecule, which indicated that the incompatibility between DTE and DT was exacerbated by the presence of the

drug. The positions of the interference peaks in these copolymers were measured at slightly lower q values (i.e., increased spacing) than measurements made under wet conditions.

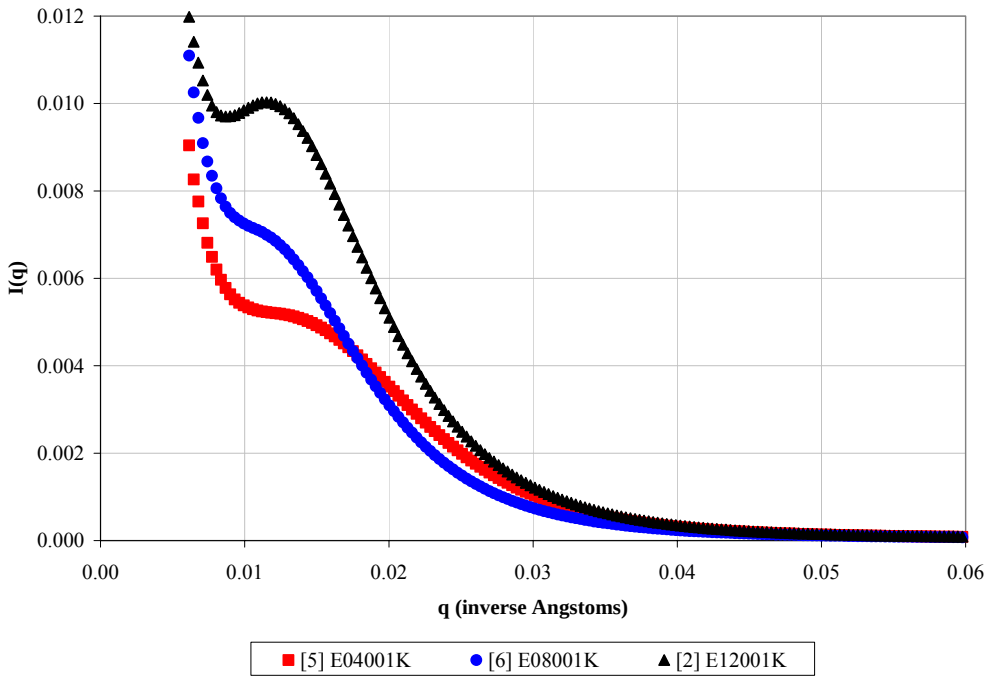

Figure 4.7. SAXS plot of intensity I(q) versus q for DTE-co-DT polycarbonate copolymers containing 30 wt.% voclosporin in the dry state.

Figure 4.8 is a plot of the x-ray scattering intensity, I(q), on a log scale versus the scattering vector, q, for two PEG-containing polycarbonates loaded with 30 wt.% voclosporin before and after hydration-induced phase separation of its PEG and DTR regions. The data in Figure 4.8(A) demonstrated a potential irreversible phase separation observed in DTE-co-DT-co-PEG_{1K} terpolymers. The drug loaded E1218(1K) had no signal when dry, manifested an interference peak indicative of phase separation when hydrated (28-day wet sample), and these phases remained separated within the matrix after the wet polymer was re-dried (25-day wet/redry sample). A curve for this drug

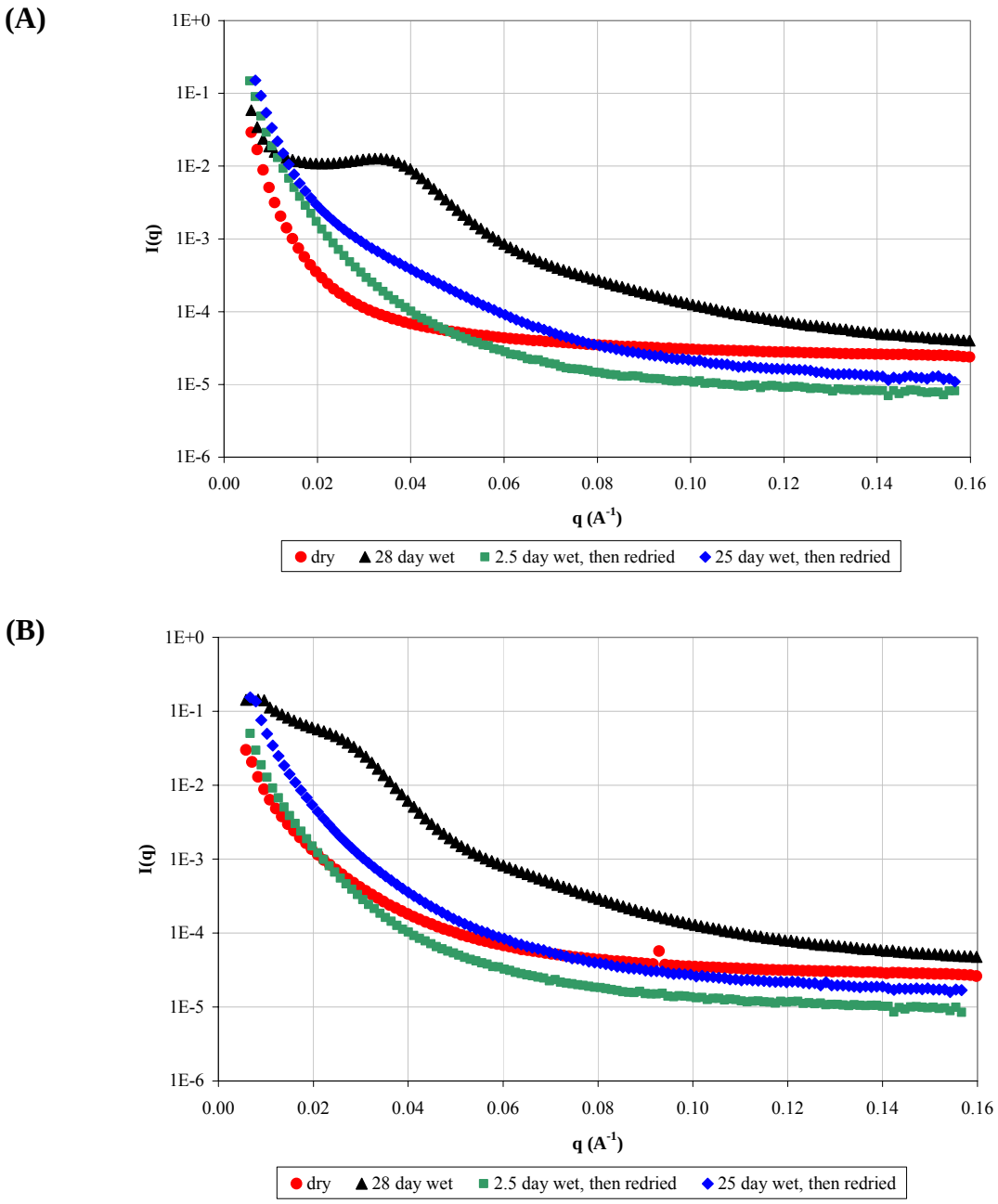

Figure 4.8. Development of (A) irreversible phase separation in E1218(1K) and (B) reversible phase separation in E0018(1K), after incubation times > 25 days in PBS at 37 °C. No significant interference peak was observed for the short incubation time of 2.5 days. All hydrated samples contained 30 wt.% voclosporin. Analysis by SAXS.

loaded polymer, hydrated for a shorter time of 2.5 days then re-dried, was also displayed in the figure to assist the reader in discerning the emergence of the interference peak

located at q ~ 0.04 $Å^{-1}$ in the 25-day hydrated/dried sample. It is noteworthy to mention that the DTE-co-DT copolymers manifested the irreversible phase separation only in the presence of the drug, which occurred after sample fabrication and remained when the sample was hydrated and when it was re-dried. Figure 4.8(B) demonstrated a potential reversible phase separation observed in DTE-co-PEG_{1K} copolymers. In this case, E0018(1K) had an interference signal only in the hydrated state. When water was removed from the sample, the phase separation vanished.

The PEG-containing polycarbonates in the wet state, with or without drug, all produced detectable broad interference peaks. Figure 4.9 is a plot of the interdomain spacing for the phase separated structures formed within these hydrated polycarbonates as a function of their PEG_{1K} content at 1, 4 and 7 weeks incubation in PBS at 37 °C in the absence of drug. Two general trends were observed in the data. First, an increase in the PEG_{1K} content of the terpolymer composition resulted in a reduction in the spacing between phase separated domains. This finding implied that more PEG chains were being packed within water clusters than were being compensated for by the potential swelling capacity[10] of the polymer. It was expected that a higher PEG content would result in more swelling of the polymer and an increase in the distance between domains, but this did not occur. In the second trend, an increase in the hydration time of the terpolymers resulted in the development of a larger interdomain spacing, which was expected. However, the slope of the domain spacing versus PEG_{1K} content for samples at

[10] The assumption is that the swelling capacity is directly related to the PEG content. For example, it would be expected that doubling the PEG content would also double the swelling capacity of the matrix. Note that this assumption may not valid for the polycarbonate terpolymers.

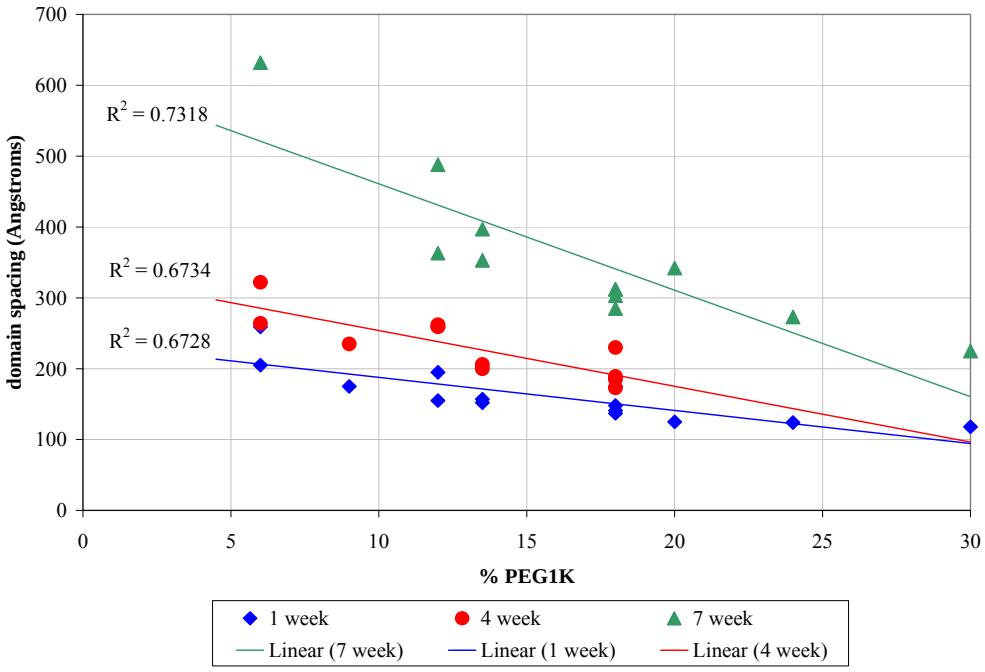

Figure 4.9. Plot of interdomain spacing versus PEG_{1K} content of DTE polycarbonate copolymers incubated for various times in PBS at 37 °C. Data obtained from SAXS analysis.

the 7-week incubation was three times greater than the slope of samples at the 1-week incubation. Based on these two trends, one potential explanation could be that higher amounts of PEG in the composition resulted in a reduction in the structural support of the matrix when hydrated. This weakness in the support was exacerbated by the presence of more water within the matrix, where an increase in the water uptake over time made the polymer more "flowable" and prone to collapse. The information given in Chapter 3 on the preferential loss of PEG_{1K} from the matrix did not contradict this conceptual picture since it was shown that an adequate amount of PEG remained within the terpolymer after seven weeks of hydration. The relationship between the polycarbonate composition, the hydration time and the distance between hydrophilic domains within the water clusters,

given in Eq. 4.2, seems valid at PEG_{1K} content < 30 mole %. At higher PEG content, the domain spacing approached an asymptotic value.

Eq. 4.2: $$\text{domain spacing} \propto \frac{\text{hydration time}}{PEG_{1K}\ \text{content}}$$

A similar trend was also observed for the polycarbonate terpolymers loaded with 30 wt.% voclosporin (figure not shown).

4.2.2 WAXS analysis of hydrated structure of polycarbonates with and without voclosporin

Structural information of interchain spacing for all of the polycarbonate polymers during wet and dry conditions in the presence and absence of drug was obtained from WAXS analysis. As an example, Figure 4.10 illustrates the x-ray scattering intensity profiles of I(q) versus the scattering vector, q, for E1218(1K) loaded with 30 wt.% voclosporin in the dry state and in the wet state with PBS at 37 °C for 1, 4 and 7 weeks. For the drug loaded samples in the wet state, four broad interference peaks were detected for each sample at q values of ~ 0.6 [10.5] (peak 1), ~ 1.4 [4.5] (peak 2), ~ 1.9 [3.3] (peak 3) and ~ 2.9 [2.2] (peak 4) $Å^{-1}$. The corresponding spacing in Å is given in square brackets.

Peak 1 corresponded to an intercalation structure of drug within the polymer chains, herein referred to as the polymer-drug intercalation peak. The evidence for intercalation was obtained from polymer-only samples that showed an absence of this peak in dry and wet conditions. There was no direct proof to indicate that the hydrophobic drug was sequestered specifically within the hydrophobic segments of the

polymer, although this is likely the case during hydration of the matrix. The average spacing of the dry and wet intercalation structures was 10.5 ± 0.1 and 10.8 ± 0.2, respectively, which showed a statistical increase of 2 % ($p < 0.001$).

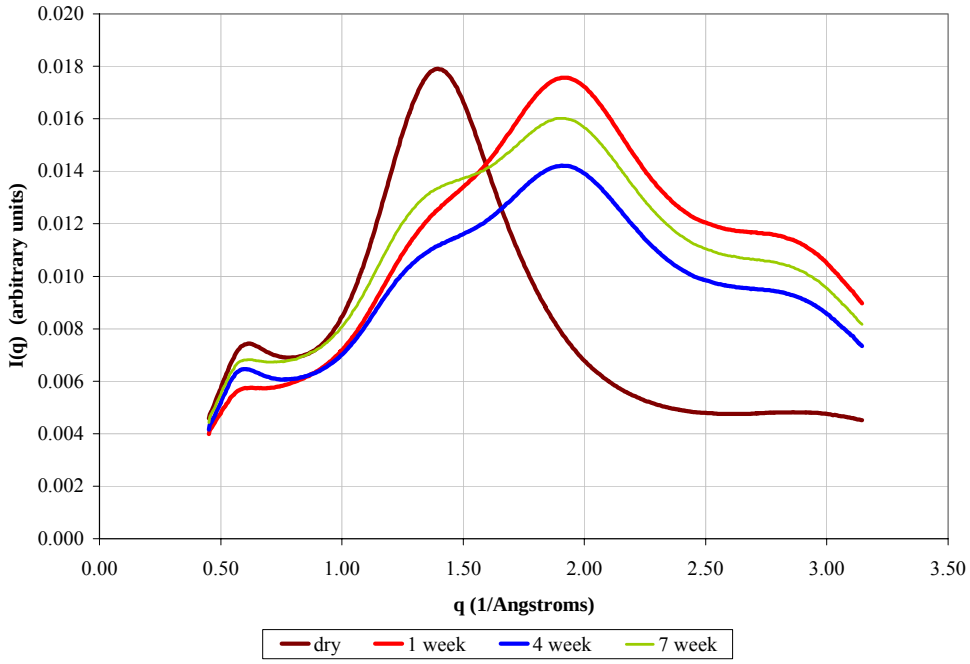

Figure 4.10. WAXS plot of intensity I(q) versus q for E1218(1K) containing 30 wt.% voclosporin at various times of hydration in PBS at 37 °C.

Peak 2 corresponded to the polymer interchain structure that had no drug molecule lying between its chains. This interference peak was observed both in the absence and presence of drug, with or without hydration. For polymer-only samples, the average spacing of the dry and wet interchain structures was 4.5 ± 0.1 and 4.4 ± 0.1, respectively (no significant difference; $p = 0.079$). For drug loaded samples, the average spacing of the dry and wet interchain structures was 4.6 ± 0.1 and 4.6 ± 0.1, respectively (no significant difference; $p = 0.968$). There was a statistical difference with respect to polymer interchain distances between polymer-only and drug loaded samples in the dry condition (2 % increase in spacing; $p < 0.001$), and in the wet condition (5 % increase in

spacing; $p < 0.001$). These findings indicated that the drug molecule was able to create a small perturbation in the interchain spacing of the polymer, and water molecules were able to slightly perturb the drug, but was too small to produce a global change within the polymer interchain spacing.

The remaining peaks 3 and 4 were attributed to the structure of water since they coincided with the scattering obtained from a PBS blank sample analyzed in the x-ray beam. These peaks were absent in dry samples.

The individual interference peak positions in q were resolved by Gaussian peak profiling methods using Jade Plus software. Polymer-drug intercalation and polymer interchain distances corresponding to peaks 1 and 2, respectively, were calculated using the Bragg relationship in Eq. 4.1. These spacing for all the polycarbonates is compiled in Table 8-10 and Table 8-11 of the Appendix.

Figure 4.11 is a series of WAXS profiles of intensity I(q) versus the scattering vector, q, for dry E1818(1K) polymer containing increased loadings of 10, 30, 50, 60, 70 and 80 wt.% voclosporin. This data provided further evidence of drug intercalation within the polymeric matrix. At drug loading ≥ 30 wt.%, an interference peak was observed at a q value of 0.60 ± 0.01 $Å^{-1}$ that became larger in intensity as the percentage of drug loading was increased. This peak was attributed to the intercalation spacing previously mentioned, and was measured on the Rigaku benchtop x-ray machine at 10.5 ± 0.2 Å. A second interference peak was also observed in all samples at a q value of 1.33 ± 0.05 $Å^{-1}$. This peak was attributed to a polymer interchain distance of 4.7 ± 0.2 Å. The individual interference peak positions in q were resolved by Gaussian peak profiling methods using Jade Plus software, and the interchain spacing was calculated using Eq.

4.1. Careful examination of this peak revealed that it might be comprised of two Gaussian distributions, which were most notable at > 50 % drug loading. It is hypothesized that a second order peak at slightly higher q could result from a drug-polymer-drug structure. As the drug loading was increased, the relative proportion of this structure became greater compared to the polymer-polymer interchain structure. This was manifested as a more dominant peak, and its contribution to the overall peak at ~ 1.33 $Å^{-1}$ created an apparent shift towards lower q values.

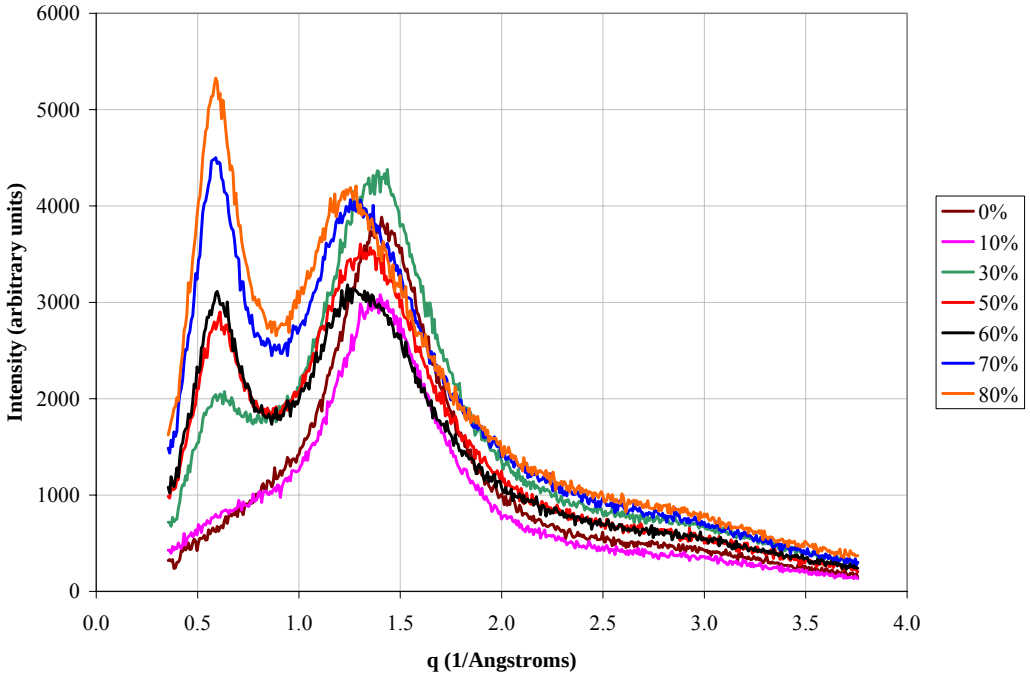

Figure 4.11. WAXS profiles of dry E1818(1K) with variable weight percentage voclosporin loading.

4.3 Optimization of the DTE-co-DT/drug complex configuration

The purpose of this simulation was to deduce whether a DTE-co-DT/voclosporin conformation existed that matched the intercalation spacing obtained from the WAXS

data (refer to Section 4.2.2). A simplistic stick model depicted in Figure 4.12 shows the 16 possible configurations of DTE-co-DT chain fragments oriented in a head-to-head conformation containing the four orientations of the drug molecule. An additional 16 configurations are possible when the DTE-co-DT fragment is in a head-to-tail conformation.

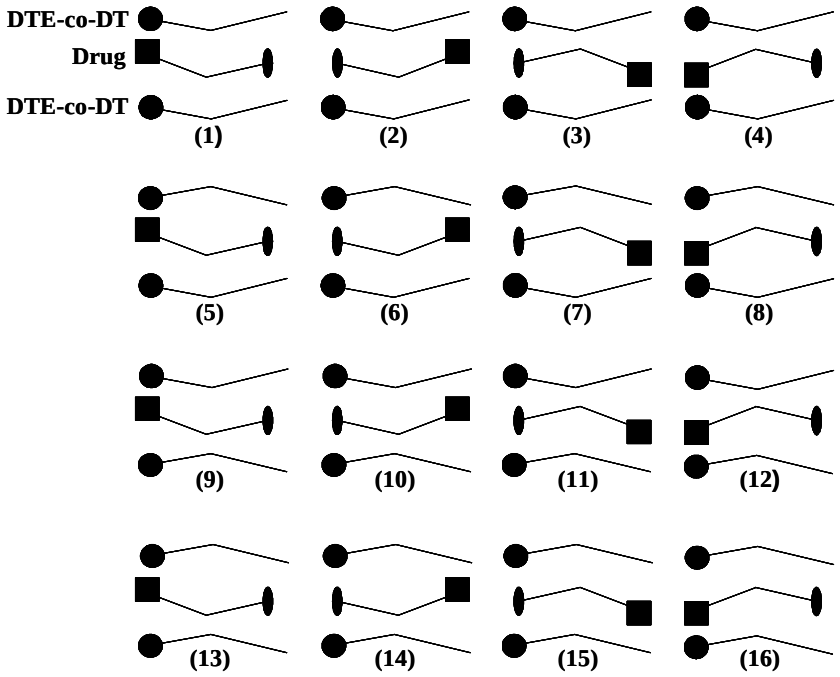

Figure 4.12. Stick model showing the 16 possible configurations of head-to-head DTE-co-DT segment complexed with a drug molecule.

Figure 4.13 shows the space filling model of a voclosporin molecule inserted between two DTE-co-DT fragments aligned in a head-to-head arrangement. The maximum distance between polymer chains was estimated at 6.58 Å which was slightly larger than the 6 Å spacing measured by WAXS. However, all possible combinations of drug and polymer chain were not simulated and the drug molecule was restrained from moving along its planar surface during the optimization.

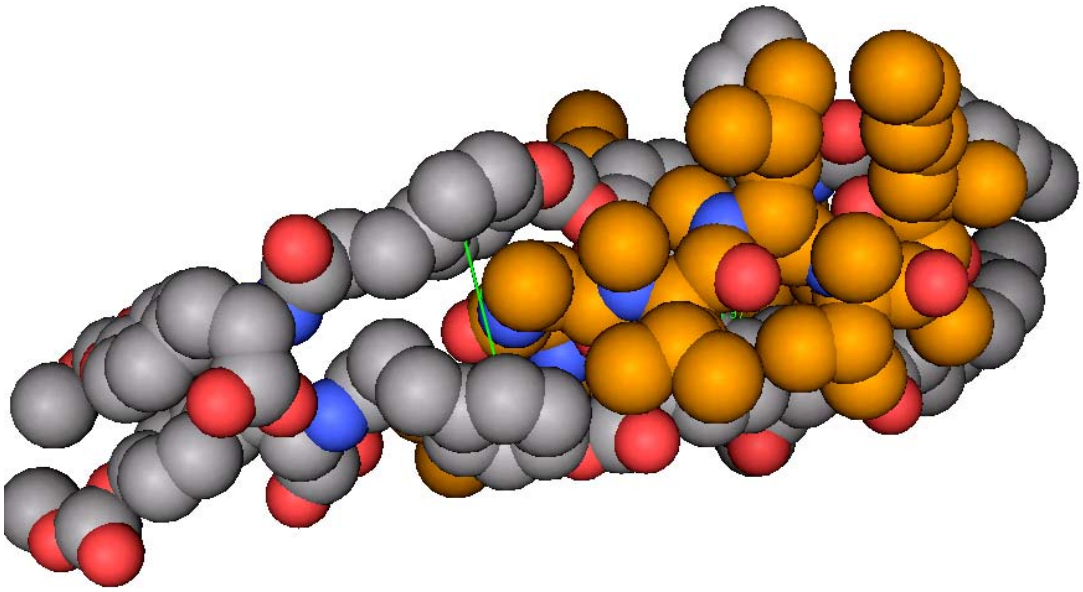

Figure 4.13. Space filling representation of voclosporin lying between two DTE-co-DT (head-to-head arrangement) segments. Gold is the carbon atoms of the drug, grey is the carbon atoms of DTE-co-DT, red is the oxygen atoms and blue is the nitrogen atoms. The distance between polymer chains was estimated by the simulation at 6.58 Å.

4.4 SAXS/WAXS analysis of hydrated structure of PLGA with and without voclosporin

No detectable SAXS interference peaks were obtained for PLGA compositions incubated for up to 7 weeks in PBS at 37 °C. However, there was considerable structural information obtained from WAXS analysis of these hydrated compositions. Figure 4.14 illustrates the scattering intensity I(q) versus the scattering vector, q, obtained from WAXS of PLGA 50:50 loaded with 30 wt.% voclosporin incubated for 1, 4 and 7 weeks in PBS at 37 °C. Also included in the figure is the WAXS profile for the dry drug loaded polymer sample. A broad interference peak located at ~ 0.60 $Å^{-1}$ [10.5] (peak 1) was found only in polymers containing the drug. Four additional interference peaks were

located at q values of ~ 1.25 $Å^{-1}$ [5.0] (peak 2), ~ 1.50 $Å^{-1}$ [4.2] (peak 3), ~ 2.05 [3.1] $Å^{-1}$ (peak 4) and ~ 2.90 [2.2] $Å^{-1}$ (peak 5). The corresponding spacing in Å is given in square brackets. At 4 weeks hydration, drug crystallization out from the polymer began to occur, as indicated by the sharp crystalline peaks riding on the curve. At 7 weeks hydration, the interference peaks 1, 2 and 3 were no longer discernable as the crystallized

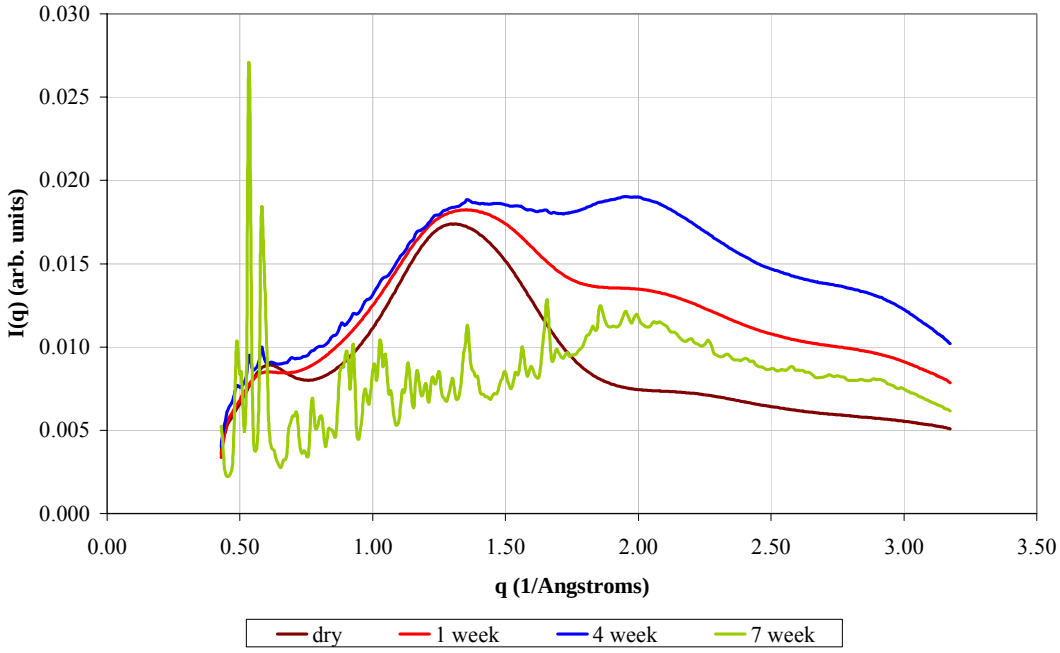

Figure 4.14. WAXS plot of intensity I(q) versus q for PLGA 50:50 containing 30 wt.% voclosporin for various times of incubation in PBS at 37 °C.

drug became prominent. Figure 4.15 is a comparison of the WAXS profiles between dry voclosporin only and the drug loaded PLGA 50:50 at 7 weeks hydration. The figure demonstrates the similarity between pure drug and the recrystallized drug obtained from the degrading PLGA.

The individual interference peak positions in q were resolved by Gaussian peak profiling methods using Jade Plus software. The polymer interchain spacing

corresponding to peaks 1, 2 and 3 were calculated for the PLGA compositions using Eq. 4.1. These calculated values are listed in Table 8-10 (peak 1) and Table 8-11 (peaks 2 and 3) in the Appendix. Peaks 4 and 5 were attributed to the scattering of water, as mentioned earlier, and were not included in the tables.

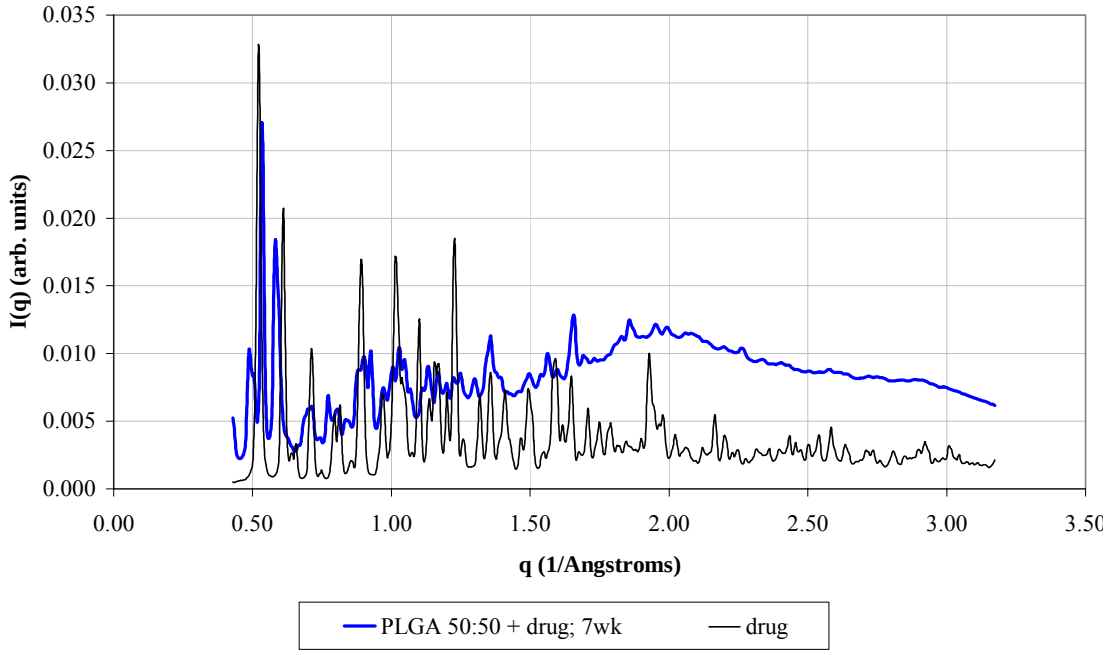

Figure 4.15. WAXS plot of intensity I(q) versus q for PLGA 50:50 containing 30 wt.% voclosporin after 7-week incubation in PBS at 37C showing recrystallization of drug from the degrading polymer. The WAXS profile of dry voclosporin (thin black line) is shown as a comparison.

4.5 Discussion

The complementary techniques of SANS to probe water domains in polymers, and x-ray scattering to probe the electron density of microphase separated domains by SAXS and polymer intrachain distances by WAXS at relatively low q values revealed interesting physical structural information about the PEG-containing polycarbonate co-

and terpolymers. SANS and SAXS analysis confirmed that hydrated terpolymer compositions containing an increased amount of PEG caused more nucleation of clusters of water domains, with close packing of PEG chains without proportional swelling[11] as the incubation time increased (refer to Figure 4.9). WAXS analysis confirmed the formation of voclosporin intercalation with the hydrophobic segments of the polycarbonate chains at the time of fabrication, and demonstrated that drug molecules remained in this configuration during the different hydration times. The absence of x-ray diffraction peaks for voclosporin within the polymer indicated that the drug was molecularly dispersed throughout the matrix where its crystalline lattice was disrupted. Polymer chain spacing devoid of drug remained constant in dry and wet conditions indicating that there was little to no effect of water molecule penetration at that length scale.

4.5.1 Intercalation of drug and polymer

Voclosporin molecules are not randomly oriented within the polycarbonate matrix. Instead, single drug molecules are sandwiched with a lateral orientation between polymer chains in a layered structure, termed as intercalation of drug molecules in polymer matrix. The estimated dimensions of the drug molecule are 22.5 Å long x 13.5 Å wide x 4.5 Å thick, based on measurements made with the MOE software. The dry WAXS spacing of the drug intercalated within polymer chains was estimated at 10.5 Å, leaving a distance of ~ 6 Å to fit the drug molecule[12]. The molecule can therefore only fit in a lateral orientation, possibly forming alternating polymer and single-drug layers in

---

[11] Proportional swelling would be indicated by identical slopes for the three incubation times.

[12] The thickness of the polymer chain was estimated at 4.5 Å based on polymer interchain measurements made in Section 4.2.2.

regions densely populated with drug. In the absence of voclosporin, no intercalation peak was observed. The spacing determined from *in silico* minimization routines of one possible orientation of a DTE-co-DT fragment and the voclosporin molecule was consistent with the WAXS intercalation distance.

In the presence of increasing amounts of drug, the intercalation peak remained at a fixed q, but its peak intensity increased accordingly (Figure 4.11). From dry to wet conditions of the matrix, the q position of the drug intercalation peak remained constant (Figure 4.10). Swelling of the terpolymer during hydration would have changed the drug interchain spacing if the drug resided within the mobile hydrophilic segments of the chain. The hydration-induced phase separation of PEG chains seemed to have little or no effect on moving the intercalated drug. The spacing was perturbed only slightly by the presence of water molecules, but not enough to change the local ordered structure. These features are consistent with the idea that the drug molecules predominately reside within the hydrophobic DTR-co-DT regions of the polymer chain. Intercalation structures in nanocomposites of hydrogels with layered silicates (113, 114) and PLA with layered silicates (115) are a few examples cited from the literature that indirectly support the concept of a polymer-drug intercalation presented in this thesis. A review article by Alexandre and Dubois (116) provides an excellent introductory treatment of polymer-layered silicate nancomposites for the interested reader.

4.5.2 Explanation for drug retention

Three plausible explanations exist for the drug retention phenomenon. One explanation is that the drug becomes physically entrapped within a collapsing polymeric matrix. The polycarbonate terpolymers are very tacky and flowable when hydrated at 37

°C, and it is conceivable that any developing porosity within the degrading polymer would be eventually closed up by the flowing polymer. Figure 4.16 shows a SEM photograph of the E1206(1K) terpolymer hydrated for 32 weeks in PBS at 37 °C as evidence of non-connecting craters of approximately 10 to 40 microns in diameter within the thickness of the sample. However, the notion of a collapsing matrix does not account

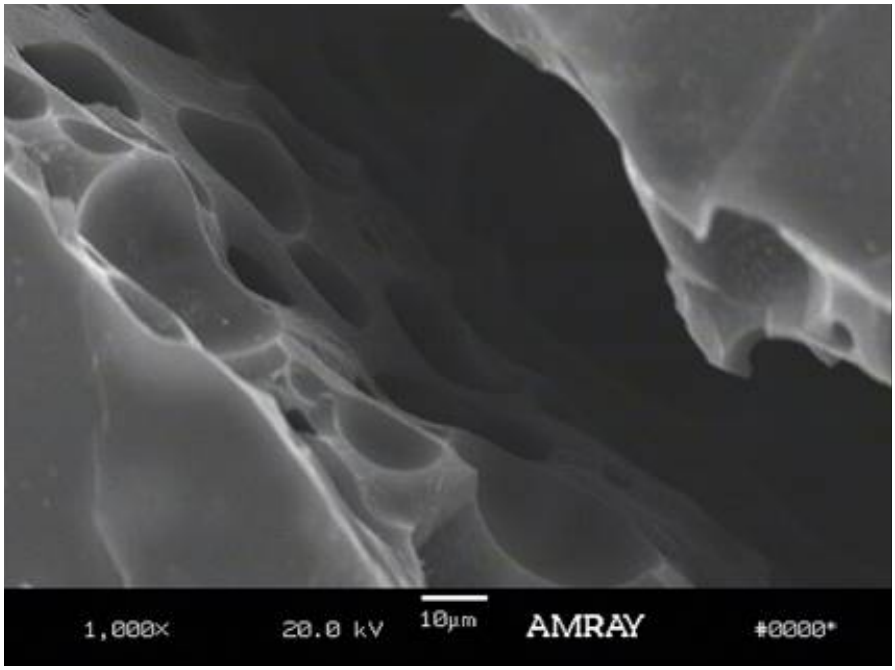

Figure 4.16. SEM of E1206(1K) disk containing 30 wt.% voclosporin incubated for 32 weeks in PBS at 37 °C (from erosion study). The picture shows non-connected craters in the thickness of the sample (magnification 1,000X).

for the relatively high drug release measured during the three weeks prior to the onset of drug retention. A second explanation is that the drug and polymer forms a complex that hinders drug release from the matrix, specifically through the formation of hydrogen bonding between the carboxyl group on the DT molecules and the NH groups on amino acid positions 2, 5, 7 and 8 of the voclosporin molecule (refer to Figure 1.1). However,

the data obtained from WAXS shows that voclosporin is already intercalated with the polymer chains during the casting operation and remains in this configuration during hydration. Relatively high levels of drug were released from this structure during the first 4 weeks of hydration. The third explanation is that phase separation of PEG within terpolymer matrix creates hydrophobic domains that sequester the drug, restricting its association with water molecules thereby increasing its resistance to transport out of the carrier. The water rich domains become surrounded by a hydrophobic exterior which slows down the transport of all species in the matrix. The supporting evidence for this proposed structure is outlined in this chapter.

The hypothesis emerging from the x-ray and neutron scattering measurements was consistent with the drug release behavior of the hydrated tyrosine-based polycarbonate homo-, co- and terpolymers. This hypothesis stated that early-stage drug release from the polymer matrix was due to an enhancement of drug diffusion brought about by PEG_{1K} segment mobility in the polymer chain. Structural changes in the polymer at ~100 Å length scale, detectable by both SAXS and SANS, indicate the nucleation, growth and redistribution of PEG_{1K} rich domains and water domains upon hydration (refer to Figure 4.1 for the SANS data and Figure 4.6 for SAXS data of E1218(1K) terpolymer). It is believed that the increased PEG_{1K} segment mobility brought about by the hydration-induced phase separation caused a transient localized mixing that increased drug transport out of the matrix. Adding to this proposed mechanism is the fact that the polymer also undergoes preferential hydrolytic degradation of PEG segments and bulk erosion which loosens up its structure, and the inflow of water causes swelling of the matrix which increases both the size and interdomain spacing of

the PEG-rich regions. It was expected that transport of the byproducts of polymer degradation (i.e., monomers and low molecular weight oligomers) throughout the matrix would also be enhanced by the mobility of the phase separating PEG_{1K} segments.

4.5.3 Microphase separation of DTE-co-DT and drug

The evidence for the microphase separation of DTE-co-DT polymer segments and the drug is given in Table 8-9 in the Appendix. In the dry state, the DTE-co-DT copolymers containing drug were the only matrices to manifest a SAXS interference structure. No structure was observed in the poly(DTE carbonate) or the poly(DT carbonate) dry amorphous polymers containing drug, or in the DTE-co-DT copolymers without drug in both the dry and wet state. Poly(PEG_{1K} carbonate) did have a detectable structure both in the presence and absence of drug at higher q values when dry, which is expected since the polymer is semicrystalline and has long range ordering. The fact that there is no interference peak detected either for drug loaded poly(DT carbonate) or for drug loaded poly(DTE carbonate) meant that the inhomogeneity between DT and DTE segments were exacerbated by the presence of the drug. It is unknown at this time whether the association of drug is though hydrogen bonding with the carboxyl group on the DT, or hydrophobic-hydrophobic interaction with the DTE segment.

4.5.4 Conceptual description of drug release from polycarbonates

The overall description of *in vitro* release of voclosporin from the polycarbonate terpolymers is outlined here. Water rapidly penetrates and forms water-rich domains within the drug loaded terpolymer. The presence of water causes mobility of the PEG_{1K} segments of the polymer chain (i.e. hydration-induced phase separation of PEG). This

redistribution of PEG, or phase separation, creates a "stirring" effect within the matrix. "Free" drug molecules that are not intercalated with the hydrophobic polymer regions become perturbed, dissolved by water and carried away by the mobile PEG. The amount of drug dissolution is limited by its extremely low solubility in aqueous media. This scenario describes the early-stage enhanced release of voclosporin from the polycarbonate terpolymers. Coupled to the mobility of PEG is the underlying influx of water molecules causing swelling and mass loss of the polymer matrix which also enhances drug release. Over time (on the order of weeks), continued and irreversible phase separation of PEG buries these hydrophilic domains as non-connected bodies within hydrophobic domains rich in DTE-co-DT segments. Within the DTE-co-DT regions lies the intercalated drug which has become isolated from the bulk water residing in the PEG. Recall that DTE-co-DT copolymers were unable to release significant amounts of voclosporin from its matrix, as demonstrated in the kinetic drug release studies given in Chapter 3. The drug therefore becomes trapped, and with PEG no longer available for localized perturbation of the matrix, drug retention therefore sets in and the diffusion of voclosporin becomes similar to the low rates of drug release as measured in DTE-co-DT copolymers. Figure 4.17 summarizes the regions of early and late-stage drug release for the E1218(1K) terpolymer and the corresponding morphological changes that occur during hydration of the drug-loaded matrix. Note that the transition between early-stage and late-stage release was attributed to an increasing hydrophobic barrier that separated PEG (and water) domains thereby increasing the resistance to species transport (refer to Figure 4.18).

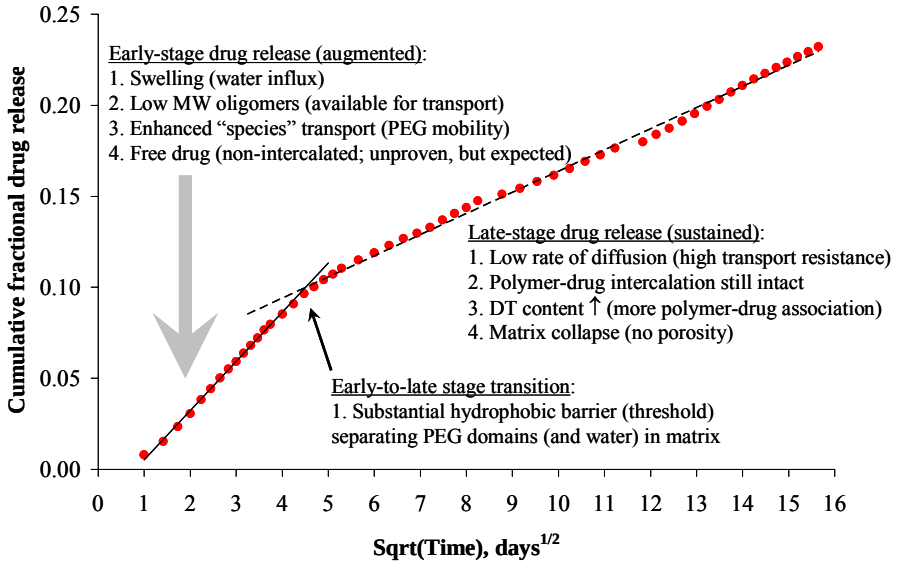

Figure 4.17. Cumulative fractional drug release versus square root of time for E1218(1K) loaded with 30 wt. % and incubated in PBS at 37 °C. Annotations describe morphological changes occurring within the polymer as determined by SAXS/WAXS.

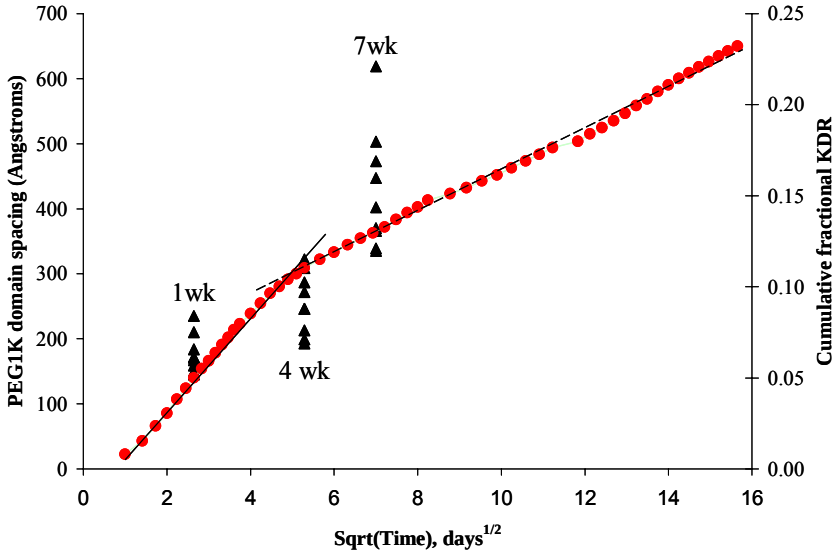

Figure 4.18. Spacing of microphase separated PEG_{1K} domains at 1, 4 and 7 weeks hydration (shown as filled triangle) in PBS at 37 °C for PEG-containing polycarbonates loaded with 30 wt.% drug. Overlay with cumulative fractional drug release versus square root of time for E1218(1K) loaded with 30 wt. % is. Figure demonstrates the range of PEG_{1K} domain spacing during drug release from the E1218(1K) polymer.

5 Destabilization of voclosporin in the presence of PEG-containing polycarbonate terpolymers

This chapter presents data on the effects of heat and radiation on voclosporin stability in the presence of the PEG_{1K}-rich DTR polycarbonate terpolymers. Other polymeric systems were described in the literature either omitting to investigate, or stating that there was no effect of these conditions on peptide drug molecules held within the matrix. Sternberg, et al. (117), found that CsA contained within PLLA thin coatings was unaffected by beta-radiation at doses up to 40 kGy even though the surrounding polymeric matrix was degraded by the sterilization process. Analysis by Kanjickal, et al. (118), of gamma sterilized (25 kGy) hydrogels containing PEG, crosslinked with triphenyl methane triisocyanate and loaded with CsA, revealed significantly higher quantities of peroxy and triphenyl methyl carbon free radicals relative to the amount found in non-sterile material. No effect of these free radicals on CsA activity was discussed in the article. Rothen-Weinhold, et al. (119), studied both the heat and gamma radiation stability of the hydrophobic octapeptide molecule vapreotide in poly(lactic acid), PLA. They found that the drug did not thermally degrade at temperatures between 80 and 90 °C and incubation times less than one hour. Similarly, the authors found that gamma radiation dose up to 50 kGy had no significant deleterious effect on the stability of vapreotide in the presence of PLA.

The effect of gamma radiation on tyrosine-based polycarbonate homopolymers have been studied in the Kohn laboratory by Hooper, et al. (120). Preliminary studies conducted during the present research demonstrated that voclosporin degradation was

exacerbated during heat exposure in the presence of PEG-containing polycarbonates compared to the drug degradation in either the DTE homopolymer or the DTE-co-DT copolymers (refer to Table 8-13 in the Appendix). The PEG-containing polycarbonates described in this chapter were shown to significantly degrade voclosporin, both during thermal exposure and gamma sterilization. Free radical scavengers, or antioxidants, were formulated into the polycarbonate-drug matrix to demonstrate that the drug could be protected from the harmful effects caused by thermal and radiation exposure. The PEG content in the terpolymer composition was implicated as a likely culprit that generated free radicals and destroyed the drug.

5.1 Measurement of the thermal stability of voclosporin in the presence of PEG-containing polycarbonates

The melting point of voclosporin was measured at 148 °C by DSC and its onset of the heat degradation occurred at 362 °C as determined by TGA. Table 5-1 shows the effect of heat on voclosporin stability at temperatures of 100 °C and 120 °C for 60, 180 and 480 minutes. A drug recovery of 100 % from the sample after heat exposure, using the HPLC method described in Chapter 2, denoted thermal stability. Statistical analysis using a one-way ANOVA and the Tukey test indicated that there was no statistical difference between any of the test parameters, except for the condition of 120 °C for 480 minutes ($p \leq 0.004$). This finding implied that the drug was heat stable for exposure times up to eight hours at 100 °C and for exposure times up to three hours at 120 °C. However, an 8-fold increase in thermal exposure from one to eight hours at 120 °C

resulted in a 21 % decrease in drug stability, demonstrating that temperatures closer to the melting point of the drug (148 °C) had a greater effect on drug thermal stability.

Table 5-1. Percentages of active voclosporin remaining after heat treatment at various times and temperatures.

Temperature	60 min	180 min	480 min
100 °C	101 ± 0	99 ± 1	98 ± 0
120 °C	100 ± 1	95 ± 0	79 ± 9 (*)

The symbol (*) indicates statistical significant difference.

Table 5-2 shows the results of voclosporin stability obtained by running a full factorial experimental design at two times and three temperatures (ordinal categories) in the presence of seven polymer compositions (nominal category). The lower and middle temperature limits of 60 °C and 90 °C were chosen as conditions that allowed melt flow of the polycarbonate terpolymers during compression molding. The high temperature limit of 130 °C was chosen to be approximately 20 °C below the melting point of the drug. The two times of 30 and 180 minutes were chosen based on potential minimum and maximum times the material would reside in an extrusion machine for fabrication of fibers or rods. Statistical analysis of the data using Design Expert® software indicated a strong interaction between time and temperature for all polymer types ($p < 0.01$), where longer times and higher temperatures caused considerable damage to the drug.

The data presented in Table 5-2 for heat exposure at 60 °C for 30 minutes demonstrated that voclosporin, in the presence of the terpolymers, was heat stable at the processing temperatures and times used in this study for fabricating devices by hot compression molding. However, drug stability rapidly declined as the exposure time was increased to three hours or as the temperature was increased to 130 °C. In Table 5-1, the

drug by itself was shown to be heat stable at 100 °C for eight hours whereas in Table 5-2 approximately 15-87 % of the drug, in the presence of the polymers, was destroyed after three hours at 100 °C.

Table 5-2. Percentages of active voclosporin remaining in 15 wt.% drug loaded polymer after heat treatment at different times and temperatures.

Polymer composition	30 min			180 min		
	60 °C	100 °C	130 °C	60 °C	100 °C	130 °C
M1218(1K)	100 ± 2	87 ± 1	23 ± 5	99 ± 1	13 ± 3	6 ± 5
M1420(1K)	97 ± 10	92 ± 4	11 ± 6	112 ± 9	20 ± 11	4 ± 3
M1224(1K)	101 ± 1	89 ± 3	23 ± 3	101 ± 2	38 ± 2	3 ± 0
E1218(1K)	100 ± 2	94 ± 3	58 ± 8	100 ± 3	85 ± 1	28 ± 11
E1420(1K)	106 ± 9	82 ± 2	24 ± 3	94 ± 5	33 ± 8	2 ± 2
E1224(1K)	95 ± 5	92 ± 1	31 ± 6	99 ± 2	37 ± 2	6 ± 5
1:1 blend E1224(1K) +PLGA 50:50	94 ± 1	82 ± 5	30 ± 7	89 ± 2	36 ± 7	14 ± 16

5.2 Effect of antioxidants on the thermal stability voclosporin in the presence of PEG-containing polycarbonates

Five antioxidants (BHT, BHA, Vitamin C, Vitamin E and TPGS) were investigated to determine whether these free-radical scavengers could protect the drug at a relatively high temperature of 100 °C (in this case) and a relatively long exposure time of three hours. A comparison of the effectiveness of the five antioxidants on voclosporin heat stability in the presence of the M1420(1K) terpolymer is shown in Table 5-3. This polymer was chosen since it showed almost complete drug destruction after heat exposure of 100 °C for three hours (refer to Table 5-2). Two thermal exposure times of one and three hours were investigated at two levels of antioxidant (0.1 % and 1 % per weight of the polymer) in the formulation of the drug loaded polymer. All data were

normalized by dividing the amount of drug recovered post-heat treatment by the amount recovered pre-heat treatment.

Statistical analysis using a one-way ANOVA and Tukey's HSD test indicated no statistical difference in drug stability for the M1420(1K) polymer containing BHT at all antioxidant levels and heat exposure times. Similar results were obtained for the same polymer containing Vitamin E. Data for BHT and Vitamin E samples were therefore separately pooled and found to be statistically different when compared to each other using a two-sample t-test ($p = 0.017$). The average normalized drug recovery for BHT and Vitamin E samples was 98 ± 3 % and 94 ± 4 %, respectively.

A statistical comparison (one-way ANOVA; Tukey's HDS; LSD) of all five antioxidants was performed for samples subjected to 100 °C for three hours at the level of 1 wt.% antioxidant (per weight of polymer). At this level, three groups were distinguished as homogeneous subsets: (1) BHT, BHA and Vitamin E (96 % of drug recovered; pooled data), (2) Vitamin C (88 % of drug recovered) and (3) TPGS (76 % of drug recovered). These results showed that the antioxidants BHT, BHA and Vitamin E were more effective than Vitamin C or TPGA at the level of 1 % antioxidant within the polymer M1420(1K).

Table 5-3. Percentages of active voclosporin remaining in 15 wt.% drug loaded M1420(1K) with antioxidant after heat treatment at 100 °C. Levels of antioxidants are 0.1 % and 1.0 % per weight of polymer.

Time	%Antiox.	BHT	BHA	Vit E	Vit C	TPGS
60 min	0.1%	101 ± 4	91 ± 1	97 ± 7	99 ± 1	88 ± 1
	1.0%	96 ± 2	98 ± 3	94 ± 2	89 ± 7	95 ± 9
180 min	0.1%	97 ± 3	91 ± 1	92 ± 1	97 ± 2	40 ± 4
	1.0%	97 ± 3	97 ± 1	93 ± 1	88 ± 3	76 ± 4

5.3 Measurement of gamma radiation stability of voclosporin in the presence of M1420(1K) terpolymer

The next step in evaluating the stability of voclosporin within the tyrosine-based terpolymers was to examine the effect of gamma radiation. A drug recovery of 100 % from polymer samples after gamma irradiation, using the HPLC method described in Chapter 2, denoted radiation stability in the presence of the polymer. The normalized percentage of active voclosporin recovered in the absence of both polymer and antioxidants after gamma sterilization (~ 22 kGy) was 92 ± 7 %. In contrast, the stability of the drug was reduced by 39-55 % in the presence of the terpolymer (no antioxidant present) after radiation exposure, as shown in Table 5-4.

Table 5-4. Percentages of active voclosporin remaining in 15 wt.% drug loaded polymer after gamma irradiation at 22 kGy.

Polymer composition	Percent voclosporin recovered
M1218(1K)	54 ± 3
M1420(1K)	54 ± 4
M1224(1K)	47 ± 3
E1218(1K)	61 ± 10
E1420(1K)	45 ± 1
E1224(1K)	46 ± 2
1:1 blend of E1224(1K)+PLGA 50:50	56 ± 8

5.4 Effect of antioxidants on voclosporin gamma radiation stability in the presence of M1420(1K) terpolymer

It was determined from the previous section that antioxidants were necessary in the formulation in order to protect voclosporin. Table 5-5 gives a comparison of the effectiveness of each of the five antioxidants (BHT, BHA, Vitamin E, Vitamin C and

TPGS) at two antioxidant levels (0.1 and 1 % per weight of polymer) to protect voclosporin from gamma radiation in the presence of the terpolymer M1420(1K). This polymer was chosen since it showed approximately 50 % drug destruction after gamma radiation exposure of ~22 kGy (refer to Table 5-4). Analysis using a two-sample t-test indicated a statistical difference in drug activity between the 0.1% and 1% antioxidant levels for samples containing BHT ($p = 0.003$) and Vitamin E ($p = 0.02$) after gamma irradiation. Polymer formulations containing 1 % antioxidant showed a 12 % and 14 % increase in drug recovery compared to the lower antioxidant level for BHT and Vitamin E, respectively, after gamma irradiation. A statistical comparison (one-way ANOVA and Tukey's HDS) of M1420(1K) polymer samples containing 1 % antioxidant indicated no statistical difference between BHT, BHA and Vitamin E. The pooled average drug recovery for this group of 92 ± 4 % was similar to the drug recovery obtained for gamma-irradiated voclosporin. The M1420(1K) polymer sample containing 1 % TPGS was statistically different ($p < 0.001$) from the BHT/BHA/Vit E group, losing approximately 27 % of the drug after radiation exposure. Vitamin C was not analyzed due to its high standard deviation.

Table 5-5. Normalized percentages of active voclosporin remaining in 15 wt.% drug loaded M1420(1K) with antioxidants after gamma irradiation at 22 kGy.

Antioxidants	0.1 % antioxidant	1 % antioxidant
BHT	86 ± 2	96 ± 2
BHA	86 ± 6	91 ± 1
Vitamin E	77 ± 1	88 ± 5
Vitamin C	70 ± 1	67 ± 21
TPGS	N/A	73 ± 2

5.5 Effect of gamma irradiation on polymeric carriers in the absence and presence of antioxidants

Table 5-6 shows the change in molecular weight and corresponding change in polydispersity for the seven polymer formulations in the absence of antioxidants before and after gamma sterilization (~22 kGy). Statistical analysis using the paired t-test between samples before and after gamma sterilization indicated statistical difference in molecular weight for all polymers M1218(1K) ($p = 0.006$), M1420(1K) ($p < 0.001$), M1224(1K) (p = 0001), E1218(1K) ($p = 0.014$), E1420(1K) ($p = 0.001$), E1224(1K) ($p < 0.001$) and 1:1 blend of E1224(1K)+PLGA 50:50 ($p = 0.004$). The DTM terpolymers showed a decrease in the initial M_n ranging from 22 to 36 % and an average increase in polydispersity ranging from 14 to 15 %. The DTE terpolymers showed a decrease in the initial M_n ranging from 13 to 28 % and an average increase in polydispersity ranging from 7 to 14 %. This general trend of decreasing molecular weight and increasing polydispersity after radiation exposure indicated that radiation-induced crosslinking of the terpolymers did not occur. However, the data confirmed that gamma sterilization induced radiation damage to the polymer backbone. The 1:1 blend of E1224(1K)+PLGA 50:50 was not statistically evaluated since its analysis was complicated by having two polymers with different chemistries.

The use of the two top performing antioxidants (BHT and Vitamin E) was examined for their effectiveness at maintaining molecular weight of the terpolymers during sterilization. The two polymers, E1218(1K) and the 1:1 blend of E1224(1K)+PLGA 50:50, were formulated with either BHT or Vitamin E and subjected to gamma radiation (~22 kGy). The molecular weights before and after sterilization are

Table 5-6. Change in number average molecular weight (M_n) and polydispersity (PD) of polymers containing 15 wt.% voclosporin after gamma sterilization at 22 kGy.

Polymer Composition	M_n (kDa)		PD	
	Non-sterile	Gamma sterile	Non-sterile	Gamma sterile
M1218(1K)	159 ± 3	122 ± 3	1.4	1.6
M1420(1K)	220 ± 2	141 ± 1	1.4	1.6
M1224(1K)	175 ± 3	136 ± 1	1.3	1.5
E1218(1K)	110 ± 2	96 ± 1	1.4	1.6
E1420(1K)	173 ± 3	124 ± 2	1.4	1.6
E1224(1K)	143 ± 1	118 ± 1	1.4	1.5
1:1 blend of E1224(1K)+PLGA 50:50	139 ± 5	84 ± 2	1.6	1.5

Table 5-7. Change in number average molecular weight (M_n) and polydispersity (PD) of polymers containing 15 wt.% voclosporin and 1% antioxidants after gamma sterilization at 22 kGy.

Formulation	M_n (kDa)		PD	
	Non-sterile	Gamma sterile	Non-sterile	Gamma sterile
E1218(1K); 1% BHT	104 ± 1	102 ± 2	1.4	1.5
E1218(1K); 1% Vitamin E	107 ± 0 (*)	99 ± 1 (*)	1.4	1.5
1:1 blend of E1224(1K)+PLGA 50:50; 1% BHT	116 ± 6	112 ± 1	1.5	1.5
1:1 blend of E1224(1K)+PLGA 50:50; 1% Vitamin E	108 ± 13	118 ± 5	1.5	1.6

The symbol (*) indicates statistical significant difference.

given in Table 5-7. Statistical analysis using the paired t-test between pre- and post-sterile samples indicated no statistical difference in molecular weight for all formulations, except for the E1218(1K) polymer containing Vitamin E ($p = 0.007$) which showed a 7 % reduction in initial M_n and an increase in average polydispersity of 7 %. This difference

was not considered to be substantial given the fact that GPC data[13] can vary by ± 5%. For all other formulations, there were no statistical differences in molecular weight indicating that the antioxidants seemed to protect the polymer from chain scission after radiation exposure.

5.6 Discussion

Voclosporin instability in the presence of the polycarbonate terpolymers during thermal exposure and gamma irradiation was mainly attributed to the formation of free radicals associated with the PEG component of the polymer by way of circumstantial evidence. The control samples, given in Table 8-13 of the Appendix, were tested during a preliminary study of the drug thermal stability in the presence of either non-PEG or PEG containing polycarbonates. A comparison of heat-treated samples to their controls indicated that the drug might be marginally affected by the DTE homopolymer and significantly affected by the DTE-co-DT copolymer, DTE-co-PEG_{1K} copolymer and DTE-co-DT-co-PEG_{1K} terpolymer. Drug destruction in these samples was more prominent in the presence of PEG. No similar control samples were used in the gamma sterilization study since its focus was to demonstrate the benefit of using an antioxidant within the formulation to protect the drug. In hindsight, this decision was a poor judgment since it prevented the determination of the extent of PEG contribution to the drug instability. To this end, citations from the literature were used to provide circumstantial evidence for the potential formation of free radicals on PEG and its probable mechanism of action for drug destruction.

---

[13] Absolute molecular weight was not measured since the in-house equipment (Viscotek® with light scattering detector) was not configured for these relatively low molecular weights.

PEG has been shown to randomly oxidize along its chain into heat labile α-hydroperoxides that can decompose on heating to form secondary α-alkoxyalkyl radicals attached as side groups on the PEG (121) [refer to Figure 5.1; steps 1 and 2]. Likewise, studies by Decker (122, 123) demonstrated a potential mechanistic scheme for the formation of PEG backbone secondary alkyl radicals, and the formation of PEG side chain secondary α-alkoxyalkyl peroxy and α-alkoxyalkyl radicals, during gamma irradiation of the solid form of PEG [refer to Figure 5.1; steps 3, 4 and 5]. This scheme proposed by Decker was based on identification and quantitative measurements of degradation byproducts containing formate and hemiformal groups, hydroperoxide groups, and volatiles such as formaldehyde and carbon dioxide. Decker also provided

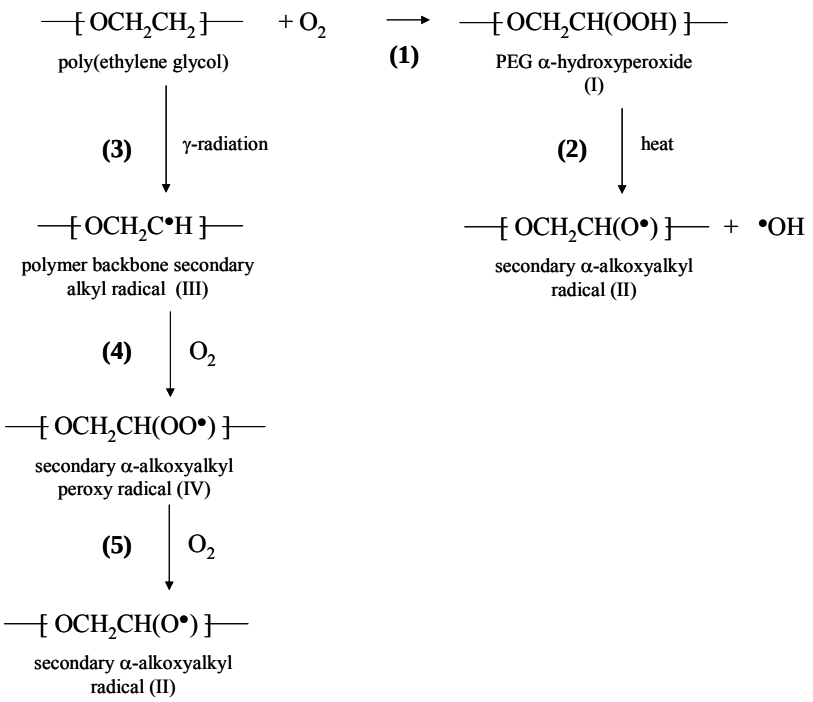

Figure 5.1. Proposed mechanisms of free radical formation during thermal degradation of PEG [steps 1 and 2; adapted from Han et. al., 1997 (121)] and during gamma radiation of PEG [steps 3, 4 and 5; adapted from Decker, 1977 (122)].

circumstantial evidence for the formation of these free radicals to be within the amorphous phase of the semicrystalline PEG which is more accessible to the diffusion of oxygen.

The data in Table 5-6 and Table 5-7 demonstrated that the molecular weight of PEG-containing tyrosine-based terpolymers was susceptible to gamma irradiation, and that these polymers were protected from significant radiation damage in the presence of radical scavengers such as BHT and Vitamin E. Similarly, Table 5-4 and Table 5-5 showed that the recovery of voclosporin from gamma sterilized PEG-containing terpolymer matrices was significantly reduced compared to the gamma sterilized drug-only control, and that the drug was protected from significant radiation damage in the presence of the radical scavengers. Additional gamma sterilization testing of E1218(1K) loaded with 15 wt.% voclosporin and 0.1 % (per weight of total polymer) antioxidant showed that ~ 4 % of BHT and ~ 19 % of Vitamin E were consumed after radiation exposure in protecting 95 % and 90 % of the loaded drug, respectively. The fact that these antioxidants were able to protect both the drug and the terpolymer from degradation indicated that free radical formation played a prominent role in the mechanism of degradation.

Radicals on the PEG segment of the polycarbonate terpolymer can potentially remove hydrogen from susceptible sites on the peptide molecule voclosporin. Hydrogen abstraction from the backbone α-carbons of the solid peptide can lead to the formation of free radicals $CONHC^{\bullet}(R)$, with eventual cleavage of the peptide main chain at most aliphatic amino acid sites (124). Voclosporin is composed of several aliphatic amino acid derivatives that are susceptible to radiolysis, such as aminobutyric acid (Abu), methylated

glycine (Me-Gly) and methylated leucine (Me-Leu). Meents, et.al. (4), studied the "global" radiation-induced structural changes in cyclosporine A and speculated that these localized motions could be a precursor to free radical formation by hydrogen abstraction from the α-carbon of aliphatic amino acids. Although not explicitly illustrated with examples, a similar attack on voclosporin is anticipated for prolonged thermal exposure of the drug in the presence of alkoxy free radicals on PEG segments of the terpolymer. Other likely possibilities for the destruction of drug activity may occur through (i) radiation-induced oligomerization of voclosporin at the conjugated double bond on amino acid position 1 (refer to Figure 1.1) with free radicals on the polymer chain, and (ii) thermal dimerization of voclosporin via a Diels-Alder type mechanism also at the conjugated double bond of the drug.

Reduction in the molecular weight of non-PEG containing tyrosine-based polycarbonates after thermal exposure for extended periods or after gamma irradiation is also known to occur. Hooper, et.al. (120), demonstrated that the poly(DTE carbonate) molecular weight decreased by approximately 10 % when gamma sterilized at a dose of 25 kGy. Additionally, it is common knowledge in the Kohn laboratory that the molecular weights of dry tyrosine-based homo-, co- and terpolymer polycarbonates decrease as a function of their incubation temperature and heat exposure time. For drug loaded matrices, the recovery of voclosporin from heat treated non-PEG containing polycarbonates was measured at approximately 91% and 73% for poly(DTE carbonate) and poly(DTE-co-12 % DT carbonate), respectively (refer to Table 8-13). The information gathered for molecular weight decrease of non-PEG containing polycarbonates and the decrease of voclosporin recovery from these polymers indicated

that radical formation on PEG segments may not be the only mechanism responsible for drug instability. Future work on this topic is expected to clarify the roles of DTR, DT and PEG in the formation of radicals and their effect on drug stability, and to quantify the level of hydroperoxides on PEG.

6 *In vivo in vitro* studies of polycarbonate *ter*polymers

This chapter describes the work done to compare the *in vivo* and *in vitro* performance of the class of degradable PEG-containing polycarbonate terpolymers as an implantable drug delivery vehicle for potential ophthalmic applications. The first section describes a screening study where the placebo and drug loaded polymeric carriers were implanted into the subcutaneous tissue of rabbits to assess their drug release and polymer erosion characteristics. The purpose of this study was to select lead and backup polymer candidates that would be formulated with antioxidants and shaped as implantable devices that could easily fit within the limited space of the conjunctiva of the eye. The second section describes a pilot episcleral study in rabbit using the polymers selected from the first study. The two polymer formulations implanted in the episcleral study were (a) E1218(1K) containing 15 % voclosporin and 1 % (per weight of polymer) of Vitamin E and (b) a blend of E1224(1K) + PLGA 50:50 also containing 15 % voclosporin and 1 % (per weight of polymer) of Vitamin E. *In vivo* and *in vitro* KDR data are presented for all animal work.

6.1 *In vivo in vitro* performance of polycarbonate polymers in rabbit subcutaneous implantation

The *in vivo in vitro* screening study for evaluating drug release and polymer resorption utilized high PEG-containing polycarbonate DTM and DTE terpolymers, with and without voclosporin, that were implanted subcutaneously into the back of rabbits.

These samples were compared to the *in vitro* KDR performance of terpolymers taken from the same drug loaded set and tested in PBS at 37 °C. Test samples were gamma sterilized, but contained no antioxidants[14]. Gross visual observations on *in vivo* polymer resorption were made on explanted samples at 4, 10 and 20 weeks. The *in vivo* explants were also measured for drug content or were submitted for histological examination.

6.1.1 *In vitro* KDR profiles of sterile polycarbonate terpolymer carriers

Figure 6.1 is a plot of the *in vitro* cumulative fractional drug release versus time for the gamma sterilized DTM terpolymers – M1218(1K), M1420(1K) and M1224(1K) – loaded with 15 wt.% voclosporin and incubated in PBS at 37°C over a period of 20 weeks. The total drug content was adjusted for loss due to gamma sterilization (refer to Table 5-4). Error bars represent the cumulative accumulated error obtained during the experiment. At 20 weeks, the polymeric carrier M1224(1K) had the highest cumulative percent drug release of 79%, followed by M1420(1K) and M1218(1K) at 64% and 57%, respectively. This data demonstrated a general trend of increased drug release as the PEG content of the polymer composition increased from 18 to 24 mole %. Table 6-1 shows the average daily release of voclosporin that corresponded to the KDR profiles in given in Figure 6.1 for three time intervals: 1-4 weeks, 5-10 weeks and 11-20 weeks. These intervals do not represent different stages of drug release.

Figure 6.2 is a plot of the fractional cumulative release of voclosporin as a function of the square root of time for the three DTM terpolymers. A linear relationship

---

[14] The detrimental effect of gamma radiation on voclosporin in the presence of the polycarbonate terpolymers were not known at the time of this study.

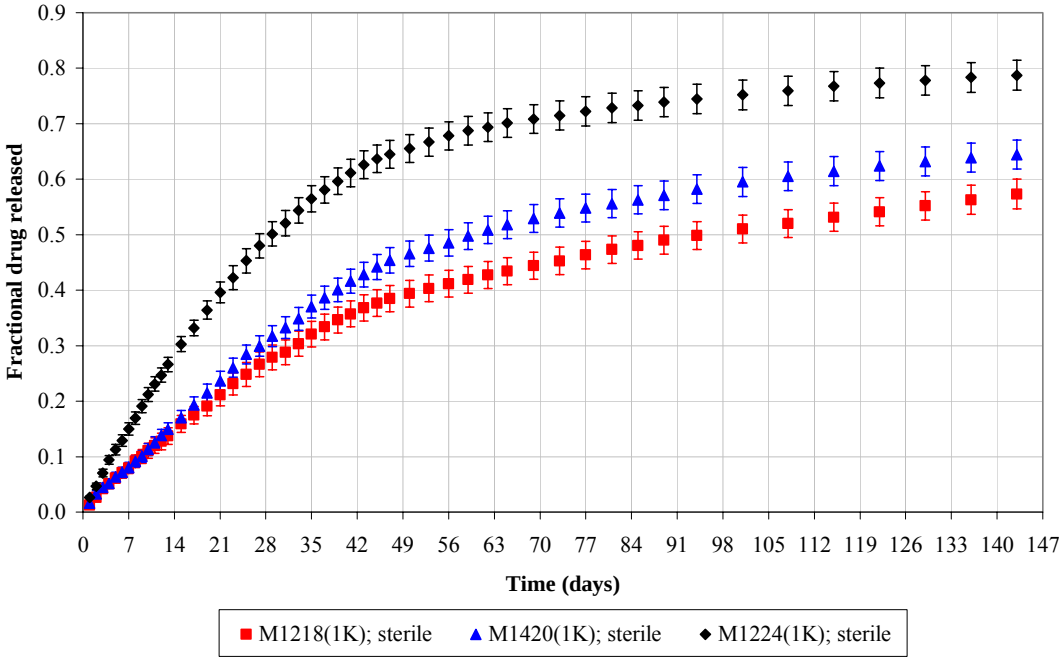

Figure 6.1. Average 20-week cumulative fractional drug release from sterile 6 mm diameter x 360 μm thick (nominal) disks of poly(DTM-co-y % DT-co-z % PEG_{1K} carbonate) loaded with 15 wt.% voclosporin in PBS at 37 °C. Error bars indicate cumulative error.

Table 6-1. Average in vitro daily release of voclosporin from sterile polymers loaded with 15 wt.% voclosporin and incubated in PBS at 37°C.

Polymer composition	Avg. daily release during 1-4 weeks (μg/day)	Avg. daily release during 5-10 weeks (μg/day)	Avg. daily release during 11-20 weeks (μg/day)
M1218(1K)	11 ± 1	5 ± 2	2 ± 0
M1420(1K)	12 ± 1	6 ± 3	2 ± 0
M1224(1K)	16 ± 3	5 ± 3	1 ± 0
E1218(1K)	10 ± 3	4 ± 2	2 ± 0
E1420(1K)	12 ± 4	4 ± 2	1 ± 0
E1224(1K)	16 ± 5	5 ± 3	1 ± 0
1:1 blend E1224(1K) +PLGA 50:50	6 ± 3	4 ± 1	2 ± 1

is indicative of a diffusion-controlled mechanism for drug release from the polymeric carrier. The figure shows two stages of release – an early release-stage that is characterized by the steeper linear region, and a late release-stage that is characterized by the second linear region occurring at a later time. The slopes of these linear regions for the polymer samples given in Table 6-2 are a measure of the rate of drug release. The data shown in the table illustrates a slowdown in diffusion (ranging from 50-85% decrease in the release rate from the terpolymers) from early-stage to late-stage drug release. The only polymer formulation that did not show a dual stage release profile was the 1:1 blend of E1224(1K)+PLGA 50:50.

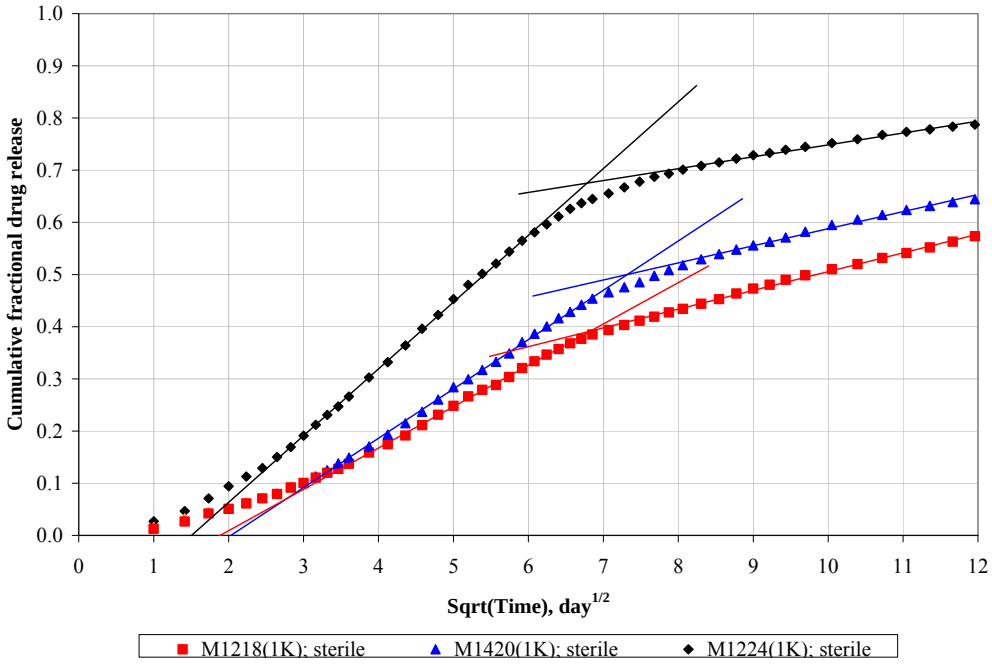

Figure 6.2. Plot of the average cumulative fractional drug release versus the square root of time for sterile 6 mm diameter x 360 μm thick (nominal) disks of poly(DTM-co-y % DT-co-z % PEG_{1K} carbonate) loaded with 15 wt.% voclosporin in PBS at 37 °C. The early- and late-release stages are depicted with lines. Error bars removed for convenience.

Table 6-2. Average early and late stage release rates of voclosporin from sterile polymers in PBS at 37°C.

Polymer	Early release-stage rate ($1/day^{1/2}$)	Late release-stage rate ($1/day^{1/2}$)	Early-to-late stage transition time (day)
M1218(1K)	0.08	0.04	46
M1420(1K)	0.09	0.03	54
M1224(1K)	0.13	0.02	46
E1218(1K)	0.07	0.03	49
E1420(1K)	0.09	0.02	46
E1224(1K)	0.13	0.02	46
1:1 blend E1224(1K) + PLGA 50:50	0.04	Not present	Not present

Figure 6.3 is a plot of the *in vitro* cumulative fractional drug release versus time for the gamma sterilized DTE terpolymers – E1218(1K), E1420(1K) and E1224(1K) – loaded with 15 wt.% voclosporin and incubated in PBS at 37°C over a period of 20 weeks. The total drug content was adjusted for loss due to gamma sterilization (refer to Table 5-4). Error bars represent the cumulative accumulated error obtained during the experiment. These polymers also show a trend similar to the DTM terpolymers of increasing drug release as the PEG content in the polymer composition increased. The cumulative percentage of drug released in 20 weeks for E1218(1K), E1420(1K) and E1224(1k) were 48%, 59% and 78%, respectively. The average daily release of voclosporin corresponding to these KDR profiles is given in Table 6-1 and the relative drug release rates at early- and late-stages are given in Table 6-2.

Figure 6.4 is a plot of the *in vitro* cumulative fractional drug release versus time for gamma sterilized polymers loaded with 15 wt.% voclosporin and incubated in PBS at 37°C over a period of 20 weeks showing how the 1:1 blend of E1224(1K)+PLGA 50:50

performed relative to the E1224(1K) polymer. The total drug content was adjusted for loss due to gamma sterilization (refer to Table 5-4). Error bars represent the cumulative accumulated error obtained during the experiment. The average daily drug release from the polycarbonate/PLGA blended matrix was relatively lower compared to the early-stage drug release of the E1224(1K) polymer. Figure 6.5 is a plot of the fractional cumulative release of voclosporin versus the square root of time over a period of 31 weeks for the blended matrix that showed a relatively linear relationship that was indicative of a single stage diffusion mechanism.

A comparison of *in vitro* cumulative voclosporin release between non-sterile (Table 6-3) and gamma-sterile (Table 6-4) polymeric drug carriers was summarized for

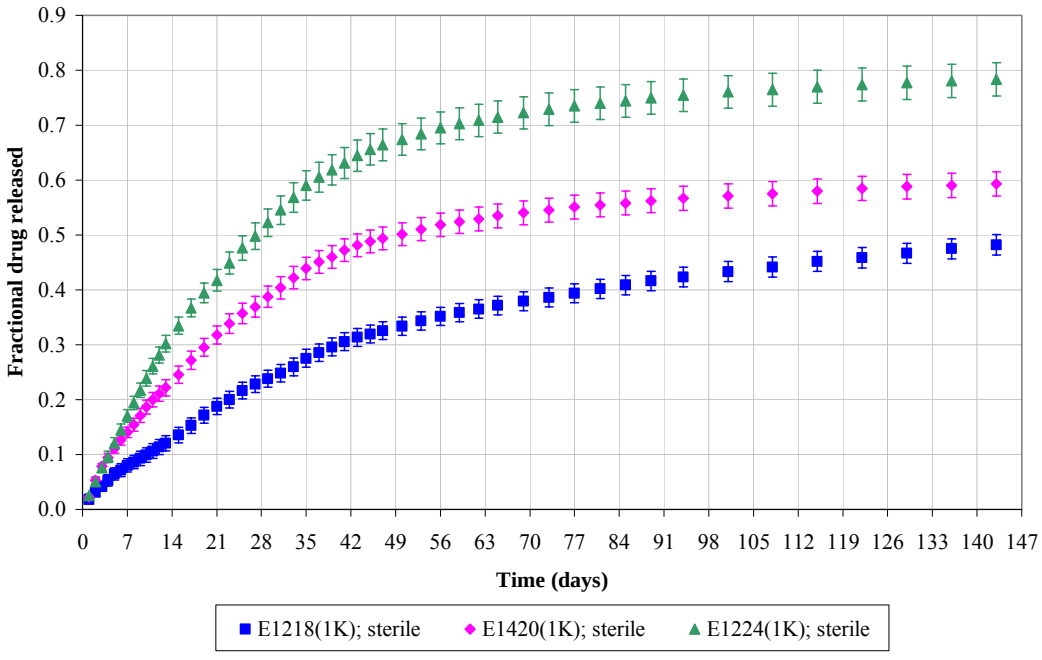

Figure 6.3. Average cumulative fractional drug release from sterile 6 mm diameter x 360 μm thick (nominal) disks of poly(DTE-co-y % DT-co-z % PEG_{1K} carbonate) loaded with 15 wt.% voclosporin in PBS at 37 °C. Error bars indicate cumulative error.

the time intervals of 4, 10 and 20 weeks. Statistical analysis using the paired t-test between polymer samples before and after gamma sterilization indicated no statistical difference in drug release between any polymers at 4 weeks, except for the polymer M1224(1K) ($p = 0.001$). Similar analysis at 10 and 20 weeks indicated no statistical difference in drug release between any polymers, except for M1224(1K) ($p = 0.003$, 10 weeks; $p = 0.001$, 20 weeks) and E1224(1K) ($p = 0.036$, 10 weeks; $p = 0.014$, 20 weeks). Drug release from the M1224(1K) polymer was increased after gamma sterilization by 25%, 16% and 22% for 4, 10 and 20 weeks, respectively. Drug release from the E1224(1K) polymer was increased by 44% and 42% after 10 and 20 weeks, respectively. All other polymers showed no statistical difference in drug release after gamma radiation.

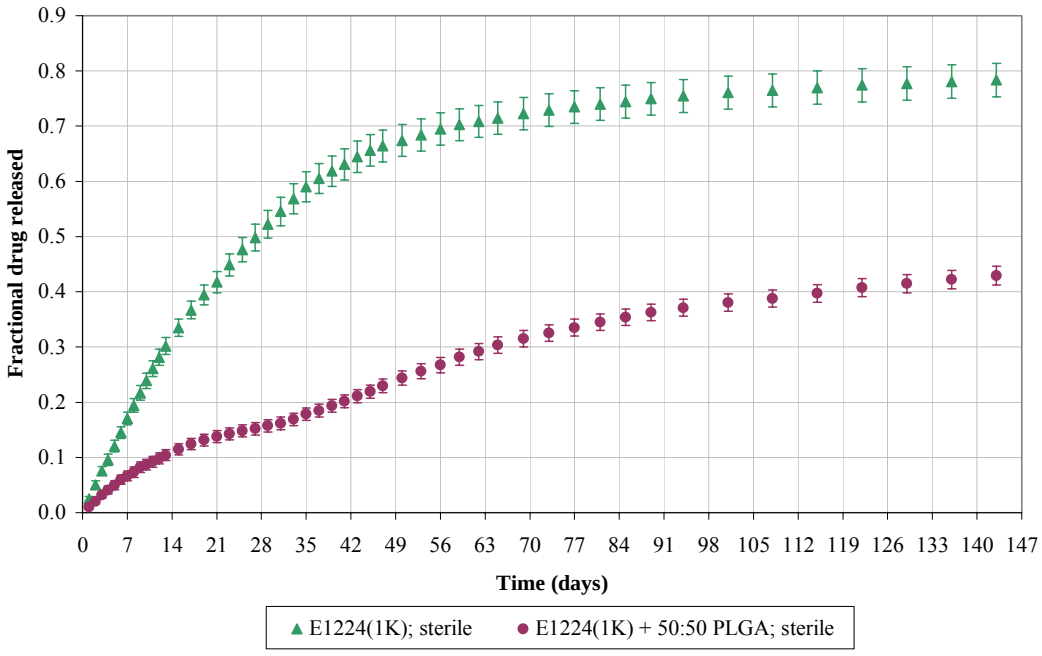

Figure 6.4. Average cumulative fractional drug release from sterile 6 mm diameter x 360 μm thick (nominal) disks of poly(DTE-co-y % DT-co-z % PEG_{1K} carbonate) loaded with 15 wt.% voclosporin in PBS at 37 °C. Comparison of E1224(1K) and the 1:1 blend of E1224(1K)+PLGA 50:50. Error bars indicate cumulative error.

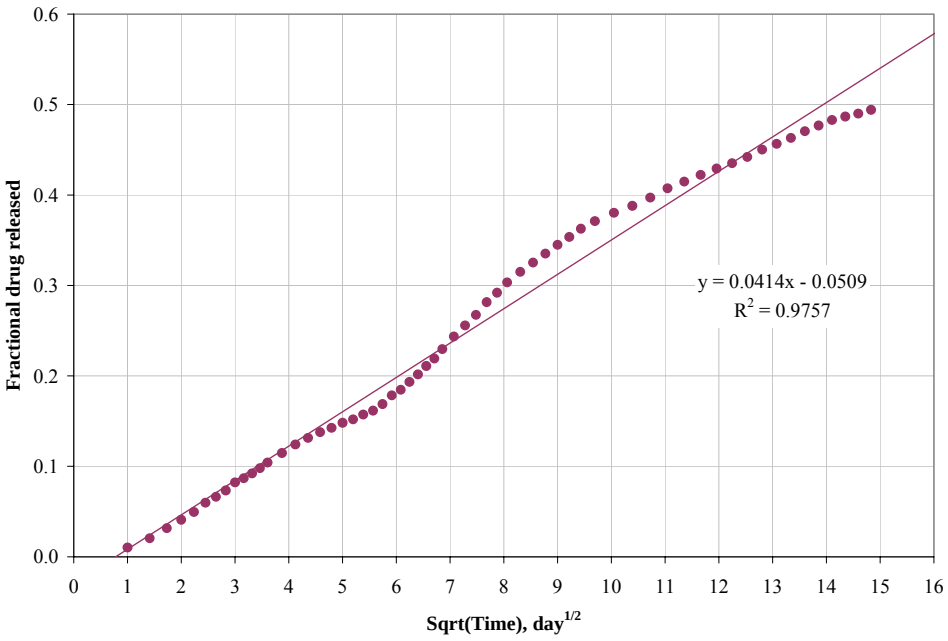

Figure 6.5. Plot of the average cumulative fractional drug release versus the square root of time for sterile 6 mm diameter x 360 μm thick (nominal) disks of 1:1 blend of E1224(1K)+PLGA 50:50 loaded with 15 wt.% voclosporin in PBS at 37 °C. Line depicts single-stage drug diffusion for 32 weeks. Error bars removed for convenience.

Table 6-3. Cumulative percent drug released from *in vitro* devices (non sterilized) loaded with 15 wt.% voclosporin and incubated in PBS at 37°C.

Polymer composition	Percent drug released after 4-weeks	Percent drug released after 10-weeks	Percent drug released after 20-weeks
M1218(1K)	28 ± 2	44 ± 3	54 ± 3
M1420(1K)	36 ± 2	59 ± 3	66 ± 3
M1224(1K)	40 ± 2	61 ± 3	65 ± 3
E1218(1K)	25 ± 2	35 ± 3	40 ± 3
E1420(1K)	31 ± 2	48 ± 2	53 ± 2
E1224(1K)	36 ± 3	50 ± 3	55 ± 3
1:1 blend of E1224(1K)+PLGA 50:50	18 ± 1	35 ± 2	43 ± 2

Table 6-4. Cumulative percent drug released from gamma sterile (~22 kGy) *in vitro* devices loaded with 15 wt.% voclosporin and incubated in PBS at 37°C.

Polymer composition	Percent drug released after 4-weeks	Percent drug released after 10-weeks	Percent drug released after 20-week
M1218(1K)	28 ± 2	44 ± 2	57 ± 3
M1420(1K)	32 ± 2	53 ± 3	64 ± 3
M1224(1K)	50 ± 2	71 ± 3	79 ± 3
E1218(1K)	24 ± 2	38 ± 2	48 ± 2
E1420(1K)	39 ± 2	54 ± 2	59 ± 2
E1224(1K)	52 ± 3	72 ± 3	78 ± 3
1:1 blend of E1224(1K)+PLGA 50:50	16 ± 1	32 ± 1	43 ± 2

6.1.2 Gross morphology of explanted polymeric drug carriers

Figure 6.6 shows representative photographs of explanted placebo polymeric devices and the surrounding subcutaneous tissue at the 4 week rabbit necropsy. No apparent redness or extreme inflammation was observed in any sample. Tissue formation around the implant did not appear fibrous in nature and a few blood vessels were observed to form over the devices. The polycarbonate terpolymer devices showed shape distortion during their degradation when compared to the PLGA 75:25 control. In general, all implants were well tolerated and did not appear to impede the normal tissue healing process.

Figure 6.7 shows representative photographs of explanted placebo polymeric devices and the surrounding subcutaneous tissue at the 10 week rabbit necropsy. The polycarbonate terpolymer devices appeared to be smaller in size compared to the four-week devices. The 1:1 E1224(1K)+PLGA 50:50 blend appeared to have more surrounding blood compared to the other polymers. The PLGA 75:25 control appeared to

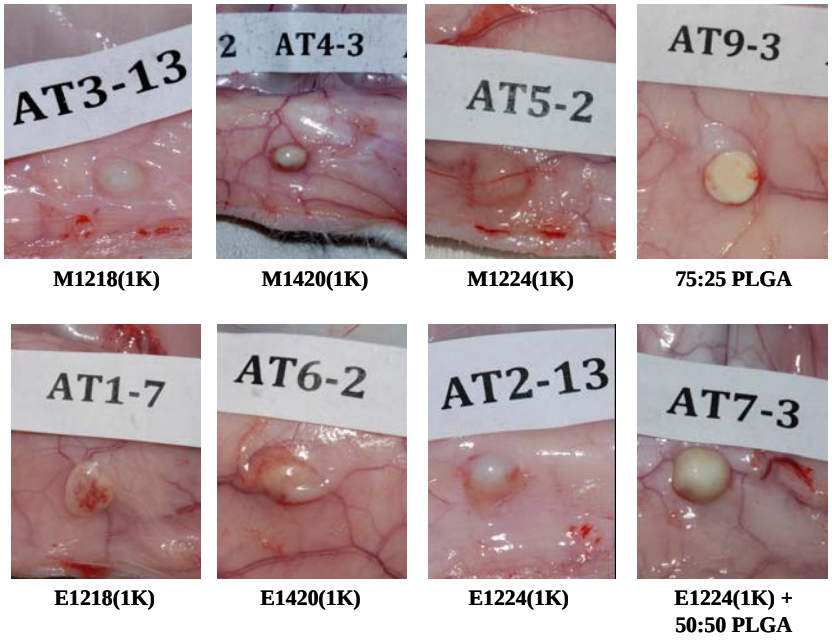

Figure 6.6. Gross morphology of 4-week rabbit subcutaneous explanted polymeric devices (6mm diameter x 360 μm nominal thickness) containing 15 wt.% voclosporin. Photos courtesy of Professor Brian Gilger, College of Veterinary Medicine, NCSU.

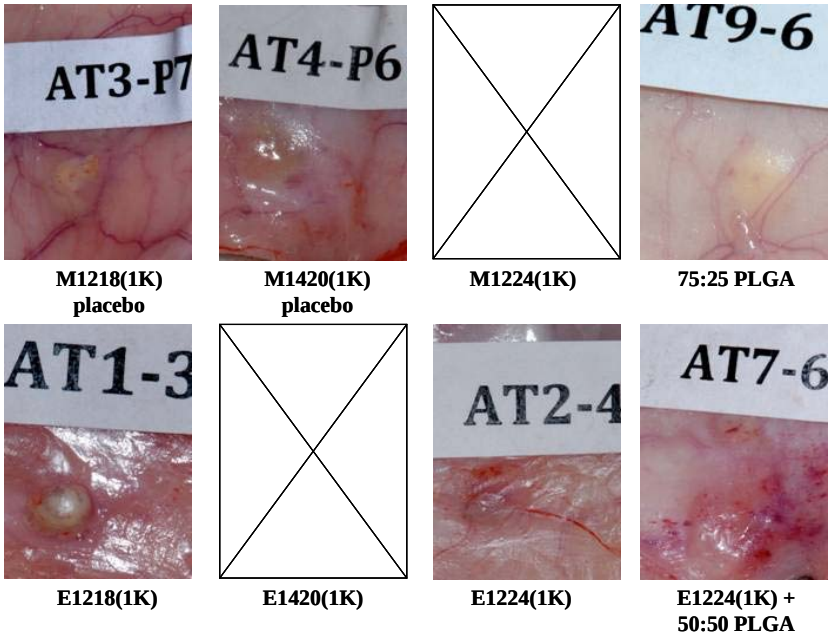

Figure 6.7. Gross morphology of 10-week rabbit subcutaneous explanted polymeric devices (6mm diameter x 360 μm nominal thickness) containing 15 wt.% voclosporin. Photo courtesy of Professor Brian Gilger, College of Veterinary Medicine, NCSU.

have more dense tissue growth compared to its four-week counterpart. No representative photographs of the explants were available for M1224(1K) and E1420(1K). No polymer samples were located at the 20 week time point, except the M1218(1K) samples. Observations from the veterinary surgeon of the conditions of all the explanted polymers at 4 and 10 weeks are presented in Table 6-5.

Table 6-5. Description of devices explanted from subcutaneous rabbit study.

	Polymer composition	4-week observation*	10-week observation*
Placebo	M1218(1K)	1/4 very small; 1/4 small; 2/4 large	1/4 very small; 3/4 not visible
	M1420(1K)	4/4 small	4/4 not visible
	M1224(1K)	4/4 very small	4/4 not visible
	E1218(1K)	1/4 small; 3/4 large	4/4 very small
	E1420(1K)	4/4 very small	4/4 not visible
	E1224(1K)	4/4 very small	4/4 not visible
	1:1 blend E1224(1K) + PLGA 50:50	3/4 large; 1/4 lost	4/4 not visible
	PLGA 75:25	3/4 large; 1/4 not visible	4/4 very small
Active (15 wt.% drug)	M1218(1K)	2/4 small; 1/4 not visible; 1/4 lost	4/4 not visible
	M1420(1K)	4/4 large	2/4 medium; 2/4 small
	M1224(1K)	2/4 very small; 1/4 small; 1/4 not visible	4/4 very small
	E1218(1K)	4/4 small	3/4 small; 1/4 very small
	E1420(1K)	2/4 very small; 2/4 small	4/4 very small
	E1224(1K)	2/4 small; 2/4 not visible	4/4 not visible
	1:1 blend E1224(1K) + PLGA 50:50	4/4 large	4/4 not visible
	PLGA 75:25	4/4 large	4/4 small

(*) Nomenclature example: "1/4 small" indicates 1 of 4 samples were small. Observations reported by Veterinary Surgeon.

6.1.3 Histology of 4-week explanted polymeric placebo devices

The dermal histopathology of placebo devices after four weeks implantation in the rabbit subcutaneous is shown in Figure 6.8 and Figure 6.9. Interpretations from the veterinary surgeon were that the explanted samples M1420(1K), M1224(1K), E1218(1K), E1420(1) and E1224(1K) did not appear different from the control tissue site (not shown) with respect to the amount of inflammation or tissue fibrosis. Sample M1218(1K) showed an increase in inflammation (i.e. moderate numbers of mononuclear cell infiltrate) surrounding the implant and in the overlying dermal tissue relative to both the control site and to the other implants sites listed above. The 1:1 blend of E1224(1K)+PLGA 50:50 had similar mild inflammation and fibrosis surrounding the implant site, but appeared to have moderate infiltration of mononuclear cells into the implant material. For the control polymer PLGA 75:25, the implant site was substantially different from the other sites. The implant was surrounded by a dense fibrotic capsule, which is characteristic for foreign body materials that are placed into an animal or human host, and had surrounding mononuclear cell infiltrate. No histopathology was available for the drug-loaded polymer explants at the time of this publication.

6.1.4 *In vivo* cumulative KDR from drug loaded polymeric carriers

Table 6-6 shows the measured amount of voclosporin retained in devices explanted from the rabbit after four and ten weeks. No statistical analysis was performed due to the low sample size and high variability in the data.

Table 6-6. Percent drug released from polymers implanted in rabbit subcutaneous loaded with 15 wt.% voclosporin (gamma sterilized).

Polymer composition	Percent drug released after 4-week implantation	Percent drug released after 10-week implantation
M1218(1K)	66 ± 40 %	38 ± 11 %
M1420(1K)	54 ± 18 %	69 ± 7 %
M1224(1K)	85 ± 12 %	92 ± 9 %
E1218(1K)	40 ± 9 %	65 ± 27 %
E1420(1K)	90 ± 10 %	90 ± 3 %
E1224(1K)	91 ± 5 %	N/A
1:1 blend E1224(1K) + PLGA 50:50	46 ± 8 %	N/A

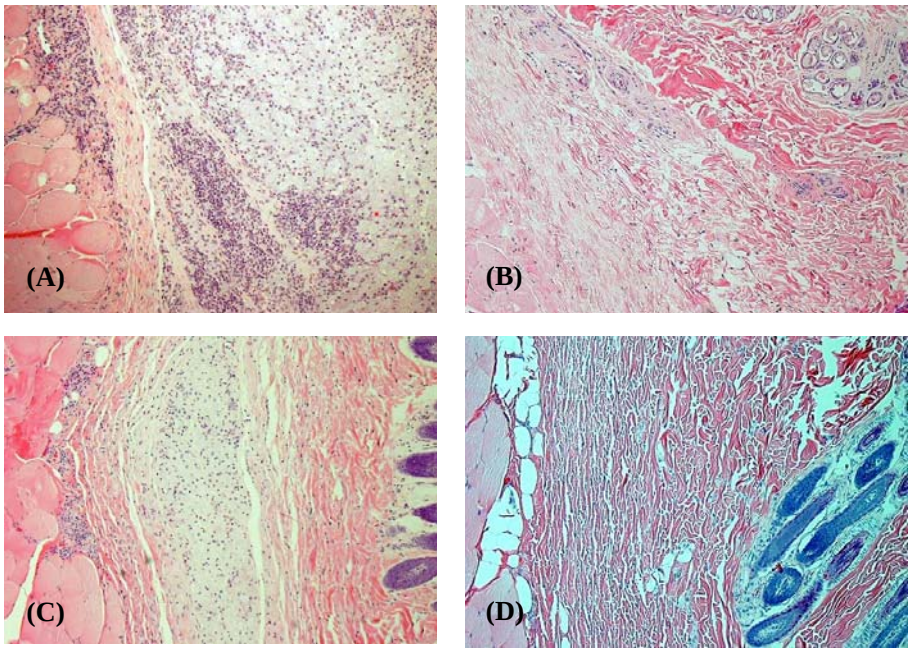

Figure 6.8. Histology of 4-week rabbit subcutaneous explants of 6mm diameter x 360 μm nominal thickness polymeric devices (placebo): (A) M1218(1K), (B) E1218(1K), (C) M1420(1K) and (D) E1420(1K). All photographs were taken at 100X magnification. Photo courtesy of Professor Brian Gilger, College of Veterinary Medicine, NCSU.

The calculated drug *in vivo in vitro* correlation (IVIVC) values were obtained by dividing the *in vivo* percent drug released values from Table 6-6 by their corresponding *in vitro* percent drug release values from Table 6-4. These IVIVC values are given in Table 6-7.

Table 6-7. IVIVC of voclosporin release from polycarbonate terpolymers (rabbit subcutaneous).

Polymer composition	4-week IVIVC	10-week IVIVC
M1218(1K)	2.4	0.9
M1420(1K)	1.7	1.3
M1224(1K)	1.7	1.3
E1218(1K)	1.7	1.7
E1420(1K)	2.3	1.7
E1224(1K)	1.8	N/A
1:1 blend E1224(1K) + PLGA 50:50	2.9	N/A

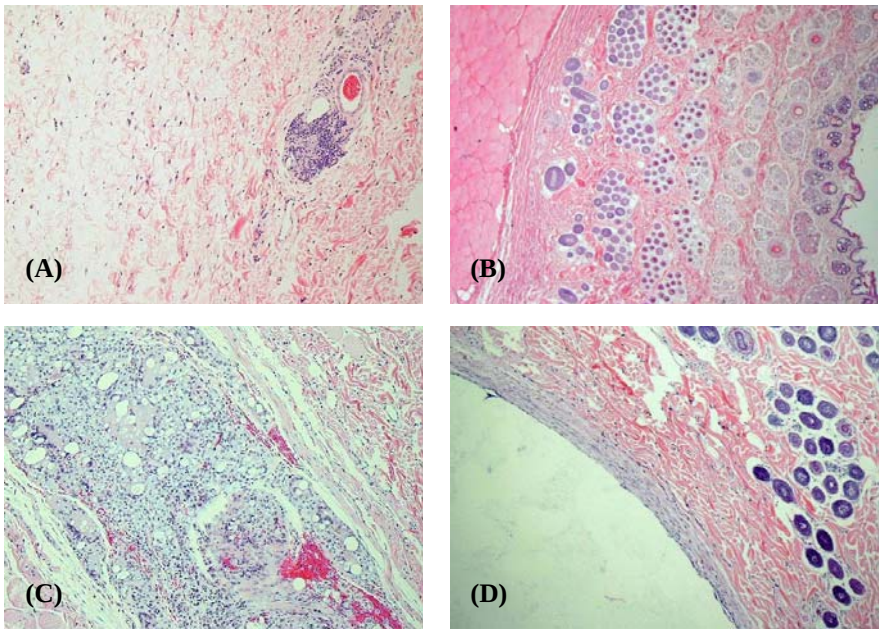

Figure 6.9. Histology of 4-week rabbit subcutaneous explants of 6mm diameter x 360 μm nominal thickness polymeric devices (placebo): (A) M1224(1K), (B) E1224(1K); 40X, (C) 1:1 blend of E1224(1K)+PLGA 50:50 and (D) PLGA 75:25. All photographs were taken at 100X magnification, except when indicated otherwise. Photo courtesy of Professor Brian Gilger, College of Veterinary Medicine, NCSU.

6.2 *In vivo in vitro* performance of polycarbonate polymers containing antioxidants in rabbit episcleral implantation

The *in vivo in vitro* episcleral study for evaluating drug release utilized two drug loaded formulations, E1218(1K) and an E1224(1K)/PLGA blend containing the antioxidant Vitamin E, that were implanted in the conjunctival space of rabbit eyes. For each rabbit, a single implant was placed into the left eye and three implants were placed into the right eye (as described in Section 2.2.22). These samples were compared to the *in vitro* KDR performance of polymers taken from the same drug loaded set and tested in PBS at 37 °C. All *in vitro* devices were gamma sterilized prior to testing. The *in vivo* explants were measured for drug content or were submitted for histological examination.

6.2.1 *In vitro* KDR profiles of sterile formulations containing Vitamin E

Figure 6.10(A) is a plot of the *in vitro* cumulative fractional drug release versus time for gamma sterilized polymers – E1218(1K) and the 1:2 blend (wt./wt.) E1224(1K)+PLGA 50:50 – containing 15 wt.% voclosporin and 1 wt.% (per wt. of polymer) of Vitamin E, incubated in PBS at 37 °C over a period of 17 weeks. The total drug content was adjusted for the loss of approximately 10 % voclosporin due to gamma sterilization in the presence of Vitamin E. Error bars represent the cumulative accumulated error obtained during the experiment. The *in vitro* average cumulative percent release of voclosporin from the E1281(1K) and E1224(1K)/PLGA blend carriers after 4 weeks was 11.7 ± 0.4 % and 11.6 ± 0.5 %, respectively, and after 11 weeks was 22.0 ± 0.6 % and 32.4 ± 1.3 %, respectively. The *in vitro* average daily release of voclosporin from the E1218(1K) and the E1224(1K)/PLGA blend carriers were 8 ± 4 and

(A)

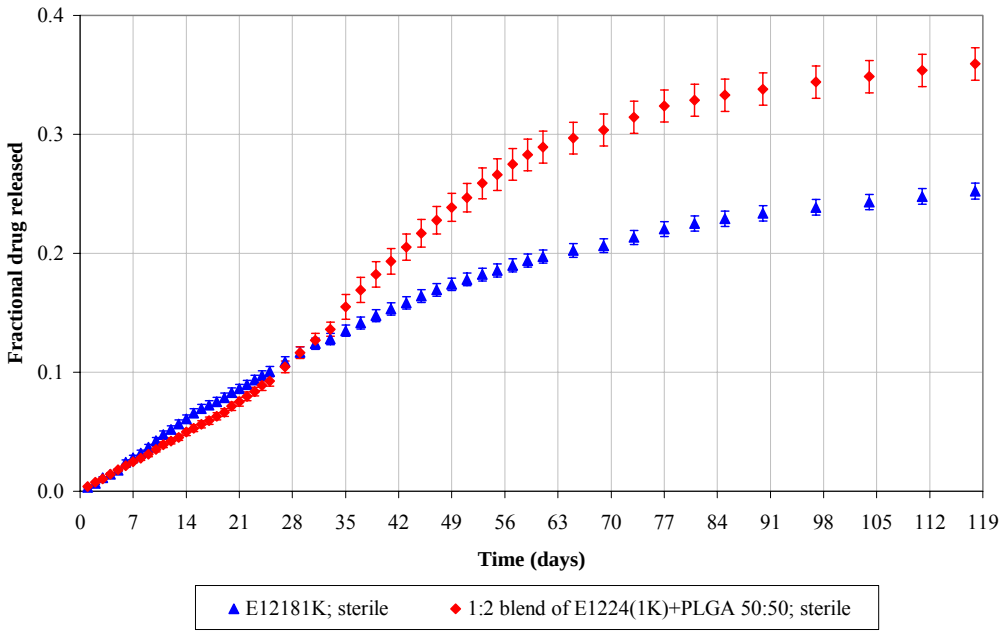

(B)

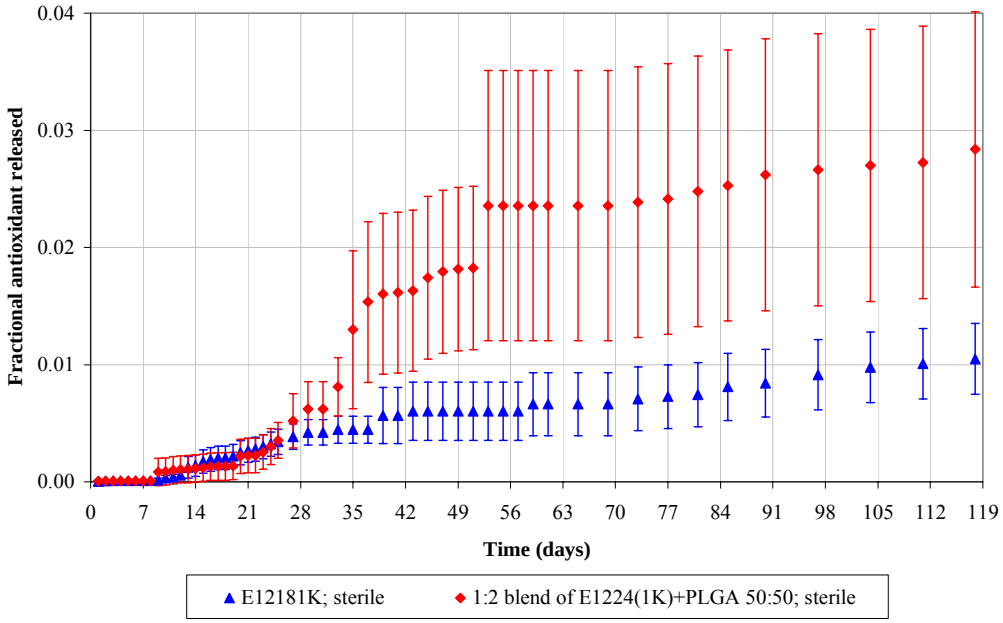

Figure 6.10. Average cumulative fractional release of (A) voclosporin and (B) Vitamin E from 2 mm wide x 15 mm long x 0.5 mm thick sterile polymer devices containing 15 wt.% drug and 1 wt. % (per weight of polymer) antioxidant in PBS at 37 °C. Error bars indicate cumulative error.

7 ± 3 μg/day, respectively, over the 17 week time period. Figure 6.10(B) shows the concurrent cumulative release of Vitamin E for both polymer matrices which were less than 3 % of the total antioxidant. The antioxidant content in the polymers was also adjusted for an approximate loss of 10 to 19 % during gamma sterilization. The predicted logP values of Vitamin E and voclosporin, calculated with ACD/LogP DB software release 11.0 (Advanced Chemistry Development Inc., Ontario, Canada) was 10.96 ± 0.39 and 2.89 ± 1.08, respectively, showing Vitamin E to be 3 to 4 times more hydrophobic than voclosporin which could account for its relatively low release from the polymer matrices.

Figure 6.11 is a plot of the *in vitro* cumulative fractional drug release versus the square root of time for the two voclosporin-loaded polymer formulations containing the antioxidant Vitamin E. The profile for the 1:2 blend of the polycarbonate/PLGA appeared to deviate from a single-stage mechanism of drug diffusion compared to the 1:1 blend of polycarbonate/PLGA without antioxidant shown earlier in Figure 6.5. Additionally, the sterile carrier E1218(1K) containing voclosporin and Vitamin E appeared to be different from its characteristic dual-stage release mechanism described in Chapter 3, demonstrating a single-stage mechanism of drug release. It is expected that longer incubation times in PBS may eventually reveal the dual stage mechanism. If not, then it can be surmised that the hydrophobic Vitamin E may have disrupted the drug/polymer interaction, thereby preventing the occurrence of drug retention within the matrix.

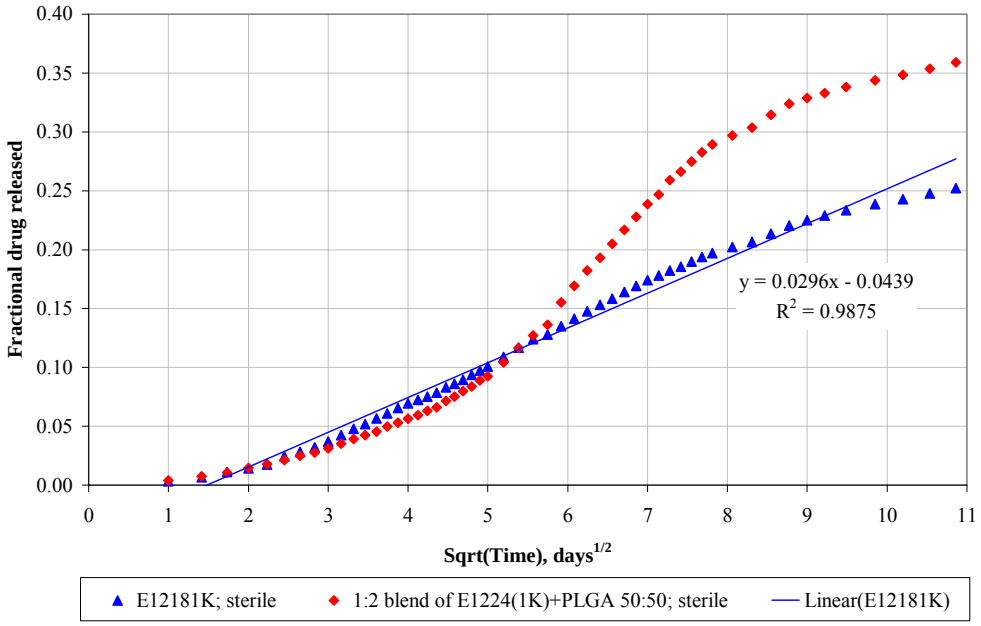

Figure 6.11. Average cumulative fractional drug release versus the square root of time for the polymer carriers E1218(1K) and E1224(1K)/PLGA blend containing 15 wt.% voclosporin and 1 wt.% (per wt. of polymer) Vitamin E, incubated in PBS at 37 °C. Error bars removed for convenience.

6.2.2 In vitro total mass loss of polymer formulations

Table 6-8 shows the *in vitro* total mass loss of the two gamma sterilized polymer formulations, E1218(1K) and the 1:2 blend (wt./wt.) of E1224(1K)+PLGA 50:50, each containing 15 wt.% voclosporin and 1 wt.% (per wt. of polymer) of Vitamin E. The pre-weighed dry test samples were hydrated in PBS at 37 °C for 4 and 11 weeks, rinsed in deionized water, dried by lyophilization and then re-weighed to determine the change in dry weight.

Table 6-8. Percent mass loss of polycarbonate formulations containing 15 wt.% voclosporin and 1 wt.% (per wt. of polymer) of Vitamin E incubated in PBS at 37 °C.

Polymer composition	Week 4	Week 11
E1218(1K)	29 ± 5	49 ± 2
1:2 blend of E1224(1K)+PLGA 50:50	26 ± 2	62 ± 3

6.2.3 Evaluation of *in vivo* polymer formulations

Clinical examination of the rabbit eyes by the veterinary surgeon indicated no signs of inflammation or toxicity related to any of the polymeric devices at 4 and 11 weeks implantation. All devices were visible at the time of excision from the ocular tissue for both time points, however the 11 week samples were visibly smaller. At 11 weeks, the hydrated devices appeared to migrate posterior from their implantation site towards the equator of the eye. Representative histological examination of the explanted single polymeric devices and surrounding ocular tissue at 4 week rabbit necropsy is shown in Figure 6.12. Mild inflammation was observed around each device that consisted of mononuclear cells and macrophages. Tissue response due to the presence of three devices was reported by the surgeon as being slightly elevated. Figure 6.13 is a photograph of a 4-week tissue section containing the three distorted forms of the hydrated

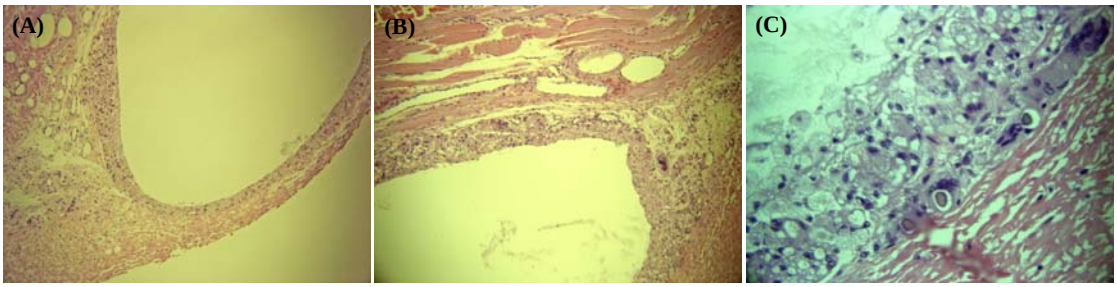

Figure 6.12. Histology of 4-week rabbit explanted episcleral devices containing 15 wt.% voclosporin and 1 wt.% (per wt. of polymer) Vitamin E: (A) E1218(1K); 20X magnification, (B) 1:2 blend of E1224(1K)+PLGA 50:50; 40X, (C) same as B; 400X magnification. All samples are single implants. Photo courtesy of Professor Brian Gilger, College of Veterinary Medicine, NCSU.

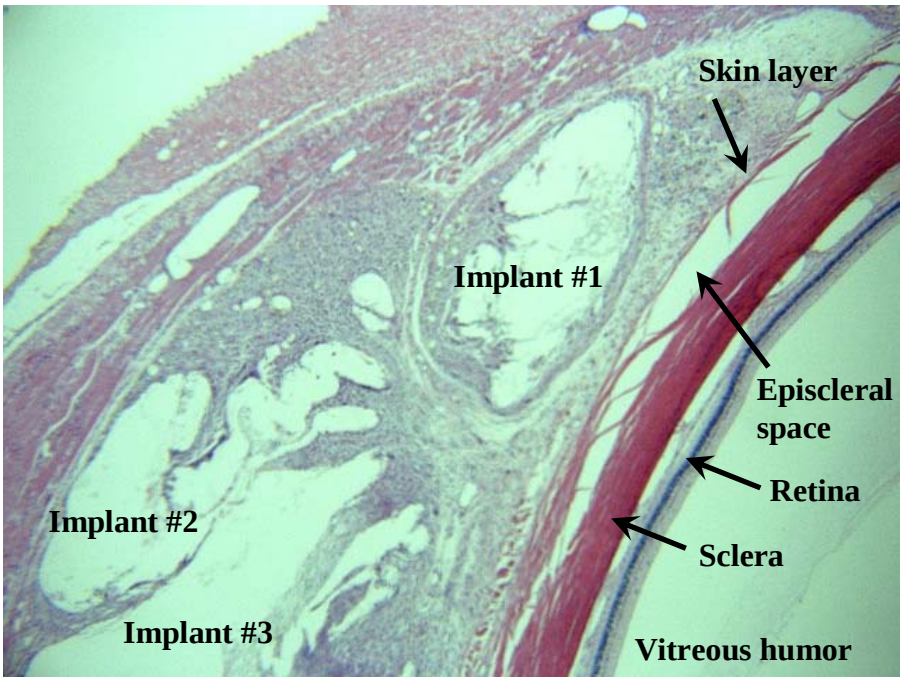

Figure 6.13. Histology of 4-week rabbit episcleral explants containing 3 sterile devices. Each device was 2 mm wide x 15 mm long x 0.5 mm thick composed of a 1:2 blend of E1224(1K)+PLGA 50:50, 15 wt.% voclosporin and 1 wt.% (per wt. of polymer) Vitamin E. Magnification is 20X. Photo courtesy of Professor Brian Gilger, College of Veterinary Medicine, NCSU.

drug-loaded polycarbonate/PLGA blend devices. No 11-week histology was available at the time of this publication.

6.2.4 *In vivo* cumulative KDR from drug loaded polymer formulations

Table 6-9 shows the measured amount of voclosporin retained in devices explanted from the conjunctival region of the rabbit eye after 4 and 11 weeks. No statistical analysis was performed since the sample size was equal to one. Missing values in the table corresponded to very low yields from the extraction process and were discarded.

Table 6-9. Percent drug released from polymer formulations implanted in the rabbit episcleral study loaded with 15 wt.% voclosporin and 1 wt.% (per wt. of polymer) Vitamin E (gamma sterilized).

Polymer composition	No. of implants	%drug release after 4 weeks	%drug release after 11 weeks
E1218(1K)	1	N/A	76
E1218(1K)	3	36	71
1:2 blend of E1224(1K)+PLGA 50:50	1	46	N/A
1:2 blend of E1224(1K)+PLGA 50:50	3	46	84

The calculated drug IVIVC values for the polymer formulations were obtained by dividing the *in vivo* percent drug release values given in Table 6-9 by the in vitro percent drug release value from Section 6.2.1. These IVIVC values are given in Table 6-10.

Table 6-10. IVIVC of voclosporin release from polycarbonate terpolymer formulations (rabbit episcleral study).

Polymer composition	No. of implants	4-week IVIVC	11-week IVIVC
E1218(1K)	1	N/A	3.5
E1218(1K)	3	3.0	3.2
1:2 blend of E1224(1K)+PLGA 50:50	1	3.8	N/A
1:2 blend of E1224(1K)+PLGA 50:50	3	3.8	2.6

7 Concluding remarks and future work

The family of PEG-containing polycarbonates is a versatile subset of the tyrosine based biodegradable polymers. Several examples of their versatility were demonstrated throughout this work, and in particular, the advantages of PEG in the composition were highlighted. It was ironic that this non-natural metabolite yielded much control on the utility of these terpolymers. Water access was a key requirement in the degradation and transport of mobile species out of the matrix, and low thermal processing conditions were a necessity to prevent degradation of the drug molecule. Both features were made possible by the presence of PEG. Conversely, PEG was also the Achilles heel of the polymer composition. The destruction of the drug molecule in the presence of free radicals generated from the PEG during thermal or gamma radiation necessitated the use of antioxidants.

Several features describing the complexity of the PEG-containing polycarbonates were mentioned: (a) the transport of water and associated swelling of the polymer matrix was shown to modulate drug release and polymer erosion, (b) the gel-like form of the hydrated polymer made the matrix flowable and non porous, (c) the hydrolysis of the polymer chain was dependant on the availability of water around the various carbonate bonds present in the polymer chain backbone, (d) the transport of oligomers (bulk erosion) was not dependant on the rate of MW degradation, (e) drug release was diffusion-controlled and was augmented during early-stage and reduced during late stage release, (f) the polymer composition was constantly changing during its resorption, (g)

microphase separation of PEG_{1K} was shown to occur during hydration of the polymer, (h) intercalation of the drug with the hydrophobic DTE-co-DT segments of the polymer chain was demonstrated, and (i) a potential interaction between voclosporin and the hydrophobic segments of the polymer was suggested. In summary, this research provided evidence that the hydration-induced microphase separation of PEG_{1K} was the most probable cause for drug retention (and the slowdown in polymer erosion) in these matrices during late-stage drug release. This phase separation of water-rich regions was responsible for the increased transport resistance of all species (drug and oligomers).

The studies presented within this thesis have spawned a range of potential research topics, if executed, would be beneficial for advanced characterization these polymer systems for many future biomedical engineering applications. These ideas are listed below.

7.1 Hydroperoxides in PEG

The preliminary work performed in this thesis on the use of antioxidants to protect the drug molecule from free radicals generated from PEG during thermal and gamma radiation exposure will need to be expanded in scope. Characterization of synthesized terpolymers and off-the-shelf raw monomers, method development for purifying PEG of hydroperoxides, method development for detecting hydroperoxides in PEG and optimization of the levels of antioxidants needed for complete protection of the drug from different polymer batches are some of the work that is required. In addition, the proper control samples are required to determine the contribution level of PEG, DT and DTR on drug instability under heat and radiation conditions. A study on the mechanism of action of the antioxidants will determine whether a cocktail of antioxidants

would be a more effective strategy for protecting the drug. Shelf stability of formed devices is also within the scope of this work.

7.2 Relevance of *in vitro* testing

A significant effort was expended characterizing the drug release and polymer erosion performance of the polycarbonate terpolymers using *in vitro* test methods in PBS. The results obtained from preliminary animal studies indicated that *in vitro* test data was marginally helpful in the selection of a suitable polymeric candidate for a Phase I GLP pilot study for commercialization of an ocular implantable drug delivery device. The need for a more relevant means of evaluating polymer performance demands that a release media be developed that closely mimic the body fluids of interest. The complexity of such a media involves the use of enzymes, lipids and salts at their correct concentrations under sterile conditions to prevent the bacterial growth. Testing for drug content and polymer degradation byproducts becomes more complicated since separation from the media contents would be required. The use of mass spectroscopy instead of HPLC may be required as the analytical method for drug and polymer detection. The author believes that such a method does provide a more controllable environment than working directly in animal models. However, animal models would be necessary to validate these more relevant bench-top procedures.

7.3 Development of TEM staining methods for polycarbonate homo-, co- and terpolymers

Neutron and x-ray scattering techniques were utilized to successfully demonstrate the phase behavior of the hydrated polycarbonate co- and terpolymers. Examination of

these polymers using a complementary technique such as cryogenic TEM would confirm the existence of these phase separated structures. The development of staining techniques for the polycarbonates to provide contrast and resolution will enable the use of TEM in the Kohn laboratory. Complications from artifacts during staining should be considered.

7.4 Deuteration of polymer components for SANS studies

The high intensity source at the High Flux Isotope Reactor (HFIR) at the SANS facility at ORNL in Oakridge, TN, provides a unique opportunity to probe the mobility of deuterated single polymer chains in real time in hydrated forms of the solid matrix. The development of deuteration techniques in the Kohn laboratory would enable the synthesis of polymer compositions with select labeled regions that can be tracked over the lifetime of the degrading hydrated polymer.

7.5 Methods for disrupting PEG phase separation

Synthesis of polycarbonate terpolymers containing low molecular weight PEG (3 to 4 repeat units in PEG) should prevent PEG mobility during hydration and should allow water molecules to be uniformly distributed throughout the matrix. Assuming that the proposed theory is correct for drug retention, this structure should allow a near-zero order release of the drug for the lifetime of the device prior to complete loss of it structural integrity.

Methods to disrupt the PEG microphase separated domains were investigated (in hindsight) through the used of PLGA. PLGA degradation might have temporarily disrupted the PEG domains causing an extension in drug release. The use of surfactants

may also assist in preventing microphase separation of PEG. A more detailed study is required.

8 Appendix

Table 8-1. *In vitro* weight-average molecular weights, M_w, for poly(DTE-co-y % DT-co-z % PEG_{1K} carbonate) disks loaded with 30 wt.% voclosporin and incubated in PBS at 37 °C at times of 1, 2, 3, 4 and 5 months.

Lattice point	Polymer composition	Weight-average molecular weight, M_w (kDa)					
		0 month	1 month	2 month	3 month	4 month	5 month
1	E0000(1K)	260	211	180	176	153	154
2	E1200(1K)	121	94	78	72	72	71
3	E0018(1K)	151	61	40	30	27	35
4	E1218(1K)	176	29	19	15	15	15
5	E0400(1K)	187	147	124	127	109	112
6	E0800(1K)	160	122	102	93	90	93
7	E0006(1K)	201	117	80	63	54	56
8	E0012(1K)	222	93	58	43	37	42
9	E1206(1K)	172	26	17	13	14	14
10	E1212(1K)	161	27	17	14	14	14
11	E0418(1K)	144	42	26	21	19	17
12	E0818(1K)	174	34	21	17	16	16
13	E0304.5(1K)	148	88	60	46	38	43
14	E0904.5(1K)	115	62	40	27	19	16
15	E0313.5(1K)	168	46	29	22	20	19
16	E0913.5(1K)	184	30	19	15	15	15
17	E0609(1K)	173	35	21	16	16	15

Table 8-2. In vitro number-average molecular weights, Mn, for poly(DTE-co-y % DT-co-z % PEG_{1K} carbonate) disks incubated in PBS at 37 °C at times of 1, 2, 3, 5 and 7 days for determination of initial rate of polymer degradation.

Lattice point	Polymer composition	Number-average molecular weight, M_n (kDa)											
		0 day	0 day	1 day	1 day	2 day	2 day	3 day	3 day	5 day	5 day	7 day	7 day
1	E0000(1K)	173	203	174	169	177	175	178	178	177	172	174	174
2	E1200(1K)	69	68	65	69	65	64	61	63	59	59	57	58
3	E0018(1K)	78	74	70	67	60	60	56	59	57	54	54	52
4	E1218(1K)	55	56	51	50	44	44	39	39	35	35	31	32
5	E0400(1K)	118	111	118	117	116	116	113	113	104	104	101	96
6	E0800(1K)	92	91	91	90	89	91	88	90	82	83	79	78
7	E0006(1K)	143	137	144	140	146	148	140	140	138	140	130	122
8	E0012(1K)	174	178	167	167	155	155	138	142	137	132	123	123
9	E1206(1K)	81	73	77	65	74	77	58	57	45	47	38	37
10	E1212(1K)	55	54	48	48	43	43	37	37	34	34	30	30
11	E0418(1K)	100	98	98	97	77	76	65	65	58	60	54	54
12	E0818(1K)	52	52	49	49	44	43	38	39	36	36	33	33
13	E0304.5(1K)	100	96	99	100	91	92	93	91	86	85	83	85
14	E0904.5(1K)	71	69	73	72	68	67	64	64	58	62	56	55
15	E0313.5(1K)	74	74	71	67	63	61	56	57	51	50	46	47
16	E0913.5(1K)	52	54	49	48	42	43	38	38	35	35	32	32
17	E0609(1K)	81	78	71	70	60	61	53	53	46	46	41	41

Table 8-3. ***In vitro*** **average cumulative fractional drug release of voclosporin (30 wt.% loading) from poly(DTE-co-y % DT-co-z % PEG_{1K} carbonate) disks incubated in PBS at 37 °C at times of 4, 8, 12, 16, 20, 24, 28, 32 and 35 weeks.**

			Average cumulative fractional release of drug								
Lattice point	Polymer composition	Initial avg. drug mass (mg)	4 wk	8 wk	12 wk	16 wk	20 wk	24 wk	28 wk	32 wk	35 wk
1	E0000(1K)	1.67	0.047	0.076	0.098	0.120	0.134	0.148	0.156	0.161	0.163
2	E1200(1K)	1.64	0.002	0.003	0.004	0.004	0.005	0.006	0.007	0.008	0.009
3	E0018(1K)	1.97	0.092	0.115	0.130	0.144	0.152	0.164	0.174	0.185	0.192
4	E1218(1K)	2.03	0.110	0.137	0.154	0.169	0.180	0.195	0.211	0.224	0.232
5	E0400(1K)	1.77	0.025	0.038	0.049	0.061	0.070	0.082	0.091	0.099	0.105
6	E0800(1K)	1.61	0.009	0.011	0.012	0.013	0.014	0.016	0.018	0.019	0.021
7	E0006(1K)	1.93	0.010	0.013	0.015	0.017	0.020	0.023	0.026	0.029	0.033
8	E0012(1K)	1.96	0.066	0.084	0.097	0.109	0.118	0.132	0.143	0.152	0.158
9	E1206(1K)	1.91	0.077	0.094	0.111	0.126	0.134	0.141	0.146	0.149	0.151
10	E1212(1K)	1.88	0.095	0.118	0.134	0.149	0.161	0.174	0.184	0.193	0.200
11	E0418(1K)	1.97	0.083	0.105	0.119	0.130	0.137	0.148	0.157	0.167	0.173
12	E0818(1K)	2.10	0.080	0.101	0.116	0.127	0.135	0.146	0.156	0.164	0.171
13	E0304.5(1K)	1.96	0.007	0.008	0.009	0.012	0.014	0.018	0.023	0.028	0.031
14	E0904.5(1K)	1.89	0.011	0.014	0.019	0.029	0.041	0.053	0.057	0.060	0.062
15	E0313.5(1K)	1.99	0.083	0.104	0.118	0.132	0.144	0.161	0.173	0.182	0.188
16	E0913.5(1K)	2.01	0.085	0.107	0.121	0.133	0.142	0.155	0.168	0.179	0.185
17	E0609(1K)	1.98	0.073	0.092	0.109	0.123	0.135	0.144	0.151	0.159	0.165

Table 8-4. ***In vitro*** **35-week kinetic drug release data for voclosporin (30 wt. % loading) from poly(DTE-co-y % DT-co-z % PEG_{1K} carbonate) compositions in PBS at 37 °C showing the early and late-stage drug release, fractional release rate coefficients k_1 (early stage) and k_2 (late-stage), onset of transition from k_1 to k_2 and persistence factor.**

Sample design point	Polymer composition	Average early-stage drug release (μg/day)	Average late-stage drug release (μg/day)	$k_1 \times 10^{-3}$ ($day^{-1/2}$)	$k_2 \times 10^{-3}$ ($day^{-1/2}$)	Early-to-late stage transition (day)	Persistence factor
1	E0000(1K)	2.0 ± 0.8	0.2 ± 0.1	12.7 ± 1.3	3.6 ± 1.1	190 ± 25	0.28 ± 0.06
2 (†)	E1200(1K)	0.1 ± 0.1	0.1 ± 0.0	0.4 ± 0.2	1.2 ± 0.3	134 ± 7	3.73 ± 1.57
3	E0018(1K)	9.1 ± 2.3	1.2 ± 0.4	23.5 ± 1.5	9.6 ± 0.9	18 ± 2	0.41 ± 0.02
4	E1218(1K)	10.2 ± 2.4	1.4 ± 0.4	26.3 ± 3.1	11.5 ± 0.5	23 ± 0	0.44 ± 0.04
5	E0400(1K)	1.7 ± 0.6	0.7 ± 0.1	4.9 ± 1.3	7.8 ± 2.2	36 ± 5	1.60 ± 0.28
6 (†)	E0800(1K)	1.4 ± 0.6	0.1 ± 0.1	2.0 ± 0.8	1.0 ± 0.6	7 ± 2	0.51 ± 0.10
7 (†)	E0006(1K)	0.5 ± 0.6	0.2 ± 0.1	1.3 ± 0.1	3.3 ± 0.2	130 ± 9	2.53 ± 0.36
8	E0012(1K)	8.8 ± 2.0	1.3 ± 0.5	19.2 ± 1.4	8.7 ± 0.4	10 ± 1	0.46 ± 0.02
9	E1206(1K)	7.6 ± 1.9	0.9 ± 0.4	20.0 ± 1.6	7.9 ± 1.2	18 ± 0	0.40± 0.06
10	E1212(1K)	9.0 ± 2.5	1.2 ± 0.4	22.7 ± 2.2	10.1 ± 0.6	21 ± 11	0.45 ± 0.03
11	E0418(1K)	8.7 ± 2.5	1.1 ± 0.4	21.3 ± 1.7	8.6 ± 0.7	16 ± 2	0.41 ± 0.03
12	E0818(1K)	8.7 ± 2.5	1.2 ± 0.4	20.4 ± 1.7	8.8± 0.5	17 ± 1	0.43 ± 0.04
13 (†)	E0304.5(1K)	0.4 ± 0.4	0.3 ± 0.0	0.8 ± 0.0	4.7 ± 0.1	130 ± 3	5.88 ± 0.12
14 (†)	E0904.5(1K)	0.7 ± 0.6	0.7 ± 0.1	1.5 ± 0.1	8.9 ± 0.6	80 ± 3	5.93 ± 0.17
15	E0313.5(1K)	9.9 ± 2.1	1.5 ± 0.8	21.1 ± 1.9	10.4 ± 1.7	13 ± 8	0.50 ± 0.12
16	E0913.5(1K)	9.5 ± 2.6	1.3 ± 0.4	21.9 ± 1.6	9.5 ± 1.0	15 ± 1	0.44 ± 0.04
17	E0609(1K)	7.6 ± 1.8	1.1 ± 0.4	18.6 ± 1.9	9.1 ± 1.2	16 ± 2	0.4 ± 0.03

(†) Contained data measured below the LOQ or LOD during HPLC analysis.

Table 8-5. ***In vitro*** **average mass loss of DTR from poly(DTE-co-y % DT-co-z % PEG_{1K} carbonate) disks loaded with 30 wt.% voclosporin incubated in PBS at 37 °C at four week intervals.**

			Average mass loss of DTR (mg)							
Lattice point	**Polymer composition**	**Initial avg. DTR mass (mg)**	**Week 0-4**	**Week 4-8**	**Week 8-12**	**Week 12-16**	**Week 16-20**	**Week 20-24**	**Week 24-28**	**Week 28-32**
1	E0000(1K)	3.94	0.00	0.00	0.00	0.00	0.00	0.00	0.00	0.00
2	E1200(1K)	3.69	0.00	0.00	0.00	0.00	0.00	0.00	0.00	0.00
3	E0018(1K)	2.99	0.09	0.11	0.09	0.09	0.08	0.05	0.04	0.02
4	E1218(1K)	2.80	0.32	0.27	0.19	0.14	0.09	0.06	0.05	0.02
5	E0400(1K)	3.92	0.00	0.00	0.00	0.00	0.00	0.00	0.00	0.00
6	E0800(1K)	3.71	0.00	0.00	0.00	0.00	0.00	0.00	0.00	0.00
7	E0006(1K)	3.71	0.00	0.00	0.00	0.00	0.00	0.00	0.00	0.00
8	E0012(1K)	3.46	0.01	0.04	0.05	0.06	0.05	0.04	0.03	0.02
9	E1206(1K)	3.88	0.23	0.27	0.22	0.13	0.06	0.04	0.03	0.01
10	E1212(1K)	3.07	0.29	0.26	0.20	0.15	0.12	0.08	0.05	0.02
11	E0418(1K)	2.66	0.13	0.17	0.15	0.14	0.11	0.07	0.04	0.01
12	E0818(1K)	2.85	0.23	0.25	0.19	0.16	0.13	0.09	0.09	0.04
13	E0304.5(1K)	3.97	0.00	0.01	0.01	0.02	0.04	0.04	0.04	0.03
14	E0904.5(1K)	3.66	0.01	0.04	0.11	0.17	0.19	0.05	0.02	0.01
15	E0313.5(1K)	3.02	0.09	0.13	0.12	0.11	0.10	0.06	0.06	0.01
16	E0913.5(1K)	3.31	0.27	0.26	0.21	0.16	0.13	0.09	0.06	0.01
17	E0609(1K)	3.63	0.13	0.20	0.18	0.14	0.09	0.05	0.05	0.04

Table 8-6. *In vitro* average mass loss of PEG_{1K} from poly(DTE-co-y % DT-co-z % PEG_{1K} carbonate) disks loaded with 30 wt.% voclosporin incubated in PBS at 37 °C at four week intervals.

			Average mass loss of PEG_{1K} (mg)							
Lattice point	**Polymer composition**	**Initial avg. PEG_{1K} mass (mg)**	**Week 0-4**	**Week 4-8**	**Week 8-12**	**Week 12-16**	**Week 16-20**	**Week 20-24**	**Week 24-28**	**Week 28-32**
1	E0000(1K)	--	--	--	--	--	--	--	--	--
2	E1200(1K)	--	--	--	--	--	--	--	--	--
3	E0018(1K)	1.94	0.28	0.23	0.12	0.08	0.07	0.04	0.02	0.02
4	E1218(1K)	1.84	0.48	0.29	0.14	0.07	0.06	0.03	0.02	0.02
5	E0400(1K)	--	--	--	--	--	--	--	--	--
6	E0800(1K)	--	--	--	--	--	--	--	--	--
7	E0006(1K)	0.70	0.00	0.00	0.01	0.00	0.01	0.00	0.01	0.00
8	E0012(1K)	1.39	0.03	0.08	0.07	0.06	0.06	0.03	0.02	0.02
9	E1206(1K)	0.74	0.06	0.09	0.10	0.03	0.01	0.01	0.01	0.01
10	E1212(1K)	1.25	0.27	0.19	0.09	0.07	0.05	0.02	0.01	0.02
11	E0418(1K)	1.73	0.24	0.26	0.13	0.09	0.08	0.04	0.03	0.02
12	E0818(1K)	1.86	0.35	0.34	0.15	0.10	0.08	0.04	0.03	0.02
13	E0304.5(1K)	0.55	0.00	0.00	0.01	0.00	0.02	0.01	0.03	0.02
14	E0904.5(1K)	0.51	0.01	0.01	0.02	0.03	0.07	0.02	0.01	0.01
15	E0313.5(1K)	1.39	0.15	0.16	0.10	0.08	0.07	0.03	0.02	0.02
16	E0913.5(1K)	1.54	0.29	0.24	0.12	0.08	0.06	0.04	0.02	0.02
17	E0609(1K)	1.06	0.07	0.13	0.08	0.05	0.03	0.01	0.02	0.02

Table 8-7. Values of the scattering vector, q, corresponding to the interference peak obtained from the short-term hydration of polycarbonate polymers with and without 30 wt. % voclosporin in deuterated PBS at 37°C for 25 and 60 hours. Data collected by SANS. Values in square brackets are the domain spacing in Å calculated from the Bragg relationship.

		Location of interference peak in terms of q value ($Å^{-1}$)			
Lattice	Polymer	Polymer only		Polymer + drug	
point	composition	25 hours	60 hours	25 hours	60 hours
1	E0000(1K)	(†)	(†)	(†)	(†)
2	E1200(1K)	(†)	(†)	(†)	(†)
3	E0018(1K)	0.037 [170]	0.037 [170]	0.032 [196]	0.034 [185]
4	E1218(1K)	0.052 [121]	0.051 [123]	0.046 [137]	0.046 [137]
5	E0400(1K)	(†)	(†)	(†)	(†)
6	E0800(1K)	(†)	(†)	(†)	(†)
7	E0006(1K)	0.018 [349]	0.018 [349]	(†)	(†)
8	E0012(1K)	0.032 [196]	0.031 [203]	0.031 [203]	0.029 [217]
9	E1206(1K)	0.043 [146]	0.035 [180]	0.040 [157]	0.037 [170]
10	E1212(1K)	0.038 [165]	0.040 [157]	0.040 [157]	0.042 [150]
11	E0418(1K)	0.046 [137]	0.045 [140]	0.042 [150]	0.048 [131]
12	E0818(1K)	0.046 [137]	0.048 [131]	0.046 [137]	0.051 [123]
13	E0304.5(1K)	(†)	(†)	(†)	(†)
14	E0904.5(1K)	(†)	(†)	(†)	(†)
15	E0313.5(1K)	0.037 [170]	0.038 [165]	0.035 [180]	0.035 [180]
16	E0913.5(1K)	0.042 [150]	0.042 [150]	0.037 [170]	0.040 [157]
17	E0609(1K)	0.037 [170]	0.035 [180]	0.032 [196]	0.034 [185]

(†) Not detected.

Table 8-8. Water uptake and ZP model parameters for SANS data of poly(DTE-co-y % DT-co-z % PEG_{1K} carbonate) compositions with and without 30 wt.% voclosporin incubated in PBS at 37 °C.

Sample design point	Polymer composition	Time (hr)	Water uptake (%)	Adjusted water uptake (%)	Peak present	Io	radius R (Å)	domain spacing, d (Å)	σ (Å)
4	E1218(1K) + drug	1	--	--	yes	8403	58	140	56
4	E1218(1K) + drug	2	--	--	yes	9270	57	138	56
1	E0000(1K) + drug	25	2.4 ± 2.4	3.4 ± 3.5	no	--	--	--	--
2	E1200(1K) + drug	25	7.7 ± 7.3	11.0 ± 10.5	no	--	--	--	--
3	E0018(1K) + drug	25	56.0 ± 8.5	80.0 ± 12.1	yes	49610	64	139	59
4	E1218(1K) + drug	25	86.7 ± 4.3	123.8 ± 6.1	yes	44516	53	112	37
5	E0400(1K) + drug	25	2.9 ± 3.5	4.2 ± 5.0	no	--	--	--	--
6	E0800(1K) + drug	25	6.3 ± 4.6	9.0 ± 6.6	no	--	--	--	--
7	E0006(1K) + drug	25	8.4 ± 5.0	12.1 ± 7.1	no	--	--	--	--
8	E0012(1K) + drug	25	20.7± 2.7	29.5 ± 3.9	yes	6581	61	176	59
9	E1206(1K) + drug	25	18.3 ± 5.1	26.1 ± 7.3	yes	3862	50	103	47
10	E1212(1K) + drug	25	57.3 ± 2.9	81.8 ± 4.2	yes	19392	52	132	42
11	E0418(1K) + drug	25	44.5 ± 8.7	63.5 ± 12.4	yes	24511	53	128	40
12	E0818(1K) + drug	25	56.4 ± 1.2	80.6 ± 1.7	yes	23452	51	114	35
13	E0304.5(1K) + drug	25	3.1 ± 1.0	4.4 ± 1.4	no	--	--	--	--
14	E0904.5(1K) + drug	25	6.1 ± 4.6	8.7 ± 6.6	no	--	--	--	--
15	E0313.5(1K) + drug	25	31.9 ± 1.0	45.6 ± 1.4	yes	27430	60	151	48
16	E0913.5(1K) + drug	25	53.4 ± 0.6	76.3 ± 0.9	yes	27400	56	136	50
17	E0609(1K) + drug	25	16.0 ± 2.6	22.8 ± 3.8	yes	2841	50	149	65

Table 8-8. (con't)

Sample design point	Polymer composition	Time (hr)	Water uptake (%)	Adjusted water uptake (%)	Peak present	Io	radius R (Å)	domain spacing, d (Å)	σ (Å)
1	E0000(1K)	25	6.9 ± 2.2	--	no	--	--	--	--
2	E1200(1K)	25	6.4 ± 4.2	--	no	--	--	--	--
3	E0018(1K)	25	77.1 ± 8.8	--	yes	44460	57	149	45
4	E1218(1K)	25	129.7 ± 8.7	--	yes	32502	41	109	31
5	E0400(1K)	25	4.0 ± 3.1	--	no	--	--	--	--
6	E0800(1K)	25	10.7 ± 8.4	--	no	--	--	--	--
7	E0006(1K)	25	4.8 ± 3.1	--	yes	2485	76	244	132
8	E0012(1K)	25	19.9 ± 4.6	--	yes	5350	56	173	55
9	E1206(1K)	25	38.6 ± 3.3	--	yes	6252	52	117	40
10	E1212(1K)	25	84.9 ± 6.7	--	yes	21452	53	142	45
11	E0418(1K)	25	54.8 ± 10.7	--	yes	13358	40	126	35
12	E0818(1K)	25	80.0 ± 8.9	--	yes	39484	46	119	35
13	E0304.5(1K)	25	5.0 ± 1.7	--	no	--	--	--	--
14	E0904.5(1K)	25	5.7 ± 5.4	--	no	--	--	--	--
15	E0313.5(1K)	25	40.9 ± 2.0	--	yes	18530	50	153	43
16	E0913.5(1K)	25	81.0 ± 1.3	--	yes	23600	47	131	39
17	E0609(1K)	25	32.2 ± 7.6	--	yes	11526	56	142	48

Table 8-8. (con't)

Sample design point	Polymer composition	Time (hr)	Water uptake (%)	Adjusted water uptake (%)	Peak present	Io	radius R (Å)	domain spacing, d (Å)	σ (Å)
1	E1218(1K) + drug	60	1.3 ± 1.3	1.9 ± 1.8	no	--	--	--	--
2	E1218(1K) + drug	60	3.0 ± 0.4	4.3 ± 0.5	no	--	--	--	--
3	E0000(1K) + drug	60	51.0 ± 3.9	72.9 ± 5.5	yes	41510	62	121	52
4	E1200(1K) + drug	60	85.0 ± 1.2	121.5 ± 1.7	yes	46504	52	111	36
5	E0018(1K) + drug	60	1.4 ± 1.4	2.0 ± 2.1	no	--	--	--	--
6	E1218(1K) + drug	60	3.5 ± 2.6	5.0 ± 3.8	no	--	--	--	--
7	E0400(1K) + drug	60	6.9 ± 2.2	9.8 ± 3.1	no	--	--	--	--
8	E0800(1K) + drug	60	18.9 ± 2.4	27.0 ± 3.4	yes	5665	63	183	61
9	E0006(1K) + drug	60	34.2 ± 2.3	48.8 ± 3.2	yes	18518	60	125	50
10	E0012(1K) + drug	60	61.7 ± 1.7	88.2 ± 2.4	yes	16427	50	131	42
11	E1206(1K) + drug	60	44.9 ± 0.7	64.1 ± 1.0	yes	10551	46	116	34
12	E1212(1K) + drug	60	60.6 ± 1.8	86.5 ± 2.6	yes	11461	45	109	31
13	E0418(1K) + drug	60	5.9 ± 2.3	8.4 ± 3.2	no	--	--	--	--
14	E0818(1K) + drug	60	3.9 ± 0.5	5.6 ± 0.7	no	--	--	--	--
15	E0304.5(1K) + drug	60	34.0 ± 0.4	48.5 ± 0.6	yes	27580	60	157	50
16	E0904.5(1K) + drug	60	54.1 ± 0.8	77.3 ± 1.2	yes	20590	52	133	43
17	E0313.5(1K) + drug	60	27.6 ± 3.1	39.4 ± 4.5	yes	8419	56	148	55

Table 8-8. (con't)

Sample design point	Polymer composition	Time (hr)	Water uptake (%)	Adjusted water uptake (%)	Peak present	Io	radius R (Å)	domain spacing, d (Å)	σ (Å)
1	E0000(1K)	60	7.9 ± 0.4	--	--	--	--	--	--
2	E1200(1K)	60	9.9 ± 1.1	--	--	--	--	--	--
3	E0018(1K)	60	73.4 ± 4.6	--	yes	52350	58	149	46
4	E1218(1K)	60	99.6 ± 20.4	--	yes	34490	46	112	31
5	E0400(1K)	60	10.9 ± 1.3	--	--	--	--	--	--
6	E0800(1K)	60	10.4 ± 0.6	--	--	--	--	--	--
7	E0006(1K)	60	6.8 ± 0.5	--	yes	2047	73	223	132
8	E0012(1K)	60	23.0 ± 1.1	--	yes	6138	61	187	57
9	E1206(1K)	60	64.5 ± 1.3	--	yes	14555	60	143	49
10	E1212(1K)	60	89.0 ± 3.1	--	yes	22413	53	135	42
11	E0418(1K)	60	49.5 ± 5.8	--	yes	14494	43	128	35
12	E0818(1K)	60	75.0 ± 10.7	--	yes	30479	46	119	34
13	E0304.5(1K)	60	4.8 ± 0.8	--	--	--	--	--	--
14	E0904.5(1K)	60	7.2 ± 0.9	--	--	--	--	--	--
15	E0313.5(1K)	60	46.9 ± 2.5	--	yes	23400	56	151	40
16	E0913.5(1K)	60	83.3 ± 4.9	--	yes	21490	48	131	39
17	E0609(1K)	60	36.6 ± 4.1	--	yes	10687	56	156	46

Table 8-9. Domain spacing (calculated using the Bragg relationship) from SAXS data of polymer disks with and without 30 wt.% voclosporin in the dry state and in the wet state in PBS at 37 °C for 1, 4 and 7 weeks.

		Domain spacing for polymer only (Å)				Domain spacing for polymer + drug (Å)			
Lattice point	Polymer composition	dry	1 wk	4 wk	7 wk	dry	1 wk	4 wk	7 wk
1	E0000(1K)	(†)	(†)	(†)	(†)	(†)	(†)	(†)	(†)
2	E1200(1K)	(†)	(†)	(†)	(†)	555	806	806	686
3	E0018(1K)	(†)	175	230	303	(†)	235	322	339
4	E1218(1K)	(†)	137	173	312	(†)	150	193	370
5	E0400(1K)	(†)	(†)	(†)	(†)	537	481	620	597
6	E0800(1K)	(†)	(†)	(†)	(†)	608	658	(†)	546
7	E0006(1K)	(†)	259	264	632	(†)	264	292	528
8	E0012(1K)	(†)	195	262	363	(†)	210	272	503
9	E1206(1K)	(†)	205	322	(†)	(†)	*184	315	(†)
10	E1212(1K)	(†)	155	259	488	(†)	171	309	619
11	E0418(1K)	(†)	148	189	285	(†)	159	213	335
12	E0818(1K)	(†)	141	185	312	(†)	145	199	366
13	E0304.5(1K)	(†)	*467	*453	(†)	(†)	(†)	*402	(†)
14	E0904.5(1K)	(†)	*161	*575	(†)	(†)	(†)	*644	(†)
15	E0313.5(1K)	(†)	157	200	353	(†)	172	246	402
16	E0913.5(1K)	(†)	152	206	397	(†)	167	287	447
17	E0609(1K)	(†)	175	235	(†)	(†)	184	246	473
-	p(DT carbonate)	(†)	(†)	(†)	--	(†)	(†)	(†)	(†)
-	p(PEG_{1K} carbonate)	193	--	--	--	231	--	--	--
-	E1224(1K)	(†)	124	--	273	(†)	132	--	277
-	E1230(1K)	(†)	118	--	225	(†)	123	--	197
-	E1420(1K)	(†)	125	--	342	(†)	125	--	282
-	E1818(1K)	(†)	--	--	429	(†)	--	--	322
-	E2418(1K)	(†)	--	--	--	(†)	--	--	--
-	E4018(1K)	(†)	--	--	--	(†)	--	--	--
-	E6018(1K)	(†)	--	--	--	(†)	--	--	--
-	M1218(1K)	(†)	129	177	350	(†)	141	--	383
-	M1420(1K)	(†)	123	161	287	(†)	123	--	268
-	M1224(1K)	(†)	125	170	312	(†)	124	166	298
-	PLGA 50:50	(†)	(†)	(†)	--	(†)	(†)	(†)	(†)
-	PLGA 75:25	(†)	(†)	(†)	(†)	(†)	(†)	(†)	(†)
-	PLGA 85:15	(†)	(†)	(†)	(†)	(†)	(†)	(†)	(†)

(†) No interference peak detected.

* Data suspicious; not used for trend analysis.

-- Sample fragmented. Not able to test.

Table 8-10. Intercalated drug-chain spacing from WAXS data for polymer disks with 30 wt.% voclosporin in the dry state and in the wet state in PBS at 37 °C for 1, 4 and 7 weeks.

Lattice point	Polymer composition	Intercalation spacing for polymer-drug (Å) dry	1 week	4 week	7 week
1	E0000(1K)	10.4	10.7	10.8	10.8
2	E1200(1K)	10.4	10.8	11.0	10.9
3	E0018(1K)	10.4	10.8	10.8	10.9
4	E1218(1K)	10.4	11.0	10.8	10.9
5	E0400(1K)	10.4	10.8	10.7	10.8
6	E0800(1K)	10.6	10.9	11.0	10.8
7	E0006(1K)	10.5	10.8	10.6	10.7
8	E0012(1K)	10.5	10.7	*11.0	*10.9
9	E1206(1K)	10.4	10.6	10.6	10.6
10	E1212(1K)	10.4	10.8	10.7	10.6
11	E0418(1K)	10.4	10.9	10.8	10.7
12	E0818(1K)	10.5	10.8	10.8	10.8
13	E0304.5(1K)	10.4	10.6	10.7	10.6
14	E0904.5(1K)	10.4	10.4	10.6	*10.5
15	E0313.5(1K)	10.5	10.8	10.6	10.8
16	E0913.5(1K)	10.6	10.8	10.8	10.7
17	E0609(1K)	10.5	10.7	*11.0	*10.5
-	p(DT carbonate)	10.7	11.1	11.0	11.0
-	p(PEG_{1K} carbonate)	*10.4	--	--	--
-	E1224(1K)	10.3	11.0	--	11.0
-	E1230(1K)	10.3	11.1	--	10.8
-	E1420(1K)	10.5	11.0	--	*11.2
-	E1818(1K)	10.5	--	--	10.6
-	E2418(1K)	10.5	--	--	--
-	E4018(1K)	10.6	--	--	--
-	E6018(1K)	10.7	--	--	--
-	M1218(1K)	10.6	11.0	--	10.7
-	M1420(1K)	10.4	10.8	--	10.8
-	M1224(1K)	10.6	10.9	10.9	10.7
-	PLGA 50:50	10.4	11.0	*11.2	*
-	PLGA 75:25	10.3	10.8	10.9	*
-	PLGA 85:15	10.3	10.7	10.9	*

(††) Interference peak is difficult to detect.
* Crystalline peaks present.
-- Sample fragmented. Not able to test.

Table 8-11. Interchain spacing from WAXS data for polymer disks with and without 30 wt.% voclosporin in the dry state and in the wet state in PBS at 37 °C for 1, 4 and 7 weeks.

		Interchain spacing for polymer only (Å)				Interchain spacing for polymer + drug (Å)			
Lattice point	Polymer composition	dry	1 wk	4 wk	7 wk	dry	1 wk	4 wk	7 wk
1	E0000(1K)	4.6	4.5	4.5	4.5	4.8	4.7	4.7	4.7
2	E1200(1K)	4.6	4.6	4.5	4.6	4.8	4.7	4.7	4.7
3	E0018(1K)	4.4	4.2	4.3	4.2	4.6	4.5	4.5	4.4
4	E1218(1K)	4.4	4.2	4.2	4.3	4.5	4.4	4.6	4.5
5	E0400(1K)	4.6	4.5	4.6	4.6	4.8	4.7	4.7	4.7
6	E0800(1K)	4.6	4.5	4.5	4.5	4.8	4.7	4.7	4.7
7	E0006(1K)	4.5	4.5	4.5	4.5	4.7	4.7	4.7	4.7
8	E0012(1K)	4.4	4.4	4.4	4.4	4.6	4.6	*4.6	*4.5
9	E1206(1K)	4.5	4.4	4.3	4.3	4.7	4.6	4.5	4.5
10	E1212(1K)	4.4	4.3	4.3	4.3	4.6	4.5	4.5	4.5
11	E0418(1K)	4.4	4.3	4.3	4.3	4.6	4.5	4.5	4.5
12	E0818(1K)	4.4	4.3	4.3	4.3	4.6	4.4	4.6	4.6
13	E0304.5(1K)	4.5	4.5	4.5	4.5	4.7	4.6	4.7	4.7
14	E0904.5(1K)	4.5	4.5	4.5	4.4	4.7	4.6	4.7	*4.7
15	E0313.5(1K)	4.4	4.3	4.3	4.4	4.6	4.5	4.6	4.6
16	E0913.5(1K)	4.4	4.4	4.3	4.4	4.6	4.5	4.5	4.6
17	E0609(1K)	4.5	4.4	4.4	4.4	4.6	4.6	*4.6	*4.6
-	p(DT carbonate)	4.6	4.4	4.4	--	4.7	4.7	4.7	5.0
-	p(PEG_{1K} carbonate)	*	--	--	--	*	--	--	--
-	E1224(1K)	4.4	4.3	--	4.3	4.5	(††)	--	4.5
-	E1230(1K)	4.3	(††)	--	4.2	*4.5	(††)	--	4.7
-	E1420(1K)	4.4	(††)	--	4.2	4.6	4.7	--	*4.6
-	E1818(1K)	4.4	--	--	4.3	4.5	--	--	4.5
-	E2418(1K)	4.4	--	--	--	4.6	--	--	--
-	E4018(1K)	4.4	--	--	--	4.6	--	--	--
-	E6018(1K)	4.4	--	--	--	4.5	--	--	--
-	M1218(1K)	4.4	4.3	4.2	4.4	4.6	4.6	--	4.5
-	M1420(1K)	4.4	(††)	4.3	4.3	4.5	4.6	--	4.6
-	M1224(1K)	4.4	4.2	4.3	4.4	4.5	4.5	4.5	4.5
-	PLGA 50:50	5.3; 4.3	5.4; 4.1	5.0; 3.8	--	5.5; 4.7	4.8; 4.0	4.8; 3.8	*
-	PLGA 75:25	5.7; 4.3	5.5; 4.0	5.7; 4.1	*	5.4; 4.5	5.6; 4.1	5.4; 4.0	*
-	PLGA 85:15	5.8; 4.3	5.5; 3.9	5.6; 3.8	5.6; 4.0	5.5; 4.6	5.5; 4.1	5.9; 4.2	*5.4; 3.9

(††) Interference peak is difficult to detect.
* Crystalline peaks present.
-- Sample fragmented. Not able to test.

Table 8-12. *In vitro* number-average molecular weights, M_n, for DTM and corresponding DTE terpolymers incubated in PBS at 37 °C at times up to 103 days.

Time (days)	Number-average molecular weight, M_n (kDa)					
	M1218(1K)	M1420(1K)	M1224(1K)	E1218(1K)	E1420(1K)	E1224(1K)
0	167	217	154	108	164	127
0	149	227	157	100	164	119
1	102	104	103	85	119	101
1	105	98	96	82	123	101
3	63	58	65	81	77	63
3	60	60	65	57	79	62
5	43	45	50	48	62	47
5	46	45	55	48	61	52
7	41	34	44	36	55	42
7	35	41	44	43	52	43
9	33	35	38	37	43	37
9	34	34	39	36	41	37
12	25	27	32	30	36	28
12	27	27	33	28	35	30
18	21	22	25	22	27	23
18	21	21	25	22	27	23
30	17	18	19	19	20	19
30	17	17	19	18	21	18
61	14	15	15	15	15	15
61	14	14	15	15	15	15
103	14	13	14	14	14	14
103	14	14	14	14	14	14

Table 8-13. Percentages of active voclosporin remaining in 30 wt.% drug loaded polycarbonates after heat treatment at various times and temperatures.

Polymer composition	R.T. (control)	100 °C			180 min	
		30 min	60 min	180 min	30 min	60 min
E0000(1K)	95 ± 4	93 ± 3	93 ± 2	88 ± 4	93 ± 3	86 ± 2
E1200(1K)	93 ± 1	84 ± 5	84 ± 4	82 ± 3	75 ± 4	68 ± 4
E0018(1K)	85 ± 2	61 ± 5	44 ± 3	25 ± 1	33 ± 2	25 ± 0
E1218(1K)	96 ± 3	70 ± 4	70 ± 2	59 ± 7	56 ± 2	48 ± 1

Samples analyzed by Mehdi Ashraf-Khorassani, Ph.D., at Virginia Tech.

Figure 8.1. Drug release from 6 mm diameter x 160 μm thick (nominal) disks loaded with 5 wt.% voclosporin incubated in PBS at 37 °C. Comparison of E1218(1K) versus PLGA carriers for (A) Average cumulative fractional release and (B) Average daily release. Error bars indicate cumulative error.

(A)

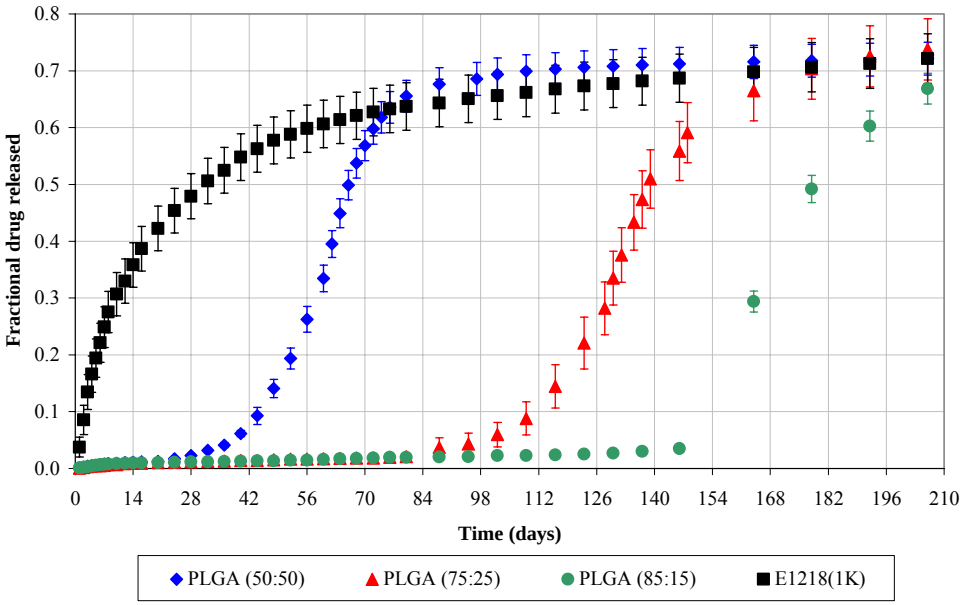

(B)

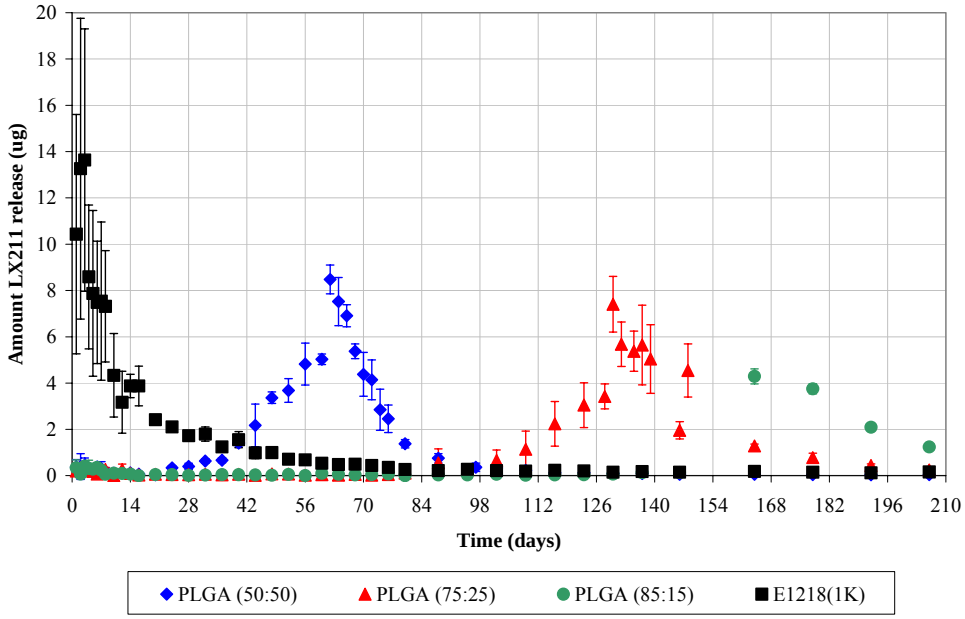

References

1. Anglade, E., Yatscoff, R., Foster, R. & Grau, U. (2007) *Expert Opinion on Investigational Drugs* **16,** 1525-1540.
2. Birsan, T., Dambrin, C., Freitag, D. G., Yatscoff, R. W. & Morris, R. E. (2005) *Transplant International* **17,** 767-771.
3. Knott, R. B., Schefer, J. & Schoenborn, B. P. (1990) *Acta Crystallographica Section C-Crystal Structure Communications* **46,** 1528-1533.
4. Meents, A., Dittrich, B. & Gutmann, S. (2009) *Journal of Synchrotron Radiation* **16,** 183-190.
5. Visiongain (2007), ed. Visiongain LTD, B. H., London, UK.
6. Ali, Y. & Lehmussaari, K. (2006) *Advanced Drug Delivery Reviews* **58,** 1258-1268.
7. Ding, S. L. (1998) *Pharmaceutical Science & Technology Today* **1,** 328-335.
8. Eljarrat-Binstock, E., Raiskup, F., Frucht-Pery, J. & Domb, A. J. (2005) *Journal of Controlled Release* **106,** 386-390.
9. McGhee, C. N. J., Dean, S. & Danesh-Meyer, H. (2002) *Drug Safety* **25,** 33-55.
10. Pijls, R. T., Lindemann, S., Nuijts, R. M. M. A., Daube, G. W. & Koole, L. H. (2007) *Journal of Drug Delivery Science and Technology* **17,** 87-91.
11. Hornof, M., Weyenberg, W., Ludwig, A. & Bernkop-Schnurch, A. (2003) *Journal of Controlled Release* **89,** 419-428.
12. Karatas, A. & Baykara, T. (2001) *Farmaco* **56,** 197-202.
13. Martinez-Sancho, C., Herrero-Vanrell, R. & Negro, S. (2006) *International Journal of Pharmaceutics* **326,** 100-106.
14. Albertsson, A. C., Carlfors, J. & Sturesson, C. (1996) *Journal of Applied Polymer Science* **62,** 695-705.
15. Di Colo, G., Burgalassi, S., Chetoni, P., Fiaschi, M. P., Zambito, Y. & Saettone, M. F. (2001) *International Journal of Pharmaceutics* **215,** 101-111.
16. Einmahl, S., Capancioni, S., Schwach-Abdellaoui, K., Moeller, M., Behar-Cohen, F. & Gurny, R. (2001) *Advanced Drug Delivery Reviews* **53,** 45-73.
17. Heller, J. (2005) *Advanced Drug Delivery Reviews* **57,** 2053-2062.
18. Hamalainen, K. M., Maatta, E., Piirainen, H., Sarkola, M., Vaisanen, A., Ranta, V. P. & Urtti, A. (1998) *Journal of Controlled Release* **56,** 273-283.
19. Gref, R., Quellec, P., Sanchez, A., Calvo, P., Dellacherie, E. & Alonso, M. J. (2001) *European Journal of Pharmaceutics and Biopharmaceutics* **51,** 111-118.
20. He, Y., Liu, Y. L., Liu, Y., Wang, J. C., Zhang, X., Lu, W. L., Ma, Z. Z., Zhu, X. A. & Zhang, Q. (2006) *Investigative Ophthalmology & Visual Science* **47,** 3983-3988.
21. He, Y., Wang, J. C., Liu, Y. L., Ma, Z. Z., Zhu, X. A. & Zhang, Q. (2006) *Journal of Ocular Pharmacology and Therapeutics* **22,** 121-131.
22. Lee, W. K., Park, J. Y., Yang, E. H., Suh, H., Kim, S. H., Chung, D. S., Choi, K., Yang, C. W. & Park, J. S. (2002) *Journal of Controlled Release* **84,** 115-123.
23. Aberturas, M. R., Molpeceres, J., Guzman, M. & Garcia, F. (2002) *Journal of Microencapsulation* **19,** 61-72.
24. Mao, H. Q., Shipanova-Kadiyala, I., Zhao, Z., Dang, W. B., Brown, A. & Leong, K. W. (2005) *Journal of Biomaterials Science-Polymer Edition* **16,** 135-161.

25. Lee, S. S., Kim, H., Wang, N. S., Bungay, P. M., Gilger, B. C., Yuan, P., Kim, J., Csaky, K. G. & Robinson, M. R. (2007) *Investigative Ophthalmology & Visual Science* **48,** 2023-2029.
26. Nair, L. S. & Laurencin, C. T. (2007) *Progress in Polymer Science* **32,** 762-798.
27. Merkli, A., Tabatabay, C., Gurny, R. & Heller, J. (1998) *Progress in Polymer Science* **23,** 563-580.
28. Coulembier, O., Degee, P., Hedrick, J. L. & Dubois, P. (2006) *Progress in Polymer Science* **31,** 723-747.
29. Okada, M. (2002) *Progress in Polymer Science* **27,** 87-133.
30. Ray, S. S. & Bousmina, M. (2005) *Progress in Materials Science* **50,** 962-1079.
31. Bourke, S. L. & Kohn, J. (2003) *Adv. Drug Del. Rev.* **55,** 447-466.
32. Tangpasuthadol, V., Pendharkar, S. M. & Kohn, J. (2000) *Biomaterials* **21,** 2371-2378.
33. Tangpasuthadol, V., Pendharkar, S. M., Peterson, R. C. & Kohn, J. (2000) *Biomaterials* **21,** 2379-2387.
34. Yu, C. & Kohn, J. (1999) *Biomaterials* **20,** 253-264.
35. Yu, C., Mielewczyk, S. S., Breslauer, K. J. & Kohn, J. (1999) *Biomaterials* **20,** 265-272.
36. Hooper, K. A., Macon, N. D. & Kohn, J. (1998) *J. Biomed. Mater. Res.* **41,** 443-454.
37. Schachter, D. (2000) *Ph.D. Dissertation, Rutgers University*.
38. Ryan, P. L., Foty, R. A., Kohn, J. & Steinberg, M. (2001) *Proc. Natl. Acad. Sci.* **98,** 4323-4327.
39. Sharma, R. I., Kohn, J. & Moghe, P. V. (2004) *J. Biomed. Mater. Res.* **69A,** 114–123.
40. Tziampazis, E., Kohn, J. & Moghe, P. V. (2000) *Biomaterials* **21,** 511-520.
41. Weber, N., Bolikal, D., Bourke, S. L. & Kohn, J. (2004) *J. Biomed. Mater. Res.* **68(A),** 496-503.
42. Hoven, V. P., Poopattanapong, A. & Kohn, J. (2004) *Macromol. Symp.* **216,** 87-97.
43. Siepmann, J. & Gopferich, A. (2001) *Advanced Drug Delivery Reviews* **48,** 229-247.
44. Larobina, D., Mensitieri, G., Kipper, M. J. & Narasimhan, B. (2002) *Aiche Journal* **48,** 2960-2970.
45. Faisant, N., Siepmann, J. & Benoit, J. P. (2002) *European Journal of Pharmaceutical Sciences* **15,** 355-366.
46. Breitenbach, A., Pistel, K. F. & Kissel, T. (2000) *Polymer* **41,** 4781-4792.
47. Wan, J. P., Yang, Y. Y., Chung, T. S., Tan, D., Ng, S. & Heller, J. (2001) *Journal of Controlled Release* **75,** 129-141.
48. Kozer, N., Kuttner, Y. Y., Haran, G. & Schreiber, G. (2007) *Biophysical Journal* **92,** 2139-2149.
49. Renner, C., Piehler, J. & Schrader, T. (2006) *Journal of the American Chemical Society* **128,** 620-628.
50. Winzor, D. J. & Wills, P. R. (2006) *Biophysical Chemistry* **119,** 186-195.
51. Claesson, P. M., Blomberg, E., Froberg, J. C., Nylander, T. & Arnebrant, T. (1995) *Advances in Colloid and Interface Science* **57,** 161-227.
52. Jonsson, M. & Linse, P. (2005) *Journal of Physical Chemistry B* **109,** 15107-15117.

53. Jonsson, M., Skepo, M., Tjerneld, F. & Linse, P. (2003) *Journal of Physical Chemistry B* **107,** 5511-5518.
54. Tsai, T. M., Mehta, R. C. & DeLuca, P. P. (1996) *International Journal of Pharmaceutics* **127,** 31-42.
55. Tsai, T. M., Mehta, R. C. & DeLuca, P. P. (1996) *International Journal of Pharmaceutics* **127,** 43-52.
56. Arifin, D. Y., Lee, L. Y. & Wang, C. H. (2006) *Advanced Drug Delivery Reviews* **58,** 1274-1325.
57. Fan, L. T. & Singh, S. K. (1989) *Controlled release: A quantitative treatment* (Springer-Verlag.
58. Kanjickal, D. G. & Lopina, S. T. (2004) *Critical Reviews in Therapeutic Drug Carrier Systems* **21,** 345-386.
59. Batycky, R. P., Hanes, J., Langer, R. & Edwards, D. A. (1997) *Journal of Pharmaceutical Sciences* **86,** 1464-1477.
60. Lemaire, V., Belair, J. & Hildgen, P. (2003) *International Journal of Pharmaceutics* **258,** 95-107.
61. Kang, J. C. & Schwendeman, S. P. (2007) *Molecular Pharmaceutics* **4,** 104-118.
62. Faisant, N., Siepmann, J., Richard, J. & Benoit, J. P. (2003) *European Journal of Pharmaceutics and Biopharmaceutics* **56,** 271-279.
63. He, J. T., Zhong, C. L. & Mi, J. G. (2005) *Drug Delivery* **12,** 251-259.
64. Grassi, M. & Grassi, G. (2005) *Current Drug Delivery* **2,** 97-116.
65. Singh, M., Lumpkin, J. A. & Rosenblatt, J. (1994) *Journal of Controlled Release* **32,** 17-25.
66. Craig, D. Q. M. (2002) *International Journal of Pharmaceutics* **231,** 131-144.
67. Miller-Chou, B. A. & Koenig, J. L. (2003) *Progress in Polymer Science* **28,** 1223-1270.
68. Costa, P., Manuel, J. & Lobo, S. (2001) *European Journal of Pharmaceutical Sciences* **13,** 123-133.
69. Narasimhan, B. (2001) *Advanced Drug Delivery Reviews* **48,** 195-210.
70. Ayres, J. W. & Lindstrom, F. T. (1977) *Journal of Pharmaceutical Sciences* **66,** 664-662.
71. Lindstrom, F. T. & Ayres, J. W. (1977) *Journal of Pharmaceutical Sciences* **66,** 662-668.
72. Chandrasekaran, S. K. & Paul, D. R. (1982) *Journal of Pharmaceutical Sciences* **71,** 1399-1402.
73. Melnichenko, Y. B. & Wignall, G. D. (2007) *Journal of Applied Physics* **102,** -.
74. Schmiedel, H., Jorchel, P., Kiselev, M. & Klose, G. (2001) *Journal of Physical Chemistry B* **105,** 111-117.
75. Shekunov, B. Y., Chattopadhyay, P., Tong, H. H. Y., Chow, A. H. L. & Grossmann, J. G. (2007) *Journal of Pharmaceutical Sciences* **96,** 1320-1330.
76. Wignall, G. D. & Melnichenko, Y. B. (2005) *Reports on Progress in Physics* **68,** 1761-1810.
77. Roe, R. J. (2000) *Methods of X-ray and neutron scattering in polymer science* (Oxford University Press, New York).
78. King, E., Robinson, S. & Cameron, R. E. (1999) *Polymer International* **48,** 915-20.

79. Noorsal, K., Mantle, M. D., Gladden, L. F. & Cameron, R. E. (2005) *Journal of Applied Polymer Science* **95,** 475-86.
80. Shekunov, B. Y., Taylor, P. & Grossmann, J. G. (1999) *Journal of Crystal Growth* **198-199,** 1335-1339.
81. Pesnell, A. (2006) *Ph.D. Dissertation, Rutgers University*.
82. Hammersley, A. P. (1998) *ESRF Internal Report, ESRF98HA01T, FIT2D V9.129 Reference Manual V3.1*.
83. Cornell, J. A. (2002) *Experiments with mixtures : designs, models, and the analysis of mixture data* (Wiley, New York).
84. Myers, R. H. & Montgomery, D. C. (2002) *Response surface methodology : process and product optimization using designed experiments* (J. Wiley, New York).
85. Laity, P. R., Taylor, J. E., Wong, S. S., Khunkamchoo, P., Norris, K., Cable, M., Andrews, G. T., Johnson, A. F. & Cameron, R. E. (2004) *Polymer* **45,** 7273-7291.
86. Guinier, A. (1963) *X-ray diffraction: In crystals, imperfect crystals, and amorphous bodies* (W.H. Freeman and Company, San Francisco).
87. Vey, E., Roger, C., Meehan, L., Booth, J., Claybourn, M., Miller, A. F. & Saiani, A. (2008) *Polymer Degradation and Stability* **93,** 1869-1876.
88. Zhu, K. J., Hendren, R. W., Jensen, K. & Pitt, C. G. (1991) *Macromolecules* **24,** 1736-1740.
89. Yoon, J. S., Jin, H. J., Chin, I. J., Kim, C. & Kim, M. N. (1997) *Polymer* **38,** 3573-3579.
90. Wu, X. S. & Wang, N. (2001) *Journal of Biomaterials Science-Polymer Edition* **12,** 21-34.
91. Yoon, J. S., Chin, I. J., Kim, M. N. & Kim, C. (1996) *Macromolecules* **29,** 3303-3307.
92. Staggs, J. E. J. (2002) *Polymer Degradation and Stability* **76,** 37-44.
93. Bose, S. M. & Git, Y. (2004) *Macromolecular Theory and Simulations* **13,** 453-473.
94. Ballauff, M. & Wolf, B. A. (1981) *Macromolecules* **14,** 654-658.
95. Emsley, A. M. & Heywood, R. J. (1995) *Polymer Degradation and Stability* **49,** 145-149.
96. Ramchandani, M., Pankaskie, M. & Robinson, D. (1997) *Journal of Controlled Release* **43,** 161-173.
97. Rothstein, S. N., Federspiel, W. J. & Little, S. R. (2008) *Journal of Materials Chemistry* **18,** 1873-1880.
98. Barnes, A. C., Bieze, T. W. N., Enderby, J. E. & Leyte, J. C. (1994) *Journal of Physical Chemistry* **98,** 11527-11532.
99. Feldstein, M. M., Kuptsov, S. A., Shandryuk, G. A., Plate, N. A. & Chalykh, A. E. (2000) *Polymer* **41,** 5349-5359.
100. Nagata, M., Sugiura, R., Sakai, W. & Tsutsumi, N. (2007) *Journal of Applied Polymer Science* **106,** 2885-2891.
101. Hammouda, B. (2006) *Journal of Polymer Science Part B: Polymer Physics* **44,** 3195-3199.
102. Arce, A., Fornasiero, F., Rodriguez, O., Radke, C. J. & Prausnitz, J. M. (2004) *Physical Chemistry Chemical Physics* **6,** 103-108.
103. Coyle, F. M., Martin, S. J. & McBrierty, V. J. (1996) *Journal of Molecular Liquids* **69,** 95-116.

104. Lundberg, J. L. (1972) *Pure and Applied Chemistry* **31,** 261-281.
105. Nguyen, Q. T., Favre, E., Ping, Z. H. & Neel, J. (1996) *Journal of Membrane Science* **113,** 137-150.
106. Siparsky, G. L., Voorhees, K. J., Dorgan, J. R. & Schilling, K. (1997) *Journal of Environmental Polymer Degradation* **5,** 125-136.
107. Starkweather, H. W. (1963) *Polymer Letters* **1,** 133-138.
108. Williams, J. L., Hopfenberg, H. B. & Stannett, V. (1969) *Journal of Macromolecular Science: Physics* **B3,** 711-725.
109. Cohn, D. & Hotovely-Salomon, A. (2005) *Polymer* **46,** 2068-2075.
110. Petrova, T., Manolova, N., Rashkov, I., Li, S. M. & Vert, M. (1998) *Polymer International* **45,** 419-426.
111. Park, J. H. & Bae, Y. H. (2003) *Journal of Applied Polymer Science* **89,** 1505-1514.
112. Misra, A., David, D. J., Snelgrove, J. A. & Matis, G. (1986) *Journal of Applied Polymer Science* **31,** 2387-2398.
113. Lee, W. F. & Chen, Y. C. (2005) *Journal of Applied Polymer Science* **98,** 1572-1580.
114. Lee, W. F. & Jou, L. L. (2004) *Journal of Applied Polymer Science* **94,** 74-82.
115. Wu, T. M. & Chiang, M. F. (2005) *Polymer Engineering and Science* **45,** 1615-1621.
116. Alexandre, M. & Dubois, P. (2000) *Materials Science & Engineering R-Reports* **28,** 1-63.
117. Sternberg, K., Kramer, S., Nischan, C., Grabow, N., Langer, T., Hennighausen, G. & Schmitz, K. P. (2007) *Journal of Materials Science-Materials in Medicine* **18,** 1423-1432.
118. Kanjickal, D., Lopina, S., Evancho-Chapman, M. M., Schmidt, S. & Donovan, D. (2008) *Journal of Biomedical Materials Research Part A* **87A,** 608-617.
119. Rothen-Weinhold, A., Besseghir, K., Vuaridel, E., Sublet, E., Oudry, N. & Gurny, R. (1999) *International Journal of Pharmaceutics* **178,** 213-221.
120. Hooper, K. A., Cox, J. D. & Kohn, J. (1997) *J. Appl. Polym. Sci.* **63,** 1499-1510.
121. Han, S., Kim, C. & Kwon, D. (1997) *Polymer* **38,** 317-323.
122. Decker, C. (1977) *Journal of Polymer Science, Polymer Chemistry Edition* **15,** 799-813.
123. Decker, C. (1977) *Journal of Polymer Science, Polymer Chemistry Edition* **15,** 781-798.
124. Garrison, W. M. (1987) *Chemical Reviews* **87,** 381-398.

Curriculum Vitae

Isaac John Khan

Education

September 2005 – October 2009 Ph.D. in Biomedical Engineering
Rutgers, The State University of New Jersey, Piscataway, NJ

September 1988 – May 1993 M.S. in Biomedical Engineering
University of Miami, Coral Gables, FL

September 1984 – May 1988 B.S. in Chemistry and Biochemistry (dual major)
University of Miami, Coral Gables, FL

Occupation

May 1999 – June 2005 Staff Engineer, R&D
Cordis, a Johnson & Johnson Company, Warren, NJ

August 1993 – March 1999 Research and Development Engineer
Corvita Corporation, Miami, FL

November 1992 – July 1993 Research and Development Engineer
Cordis Corporation, Miami Lakes, FL

Publications

Khan I.J., Murthy N.S., Kohn J. "Study of the hydration behavior of PEG-containing copolymers in the presence of a hydrophobic drug molecule using SANS". PMSE preprints: Polymeric Materials: Science and Engineering 101: 907-908, 2009.

Schut J., Bolikal D., Khan I. J., Pesnell A., Rege A., Rojas R., Sheihet L., Murthy N. S., Kohn J. "Glass transition temperature prediction of polymers through the mass-per-flexible bond principle". Polymer 48: 6115-6124, 2007.

Wilson J., Klement P., Kato Y.P., Martin J.B., Khan I.J., Alcime R., Dereume J.P., MacGregor D.C., Pinchuk L. "A Self-Expanding, Bifurcated Endovascular Graft For Abdominal Aortic Aneurysm Repair: An Initial Study". ASAIO Transactions 42(3): M386-M393, 1996.